POLYMER SINTERING AND ITS ROLE IN ROTATIONAL MOLDING

By

CÉLINE T. BELLEHUMEUR, B.Eng.

A Thesis

Submitted to the School of Graduate Studies

in Partial Fulfilment of the Requirements

for the Degree

Doctor of Philosophy

McMaster University

POLYMER SINTERING AND ITS ROLE IN ROTATIONAL MOLDING

DOCTOR OF PHILOSOPHY
(Chemical Engineering)

McMASTER UNIVERSITY
Hamilton, Ontario

TITLE:	Polymer Sintering and its Role in Rotational Molding
AUTHOR:	Céline T. Bellehumeur B.Eng. (École Polytechnique de Montréal)
SUPERVISOR:	Dr. John Vlachopoulos (Chemical Engineering)
NUMBER OF PAGES:	xix, 144

ABSTRACT

Polymer sintering can be described as the formation of a homogeneous melt from the coalescence of powder particles under the action of surface tension. Sintering is a fundamental phenomenon in processes such as rotational molding and powder coating. Rotational molding uses plastic powder to produce hollow plastic parts. The porosity of the final part produced in rotational molding depends on the completion of polymer sintering and the removal of bubbles. The objectives of this work are to study the effects of the material properties as well as the molding conditions on the sintering rate and to develop an appropriate model for polymer sintering.

An experimental study of polymer sintering has been carried out. A reliable method has been developed for the observation and the measurement of the coalescence rate for two particles. The material viscosity, elasticity, and particle size were found to affect the sintering process. Most of the results obtained corroborate observations in rotational molding experiments. The effect of the particle geometry on the sintering rate was found to be negligible. This result has led to the study of the rotomoldability of micropellets. Numerical studies have revealed that the processing conditions are severe and probably affect the micropellet rheology, which in return affects the coalescence process.

A mathematical model describing the complete polymer sintering process has been developed. The approach was similar to that of Frenkel (1945). For Newtonian fluids, the proposed model's predictions are very close to Hopper's theoretical model (Hopper, 1984) and to numerical results for viscous sintering (Jagota and Dawson, 1988, Van de Vorst, 1994). The proposed model is successful in predicting the sintering rate for most of the rotational molding grade polyethylene resins used. However, all Newtonian models predict a faster coalescence rate than that observed with the copolymer resins used in this study. This result indicates that factors other than the surface tension and the viscosity play a role in polymer sintering.

The proposed model has been generalized to describe sintering for viscoelastic fluids. As a first approach, the convected Maxwell constitutive equations were used together with the quasi-steady state approximation. The viscoelastic sintering model is capable of predicting the sintering rate observed in this study and the trends reported in the literature for the coalescence of acrylic resins.

The combination of the present experimental and modeling studies can be used for the selection of appropriate materials and for improvement of the rotational molding process.

ACKNOWLEDGEMENTS

I wish to express my sincere appreciation to my supervisor, Dr. John Vlachopoulos for his constant guidance and encouragement throughout the course of this project. I am grateful for all the opportunities he gave me to meet with people from the industry and to attend special events and conferences related with my field of study.

Financial support was provided in the form of scholarships by: Natural Sciences and Engineering Research Council of Canada, Stone-Consolidated Inc., the School of Graduate Studies and the Department of Chemical Engineering of McMaster University, and is gratefully acknowledged.

The experimental work of this project was done in the department of Material Science at the University of Toronto in the laboratories of Dr. G. J. Vancso (formerly of the University of Toronto) and of Dr. M. C. Goh, to whom I am obliged. I would like to acknowledge the following companies for supplying the resins used in this study: Borealis, Esso Chemical Canada, Miles, Millenium Petrochemical, and MSB Plastics. I am also thankful to Gala Industries for providing information about the micropelletizing die.

I would like to acknowledge Mrs. Elizabeth Takács, Mrs. Marianna Kontopoulou for the rotational molding experiments and the rheological measurements.

I am also thankful to Mrs. Takács, Mrs. Kontopoulou, Dr. Mukesh Bisaria and Mr. Ondřej Pokluda for many helpful discussions and with whom it has always been a great pleasure to collaborate.

I am grateful to Dr. George Savva, Mr. Denis Lahaie, as well as Dr. Shipping Zhu, for their helpful discussions about sintering and diffusion. Also, I would like to thank Dr. Andrew N. Hrymak for his advice and suggestions during the course of this project.

To all the people in the Centre for Advanced Polymer Processing and Design (Cappa-D) and the Department of Chemical Engineering, I would like to thank you all for providing a great and friendly environment.

Special thanks are due to Mr. Michael Lutz for his proofreading of this thesis.

Finally, I would like to thank my family and friends for their constant support, advice and encouragement.

TABLE OF CONTENTS

LIST OF FIGURES

LIST OF TABLES

LIST OF SYMBOLS

a: Particle radius

A: Center position of a sintering particle

B: Center position of a sintering particle

D: Deformation tensor

De: Deborah number (λ/t)

E: Young's modulus

J: Compliance

K: Function defined in Hopper's model (1984)

l: Distance between the sintering neck and the center position of a particle

L: Length of the sintering particles

$\bar{n}$: Unit vector normal to the surface

O: Neck position between the sintering particles

P: Pressure load

S: Surface

t: Time, characteristic flow time

$\bar{t}$: Unit vector tangent to the surface

T: Temperature

u: Velocity

V: Volume

W: Width of the sintering particles

W_s: Work of surface tension

W_v: Work of viscous dissipation

x: Position coordinate (x, y, z), mole fraction

y: Sintering neck radius

Greek characters

α: Coefficient for convected Maxwell model

β: Parameter in Hopper's model (1984)

$\dot{\gamma}$: Shear rate

Γ: Material surface tension

$\dot{\epsilon}$: Strain rate

η: Viscosity coefficient

θ: Sintering angle

κ: Surface curvature

K_1: Function defined in the viscoelastic sintering model

K_2: Function defined in the viscoelastic sintering model

λ: Material characteristic relaxation time

ν: Poisson ratio

τ: Extra-stress tensor

χ: Parameter in Hopper's model (1984)

ω: Rotational tensor

φ: Parameter in Hopper's model (1984)

Mathematical symbols

∇: Gradient of a tensor

d /dt: Time derivative

d /dT: Temperature dependence

D /Dt: Substantial derivative

∂ /∂t: Partial derivative

δ /δt: Objective derivative

$\cdot$ Dot product

: Double dot products of a tensor

Superscripts

T: Transpose

$'$ Time derivative

* Dimensionless value

Subscripts

f: Final value

o: Initial value

m: Mean value

x: Coordinate vector (x, y, z), tensor component (x, y, z)

1: Particle 1, component 1

2: Particle 2, component 2

CHAPTER 1

INTRODUCTION

1.1 Polymer sintering

Sintering is commonly defined as the formation of a homogeneous melt from the coalescence of powder particles under the action of surface tension. The sintering stages, which vary from the loose powder filling to a final, almost porosity-free, compact part are illustrated in Figure 1.1. The sintering process is used in manufacturing metallic and ceramic products. This technique allows for the processing of materials which have extremely high melting points (i.e. tungsten and some refractory metals), the combination of metals and non-metals materials, and the production of precision parts which would be otherwise economically unfeasible (Allen, 1969, Reed, 1988). The sintering process is used for the production of commodity products (bricks, porcelains, cookwares) as well as for sophisticated technologies such as semiconductor lasers, electronic packaging, capacitors, cutting tools, engine components, prostheses, catalysts and refractory structures (Allen, 1969, Reed, 1988).

Thümmler and Thomma (1967) proposed the following definition for the sintering process which summarizes most theoretical and practical aspects of the process:

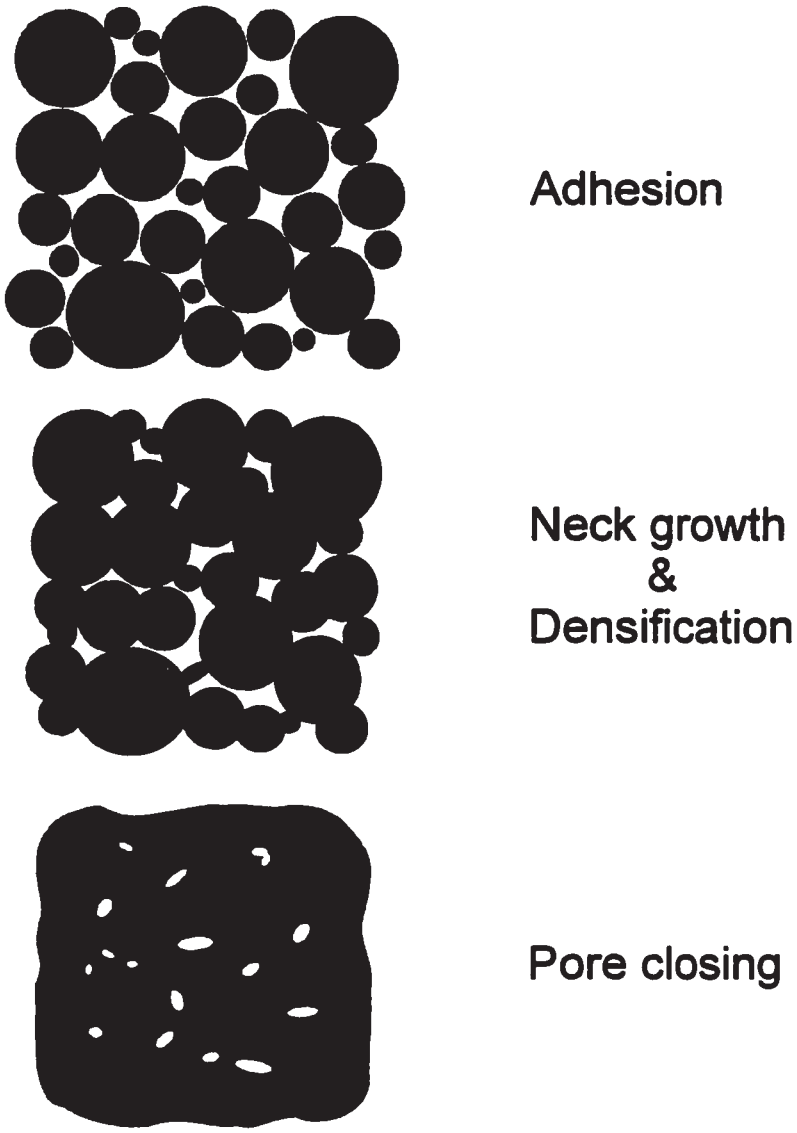

Figure 1.1 Schematic view of coalescence of particles.

> *" By sintering is understood the heat treatment of a system of individual particles or of a porous body, with or without the application of external pressure, in which some or all of the properties of the system are changed with the reduction of the free enthalpy in the direction of those of the porosity-free system. In this connection, at least enough solid phases remain to ensure shape stability. "*

The coalescence of polymer particles is often done at temperatures above their melting point for semi-crystalline material or above their glass transition for amorphous material. Yet, it is frequently referred to as polymer sintering even though the processing conditions contradict the definition of sintering. However, this terminology has been used by many authors to describe polymer coalescence, and it is now accepted in literature.

Polymer sintering is inherent to many industrial processes such as the fabrication of particulate preforms, powder coating, dispersion coating, cold compression molding, and rotational molding. Most of the research on the coalescence of polymer particles has been related to these processes. Several experimental studies have been presented and models have been proposed to describe polymer sintering. However, to date no model has been used successfully in describing the mechanisms involved in polymer sintering (Mazur, 1995). There is a need for a realistic model for polymer sintering as applicable to rotational molding.

1.2 Rotational molding

Rotational molding is used to produce hollow plastic parts and is also known as rotomolding or rotocasting. Various aspects of the rotational molding process have been presented by several authors (Rao and Throne, 1972, Throne, 1979, Crawford, 1992). The concept of rotational molding is illustrated in Figure 1.2 and can be described as follows: (i) The mold is charged with the material usually in powder form. The mold is at ambient temperature and atmospheric pressure. (ii) The mold is rotated biaxially and heated. The rotation is relatively slow and at low temperature the material remains at the bottom of the mold. As the mold is heated, the powder starts to stick and melt on the mold surface. A proper rotation ratio ensures a uniform melt covering of the mold surface by the material. After the melting of the powder is completed, the heating of the melt is continued to allow coalescence of particles and removal of bubbles formed in this process. (iii) After completion of coalescence and removal of bubbles or just before the onset of material degradation, the mold is being cooled while still in biaxial rotation. (iv) The final part is removed after the mold has reached a safe handling temperature.

Due to the nature of the process, rotational molding offers certain advantages over other polymer processes: molding extremely large containers and intricate contours is feasible, the thickness uniformity is comparable to other processes, the final part is virtually stress-free and without weld lines, and the mold is relatively inexpensive. Rotational molding is economically suited for short run production or for parts which have special constraints which could not be molded using other techniques.

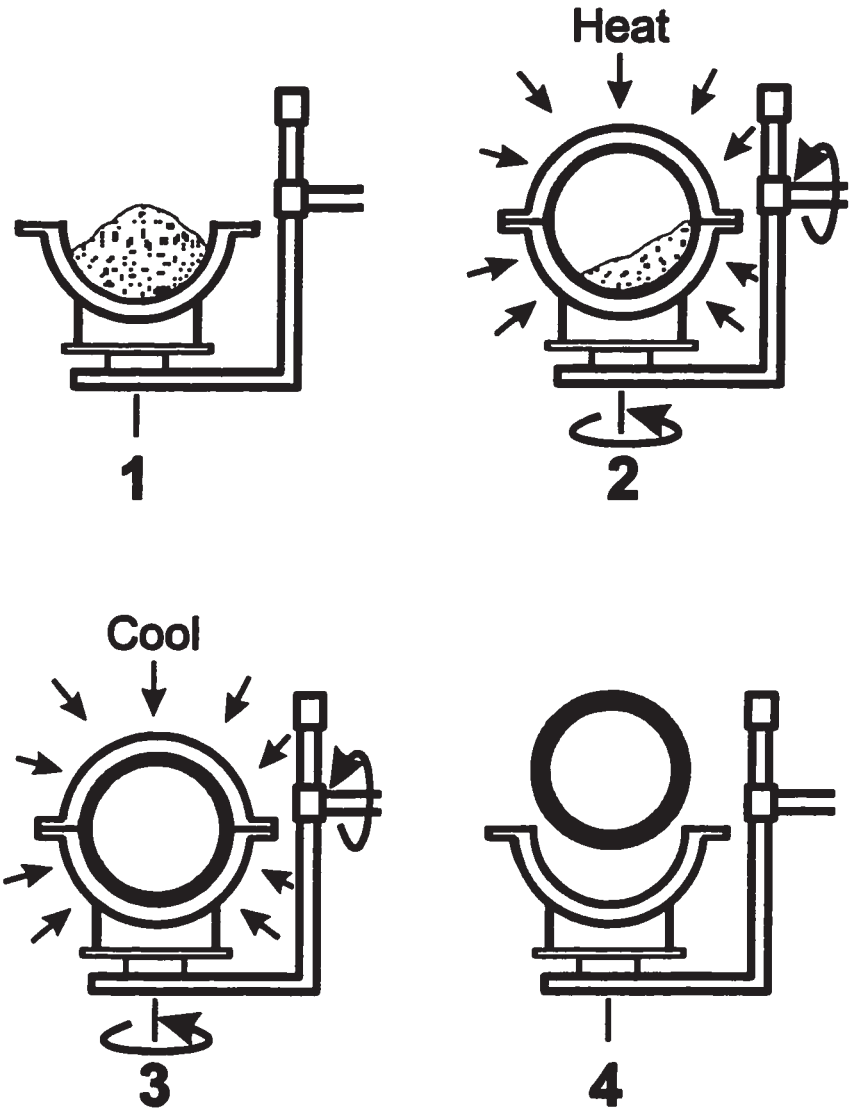

Figure 1.2 Basic operations during rotational molding (adapted from Crawford, 1992).

There are several disadvantages related to rotational molding. The material cost is high because of the need of resin pulverization. The choice of resins used in rotational molding is limited; e.g., polyethylene accounts for over 85% of the total rotomolded volume. The cycle time is relatively long (10 to 30 minutes), and automation is not used very much yet.

Rotational molding has experienced a tremendous growth in the last few years. Although there has been some progress in the molding techniques, the rotational molding industry is facing many challenges such as making more rotational molding grade engineering resins available, as well as adapting the molds, the molding equipment, and the molding conditions to reduce the molding cycle (Crawford, 1996).

Polymer sintering is a fundamental phenomenon in the process since the time required for the completion of powder coalescence controls a major part of heating time in the molding cycle (Bisaria *et al.*, 1994). As the particles coalesce and the bubbles disappear, the molded part structure is improved. A molded part with an incomplete powder coalescence will exhibit a high porosity and poor mechanical properties (Rao and Throne, 1972, Crawford and Nugent, 1989). Fundamental research on rotational molding has been directed to reduce the molding cycle time, to optimize the mechanical properties of final parts, and to examine the rotomoldability of some other high performance resins. Several attempts have been made to predict the molding cycle (Rao and Throne, 1972, Crawford and Nugent, 1989, Sun and Crawford, 1993 (a) and (b), Xu and Crawford, 1994, Bawiskar and White, 1995, Gogos *et al.*, 1997).

However, in these simulations, the densification of the melted particles has been either empirically correlated or simply neglected.

1.3 Research objectives and thesis outline

A fundamental understanding of the polymer sintering phenomenon associated with rotational molding is of immense interest. The present work focuses on a study of polymer sintering in the perspective of its role in rotational molding. The objectives are to study and explain the effects of polymer rheological properties and molding conditions on the sintering rate and to develop a suitable model for polymer sintering. A sintering model is needed to simulate and predict the cycle behavior and also to evaluate the rotomoldability of various polymer grades since the coalescence of the powder is intimately related to the porosity of the molded part. The understanding associated with such a model may also lead to the development of a greater variety of rotomoldable resins. It would also contribute to bringing rotational molding to the technological level of other polymer processes such as injection molding, thermoforming or blow molding.

This thesis is comprised of six chapters including this introduction. A review of the literature on polymer sintering and rotational molding is compiled in Chapter 2. Chapter 3 presents the microscopic approach undertaken to study the sintering of polymer particles under closely controlled conditions. The effects of material properties, particle geometry, and experimental conditions on polymer sintering are presented and discussed in this chapter. In Chapter 4, available Newtonian sintering models are reviewed and evaluated, and a new sintering model for Newtonian fluid is proposed.

The emphasis of this work is on the development of a simple but general model. Based on sintering experimental results and observations in rotational molding, viscoelastic sintering models have been proposed in Chapter 5 using the approach presented in the previous chapter. The advantages and shortcomings of the proposed sintering models are also discussed. The last chapter contains the conclusions of this thesis and the recommendations for future work on this subject.

CHAPTER 2

LITERATURE REVIEW

2.1 Polymer sintering

The sintering process has traditionally been studied for ceramic materials and metals but its application in polymer processing raised also some interest, as reviewed by Mazur (1995). Irrespective of the material used, sintering involves different stages which can be described as follows (Thümmler and Thomma, 1967, Ashby, 1974): (i) The particles adhere to each other. (ii) A neck is formed but the particles remain as individuals. (iii) The neck between the particles keeps growing, and, as the densification develops, the particles loose their identity. Most of the shrinkage takes place at this stage and a coherent network of pores is formed. (iv) The pores become spheroidised, and further densification is possible with their disappearance.

Large segments of the metallurgical and ceramic industries are based on the sintering process. Tremendous efforts have been invested to study the effect molding condition such as composition and pressure on the structure and properties of final parts as presented by German *et al.* (1996). Moreover, processing techniques keep evolving and improving with the development of thermal cycling (Beruto *et al.* 1988), plasma heating (Kim and Johnson, 1983, Johnson *et al.*, 1984, Kemer and Johnson, 1985) and microwave heating (Janney and Kimrey, 1988).

In the literature on polymer processing some attention has been given to the coalescence and sintering processes since these are inherent in industrial processes such as powder coating, dispersion coating, and rotational molding (Bisaria *et al.*, 1994, Mazur, 1995). In the production of polymer blends, it has been recognized that the coalescence process affects the morphology of the product (Utracki and Shi, 1992, Fortelný and Živný, 1995, Sundararaj and Macosko, 1995). It is also admitted that the melt elasticity affects the dissipative viscous flow around droplets in polymer blends, but its role is not completely understood (Utracki and Shi, 1992). Studies on polymer blends have been devoted mostly to model drop breakups and to the conditions causing drop collisions that could lead to coalescence.

Interdiffusion takes place in the coalescence of particles and greatly affects the cohesive strength in film formation (Fisk, 1962, Daniels and Klein, 1991, Wu, 1982). Mazur (1995) describes the molecular diffusion at the interface between the sintered particles as the equilibrium stage of the coalescence process. Theoretical aspects and experimental studies on polymer self-diffusion have been reviewed by Kausch and Tirrell (1989). Several techniques have been developed to measure and describe polymer interdiffusion (Hahn *et al.*, 1986, Pekcan *et al.*, 1990, Russell *et al.*, 1993, Liu *et al.*, 1994).

2.1.1 Transport mechanisms in sintering

The mechanisms involved in powder sintering have been studied and reviewed by numerous authors (Thümmler and Thomma, 1967, Kuczynski, 1972, Kingery *et al.* 1976). The physical significance of the transport mechanisms in solid-state sintering is illustrated in Figure 2.1. Based on surface thermodynamics it can be demonstrated that capillary forces are acting perpendicular to the surface of the neck between two sintering spheres (Kuczynski, 1972). The existence of these forces implies that viscous flow may contribute to various stages of sintering. Closely related to the tensile stress, the gradient of chemical potential can cause diffusional flow through the volume, through the surface or through the interface via grain boundaries (Kuczynski, 1972). Evaporation-condensation is also a possible transport in powder sintering (Kingery and Berg, 1955, Kuczynski, 1972). Adhesion occurs all of the time but is not a dominant mechanism in most sintering processes (Thümmler and Thomma, 1967). Moreover, although recovery and crystallization interact in grain growth, they do not directly cause coalescence (Thümmler and Thomma, 1967).

Early studies revealed that volume diffusion is the most important transport mechanism in the sintering of metals (Kuczynski, 1949 (a), Dedrick and Gerds, 1949, Kingery and Berg, 1955). Further studies with ceramics showed that volume diffusion is a dominant transport mechanism (Coble, 1961, 1964, Kuczynski, 1972). However, sintering of ceramics gains in complexity since chemical reactions often take place simultaneously (Kuczynski, 1972).

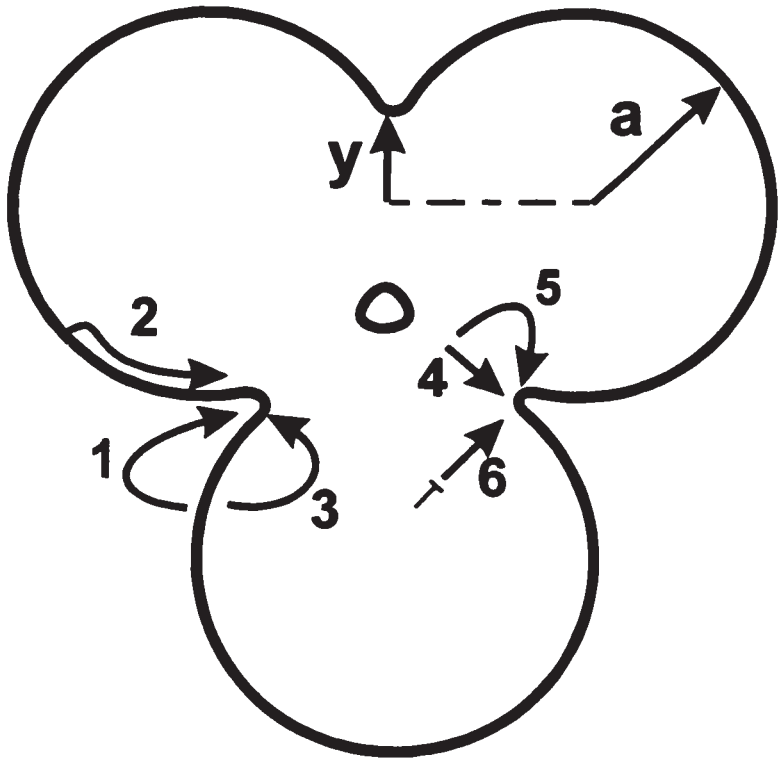

Figure 2.1 Transport mechanisms involved in solid-state sintering: **1** Evaporation-condensation, **2** Surface diffusion, **3** Volume diffusion starting from surface, **4** Grain boundary diffusion, **5** Volume diffusion starting from grain boundary, **6** Volume diffusion starting from dislocation.

Moreover, a desintering phenomenon often occurs in concurrence with the densification process in highly crystalline sintering systems (Lange, 1996).

Several attempts have been made to model sintering based on the volume diffusion mechanism (Coble, 1961, Easterling and Thöien, 1970) as well as on surface diffusion (Nichols and Mullins, 1965, German and Lathrop, 1978). However, it was later demonstrated that although volume diffusion is dominant, the contribution of other mechanisms such as surface diffusion and grain boundary diffusion were significant (Johnson and Clarke, 1964, Wilson and Shewmon, 1966). Based on this finding, sintering diagrams have been created (Ashby, 1974), and numerical models have been developed to take into account the interaction between transport mechanisms (Johnson, 1969, 1970, Eadie and Weatherly, 1975, Bross and Exner, 1979, Ting and Lin, 1994).

For glass materials, experimental studies demonstrated that sintering is due mostly to the viscous flow mechanism (Kuczynski, 1949 (b), Kingery and Berg, 1955, Exner and Petrow, 1975). Parallel to these experimental studies, Frenkel (1945) introduced the very first sintering model based on viscous flow mechanism. Ever since then models based on viscous flow have been proposed and applied to the sintering of glasses as well as ceramics (Martínez-Herrera and Derby, 1994).

As discussed in the previous chapter, although the term sintering is dubious when melting occurs, the expression has been carried on and accepted in literature for the coalescence of polymer particles. Many authors have suggested that viscous flow is the most probable transport mechanism for polymer sintering (Kuczynski, 1949 (b), Narkis, 1979, Rosenzweig and Narkis, 1980, 1981 (b)). The volume diffusion mechanism

implies the presence of a crystalline structure (Kuczynski, 1972). However, the activation energy for diffusion is very high for solid polymeric materials (Sperling, 1986) and no significant densification can be obtained without melting polymer particles (Jayaraman, 1976, Throne, 1989).

2.1.2 Experimental studies on polymer sintering

Initially, experimental work on polymer sintering aimed at identifying the dominant transport mechanisms involved (Kuczynski *et al.*, 1970, Narkis, 1979, Rosenzweigh and Narkis, 1980). There is a vast body of research on polymer sintering from the study of kinetics to the development of new processing techniques. Although particle coalescence and deformation take place in dispersion coating, drying and development of cohesive strength are also important in this process (Daniels and Klein, 1991, Mazur, 1995). Considering the context of the present study, the emphasis of the present review will be on the work performed with discrete particles and dry aggregates.

Sintering experiments have been performed with amorphous polymers (polystyrene and polymethyl methacrylate (Narkis, 1979, Rosenzweig and Narkis, 1980, 1981 (b)), and with semi-crystalline polymers (polypropylene, polyether etherketone, polyethylene) (Hornsby and Maxwell, 1992, Brink *et al.*, 1995, Liu, 1996). These experimental studies have shown that Newtonian viscous flow is dominant in polymer sintering. Liu (1996) has suggested that in addition to surface tension, gravity contributes to polymer sintering irrespective of the particle positioning. However, Rosenweig and Narkis (1981 (b)) showed that the effect of gravity strongly depends on the relative position of the

particles.

Several authors have suggested that the Newtonian viscous flow mechanism may not adequately represent polymer sintering (Lontz, 1964, Kuczynski *et al.* 1970, Mazur and Plazek, 1994). Kuczynski *et al.* (1970) found significant deviations between their experimental data obtained with poly(methyl methacrylate) and the Newtonian sintering model. Based on his experiments with poly(tetrafluoroethylene), Lontz (1964) suggested that the late stage of sintering was essentially viscoelastic. However, Lontz (1964) based this conclusion on a comparison with a Newtonian model which is only valid in the early stage of sintering (Frenkel, 1945). Mazur and Plazek (1994) experimentally measured the sintering of acrylic resins and compared their results with analytical and numerical solutions for Newtonian sintering (Frenkel, 1945, Jagota and Dawson, 1988 (a)). They found that the sintering rate is underestimated by the Newtonian models. They concluded that quasi-elastic deformation controls the early stage of sintering.

Siegmann *et al.* (1986) compared the sintering rate between polyethylene of various molecular weights. They found that the coalescence rate for the ultra-high molecular weight polyethylene (UHMWPE) was surprisingly higher than for the high molecular weight polyethylene (HMWPE), although HMWPE has a smaller viscosity than UHMWPE. They attributed this phenomenon to the morphological differences between these resins. This finding was supported by Barnetson and Hornsby (1995) who also examined the effect of the morphology on the sintering behavior of several grades of UHMWPE resins. This result favored the development of rapid polymer sintering technologies (Hornsby and Davidson, 1996).

Work on powder compaction and sintering principally aimed at studying the effect of pressure, compaction speed, powder characteristics and resin aging on the molded part structure and properties (Jayaraman *et al.*, 1976, Halldin and Kamel, 1977, Truss *et al.*, 1980, Throne, 1989, Vick and Kander, 1996). In most cases it was observed that the compaction would cause particle reorientation, particle sliding, and mechanical interlocking, but it was also observed that a part with adequate strength could be produced only with sintering above the melting point (Jayaraman *et al.*, 1976). Some welding between particles was observed at temperatures below the melting point (Throne, 1980). This welding was attributed to creep under localized load or to liquification of an intermediate by the combination of temperature and pressure (Throne, 1980).

Some attention has also been devoted to research on reactive polymeric sintering systems. Crolla and Menges (1989) studied the effect of processing conditions on the structure and properties of polyvinyl chloride during gelation.

2.1.3 Modeling of sintering based on Newtonian viscous flow mechanism

Frenkel (1945) derived the first analytical model describing the rate of coalescence occurring by viscous flow for two identical spherical particles:

$$\frac{y}{a} = \left(\frac{3}{2}\frac{\Gamma t}{\eta a}\right)^{1/2} \tag{2.1}$$

where a, t, y, η, and Γ are the particle radius, sintering time, sintering neck radius, viscosity and surface tension of the material, respectively. The validity of Frenkel's

model is limited to Newtonian flow, and is only valid in the early stages of sintering when the particle diameters remain relatively constant. This model has been assessed experimentally for glass spheres (Kuczynski, 1949 (b), Kingery and Berg, 1955) and for polymers (Narkis, 1979, Rosenzweig and Narkis, 1980, 1981 (b), Brink *et al.*, 1995, Liu, 1996). However, these assessments of Frenkel's model have been only qualitative in nature. Hornsby and Maxwell (1992) found that Frenkel's model was in good agreement with their experimental results. However, in their analysis they used the Trouton viscosity (i.e., three times larger than the shear viscosity) to generate Frenkel's model predictions. Eshelby (1949) pointed out that the continuity equation for an incompressible fluid was violated in the development of Frenkel's model. He proposed corrections which yield the following result which is subsequently referred to as the Frenkel/Eshelby model:

$$\frac{y}{a} = \left(\frac{\Gamma t}{\eta a}\right)^{1/2} \tag{2.2}$$

Several alternatives to Frenkel's model have been suggested. Rosenzweig and Narkis (1981 (b)) proposed a dimensional model which they subsequently used in a numerical simulation of the early stage of sintering (Rosenzweig and Narkis, 1983). Kuczynski *et al.* (1970) proposed the use of a shear dependent viscosity in Frenkel's model. The usefulness of this modification is questionable since the shear rates involved in sintering during rotational molding are extremely small (Rosenzweig and Narkis, 1981).

Hopper (1984, 1990, 1991) proposed an exact analytical solution of the Navier-Stokes equations for two dimensional viscous flow driven by capillary forces acting on the free-surface. He analyzed the capillary flow for two cylinders having an inverse ellipse at their cross section and presented the following sintering model (1984, 1990):

$$\frac{y}{a_f} = (1-\varphi)(1+\varphi^2)^{-1/2} \tag{2.3}$$

$$\frac{\Gamma t}{\eta a_f} = \frac{\pi}{4}\int_{\varphi^2}^{1} [\beta(1+\beta)^{1/2}K(\beta)]^{-1}\, d\beta \tag{2.4}$$

where a_f is the final particle radius and φ is the parameter of the inverse ellipse. When $\varphi=0$ the curve is one circle and as $\varphi\rightarrow 1$ the curve approaches the shape of two circles. The function $K(\beta)$ is the complete elliptic integral defined by:

$$K(\beta) = \int_{0}^{1} [(1-\chi^2)(1-\beta\chi^2)]^{-1/2}\, d\chi \tag{2.5}$$

where χ is a parameter of the elliptic integral ranging from 0 to 1. Hopper (1991) extended this theory to describe the time evolution of various geometries and generalized the model for coalescence of two cylinders in considering the initial diameter ratio (Hopper, 1992, 1993 (a) (b)). Furthermore, an analytical solution for the sintering of an array of cylinders has been proposed by Cosgrove *et al.* (1976). Based on Hopper's theory, De With and Corbijn (1995) proposed a method to determine the surface tension of glasses.

The late stage of sintering, also termed pore closing, has been studied and modeled by several authors (Mackenzie and Shuttleworth, 1949, Kuczynski and Zaplatynsyj, 1956, Van de Vorst, 1993, 1994). Scherer (1977 (b)) demonstrated the limitations of Mackenzie and Shuttleworth's model (1949) and proposed a phenomenological model for the densification of particle agglomerates (Scherer, 1977 (a) (c)). The effects of particle rearrangements, substrates, and inclusions on the coalescence of powder packing are important issues in formation of glasses and ceramics (Exner and Petzow, 1975, Rahaman, 1988, Bordia and Jagota, 1993). Hence, several attempts have been made to simulate sintering of particle packing and composite packing (Scherer, 1984, Scherer and Garino, 1985, Jagota and Dawson, 1988 (b), Jagota *et al.* 1988, 1990, Jagota and Scherer, 1993, 1995). Moreover, Jagota (1995) has extended his model to study the sintering of coated particles.

Numerical solutions for two dimensional and axisymmetric sintering systems have been presented by numerous authors (Ross *et al.*, 1981, Hiram and Nir, 1983, Jagota and Dawson, 1988 (a), 1990, Kuiken, 1990, Van de Vorst, 1994, Martínez-Herrera and Derby, 1994, 1995). The numerical simulations aimed to study the effect of the intial geometry and processing conditions on the resulting flow and coalescence rate. Van de Vorst (1994) and Martínez-Herrera and Derby (1994) showed that their numerical results for coalescence of two cylinders were in good agreement with the prediction from Hopper's model (1984).

2.1.4 Modeling of sintering based on elastic and viscoelastic mechanisms

Most elastic and viscoelastic sintering models have been derived based on the deformation of elastic bodies. Lee and Radok (1960) extended the analysis presented by Hertz (Timoshenko and Goodier, 1970) to describe the effect of pressure load for the contact deformation of two viscoelastic spheres. This approach was then refined for different geometries and load history (Graham, 1965, Yan, 1966, Ting, 1966). The drawback of these models is that they only consider the application of an external load and neglect the action of the surface tension on the sintering system. Johnson *et al.* (1971) extended the Hertz's analysis of elastic deformation by including the influence of surface tension and the adhesion force in an elastic formulation for the neck growth between two spheres of radius a_1 and a_2, respectively

$$y^3 = \frac{3a_m}{4E_m} P + 3\pi\Gamma a_m + \left(3\pi\Gamma a_m P + (3\pi\Gamma a_m)^2\right)^{1/2} \tag{2.6}$$

in which P is the applied load on the sintering spheres, and

$$\frac{1}{E} = \frac{1-\nu_1^2}{E_1} + \frac{1-\nu_2^2}{E_2} \tag{2.7}$$

$$\frac{1}{a_m} = \frac{1}{a_1} + \frac{1}{a_2} \tag{2.8}$$

where E_1 and E_2 are the Young moduli, ν_1 and ν_2, are Poisson ratios, for each sphere.

The model developed by Johnson *et al.* (1971) will be referred to as the JKR model. Experimental results obtained with latex and rubber spheres were found to fit the JKR model predictions relatively well and the model allows the calculation of the interfacial energy for polymer-polymer interaction (Kendall and Padget, 1982, 1987). However the validity of the JKR model is limited to pure elastic material.

Mazur and Plazek (1994) proposed a viscoelastic sintering model (MP model) treating the elastic and viscous flows as mutually independent contributions. The elastic contribution for the sintering neck growth is defined based on the JKR model. Firstly, the JKR model was defined in term of the compliance J with the assumptions that both particles are equal sized and that they are made from an elastic fluid (Mazur, 1995):

$$\frac{y}{a_o} = \left(\frac{9\pi\Gamma(1-\nu)J}{8a_o} \right)^{1/3} \tag{2.9}$$

Mazur and Plazek (1994) then used a time-dependent compliance $J(t)$, and the resulting model that they proposed is as follows (Mazur, 1995):

$$\frac{y}{a_o} = \left(\frac{9\pi\Gamma(1-\nu)J(t)}{2a_o} \right)^{1/3} + \left(\frac{t\Gamma}{\eta a_o} \right)^{1/2} \tag{2.10}$$

Although the trends are qualitatively consistent, the MP model predictions have been found to be significantly faster than the observed experimental results for acrylic resins (Mazur and Plazek, 1994). Mazur and his coworkers (Argento *et al.*, 1996) extended the analysis of the MP model to consider the interfacial forces originating from the

curved surface (Jagota and Dawson, 1988 (a), Hiram and Nir, 1983) and the forces arising from Van der Waals' interactions between molecules. Argento *et al.* (1996) confirmed that the extended MP model predictions qualitatively agree with the experimental results obtained by Mazur and Plazek (1994).

2.2 Rotational molding

Rotational molding is a method of making hollow plastic articles. It involves powder mixing, melting, sintering and melt solidification. Rotational molding is facing a growing competition from processes like blow molding and twin sheet thermoforming. To keep up with this competition, the rotational molding industry has invested efforts in the development of new equipment and molding techniques as well as new materials (Leaversuch, 1995, Muller and Howard, 1995, Crawford, 1996). In the following sections key aspects of rotational molding are reviewed.

2.2.1 Molding cycle and molding conditions

The molding cycle and the mold part properties are greatly affected by the molding conditions, namely the oven temperature, heating time, cooling rate, rotation speed, and rotation ratio. Handbooks have been published providing guidelines on mold design and processing parameters (Engineering Design Handbook, 1975, Association of Rotational Molders, 1982, 1989). Efforts have been principally directed to reduce the molding cycle time and to optimize the mechanical properties of the final parts. While investigating the effect of processing conditions on molded part properties, Crawford and

Nugent (1992 (b)) found that the impact strength of the molded part is highly correlated with the inside air temperature in the mold. Based on this finding, Crawford and Nugent (1992 (a)) patented a device called ROTOLOG which allows measurement of the air temperature inside the mold and which can be used to control the molding cycle. The inside air temperature profile is commonly used to represent the different stages in the molding process. A typical profile is presented in Figure 2.2 and can be described as follows (Crawford, 1992, Kontopoulou, 1995): (i) In this induction stage, the mold and powder temperatures rise steadily. The powder tumbles freely in the mold and is heated primarily through conduction and radiation up to point *A*. (ii) From *A* to *B* powder particles become sticky and adhere to the mold surface and some layers adjacent to the mold wall melt and start sintering in this stage. (iii) From *B* to *C* all the powder has melted, the neck growth between the particles (polymer sintering) is taking place, and pockets of air are trapped in the melt. (iv) From *C* to *D* the particles have lost their identity, and bubbles present in the melt decrease in size. (v) The mold is being cooled; consequently, the temperature of the melt falls to its solidification point or the crystallization point for semi-crystalline polymers (point *E*).

Several studies have been pursued to correlate the molded part mechanical properties with processing conditions. It was shown that the heating time and the oven temperature have a great effect on the impact strength of the molded part (Crawford *et al.*, 1991, Crawford and Nugent, 1992 (b)).

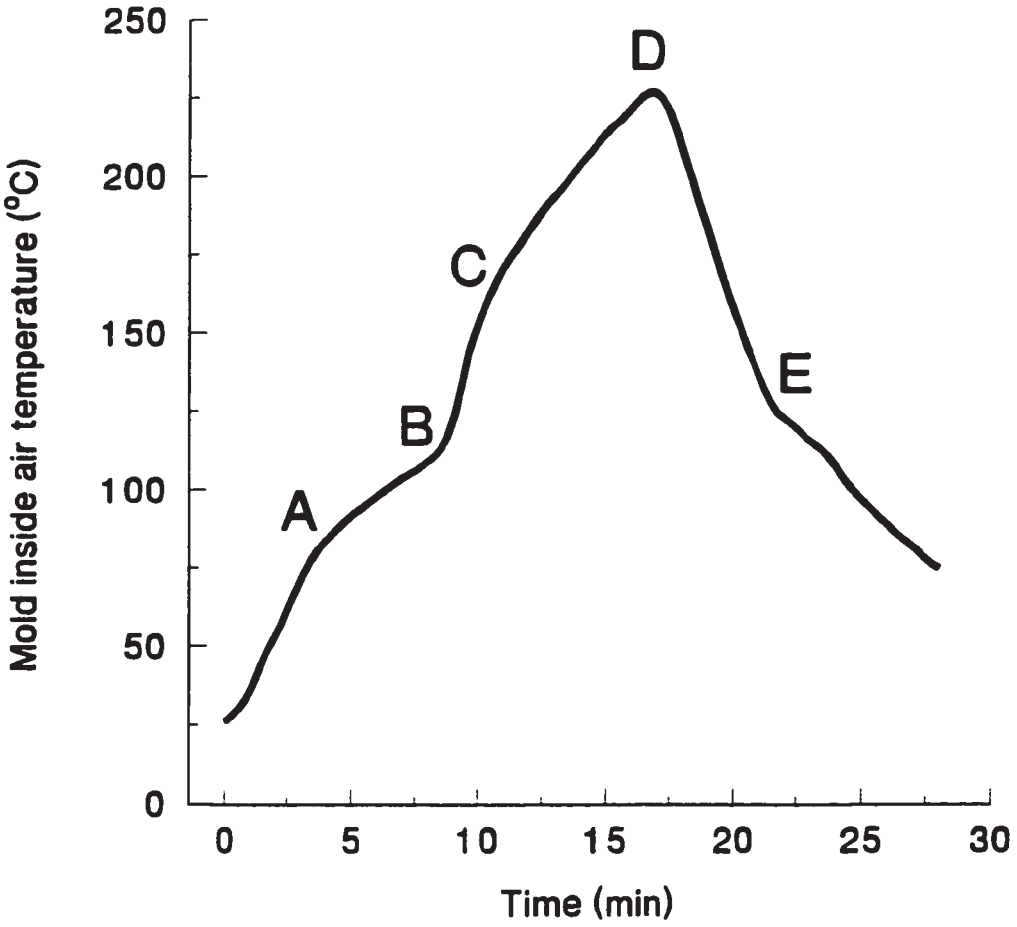

Figure 2.2 Typical mold internal air temperature during a rotational molding cycle.

Mold geometry, rotation speed and ratio along with powder properties affect the mold coverage distribution (Crawford *et al.*, 1991) and can contribute to enhanced mixing or segregating of powder in the mold (Khakhar *et al.*, 1997, McCarthy, 1996). The effects of the cooling rate on warpage, shrinkage, and mold part structure have been investigated (Chen et al., 1990, Bawiskar and White, 1994, O'Neill and Crawford, 1996). Chen *et al.* (1990) suggested a small pressurization of the mold to speed up the cycle. This idea was later considered by Crawford and his coworkers to reduce the cycle time as well as the mold part porosity (Xu and Crawford, 1993, Sun and Crawford, 1993 (b), Spence and Crawford, 1996).

2.2.2 Materials

In earlier applications of rotational molding liquid plastisol was principally used. However, the introduction of powdered resins truly revolutionized the rotational molding industry (Throne, 1979, Crawford, 1992). Research related to development of rotational molding resins included the study of pigmentation (Crawford *et al.*, 1996, Nagy and White, 1996) and the development of some alternatives to powdered resins (Gala Industries, 1995, Muller and Howard, 1995, Takács *et al.*, 1996).

There are a number of fundamental characteristics for the resin: flowability to ensure complete filling for the cavities, suitable size and shape for good heat transfer, and high thermal stability since the polymer is subject to high temperature for a relatively long period (Rao and Throne, 1972, Throne, 1979, Crawford, 1992). Studies have been completed to define the optimal powder properties and to develop methods for

characterizing resins for rotational molding according these criteria (Rao and Throne, 1972, Throne and Sohn, 1989). The flow characteristics of the melt are also very important to ensure a uniform wall thickness (Crawford, 1992) and to produce a part with reduced porosity (Rao and Throne, 1972, Kontopoulou, 1995, Vlachopoulos *et al.* 1996, Takács *et al.* 1996).

The flow characteristics of the melt have a great influence on the final part porosity and consequently on the molding cycle (Rao and Throne, 1972, Crawford, 1992, Bisaria *et al.*, 1994, Takács *et al.*, 1996, Vlachopoulos *et al.*, 1996). The zero-shear viscosity is one of the most important parameters involved in rotational molding considering the low shear character of the process (Bisaria *et al.*, 1994). It has been observed that resins with high zero-shear viscosity produce parts which show excessive porosity and poor surface finish when rotationally molded (Crawford, 1992, Bisaria *et al.*, 1994). The melt flow index (MFI), usually used to assess the resin rotomoldability, can be misleading especially in the case of blends or resins with very broad or very narrow molecular weight distribution (Vlachopoulos *et al.*, 1996). It was also observed that resins having comparable zero-shear viscosity may exhibit different behavior in rotational molding (Kontopoulou, 1995, Vlachopoulos *et al.*, 1996, Kontopoulou *et al.*, 1997 (a)). This observation was attributed to the elastic character of the resin.

Polyethylene in powder form is extensively used in rotational molding for its good impact strength properties. To compensate for the low strength of polyethylene, other resins have been considered in rotational molding such as polypropylene copolymer (Kontopoulou, 1995), nylon (Nugent, 1990), polycarbonate (Anon, 1980, Kontopoulou

et al., 1997), ethylene vinylacetate and ethylene butylacrylate copolymer (Nugent, 1990, Kontopoulou *et al.*, 1997 (b)), and acrylonitrile butadiene styrene (Tanaka, 1974, White *et al.*, undated). Reactive liquids are also used in rotational molding. The structure and properties of molded parts as well as the flow phenomena involved in reactive rotational molding have been studied for polyester (Throne and Gianchandani, 1980), syntactic foams (Narkis *et al.*, 1982), polyurethane (Rabinovitz and Rigbi, 1985), crosslinked ethylene vinylacetate and ethylene methacrylate (Espinasse *et al.*, 1993), and RIM nylon (Harkin-Jones and Crawford, 1996 (a) (b)). In many cases, promising results have been obtained, but it is still difficult to rotationally mold many engineering resins.

2.2.3 Sintering and bubble removal

The coalescence of powder particles in rotational molding was first considered by Rao and Throne (1972). In the rotational molding literature, sintering has since then been referred to as the neck growth process, while densification has been defined as the stage of bubble formation and removal (Rao and Throne, 1972, Crawford and Scott, 1987). Rao and Throne (1972) described powder coalescence in rotational molding in two stages: (i) the fusion at contact point by the powder particles to produce a porous three dimensional network and (ii) the collapsing of the network in which the bubbles are trapped. Furthermore, they suggested that the bubbles are migrating from the melt to the free surface due to the action of buoyancy forces (Rao and Throne, 1972). Progelhof *et al.* (1982) confirmed this hypothesis based on experiments performed with polyethylene pellets. Further work has been done to study the formation and removal

of bubbles in rotational molding. Based on experimental work with polyethylene powder, Kelly (undated) suggested an alternative scenario for the disappearance of the bubbles in the melt. Kelly's theory holds that bubbles, once formed, are trapped in the melt and that their disappearance is due to the diffusion of gas into the melt. He based this conclusion on microscopic observations using polyethylene powder. In a detailed study Crawford and Scott (1987) experimentally and theoretically confirmed Kelly's theory. Following up the work done by Scott (1986), Spence and Crawford (1996) investigated the effects of processing variables on the formation and removal of bubbles. They considered the material viscosity, powder characteristics, molding temperature, molding atmosphere, moisture, mold material, and mold release agent. The kinetics of bubble removal in rotational molding has been described mostly in terms of the bubble size. Other authors have suggested that the shape as well as the coordination number (i.e., number of touching particles forming the bubbles) are important properties in characterizing the coalescence of powder agglomerates (Lange, 1984, Pietsch, 1996).

Mechanistic models have been proposed to describe the bubble removal phenomenon in rotational molding. Throne (1979) generalized the model presented by Kuczynski and Zaplatynsyj (1956) to describe the disappearance of bubbles induced by capillary flow. Other authors proposed mechanistic models for the removal of bubbles due to the diffusion of gas into the melt (Crawford and Scott 1987, Xu and Crawford, 1993, Spence, 1994, Xu, 1994, Spence and Crawford, 1996).

The models proposed by Crawford and his coworkers (Spence and Crawford, 1996, Xu and Crawford, 1993) have been successfully assessed with experiments

performed with polyethylene (Scott, 1986, Spence, 1994). However, the validity of these models is limited to the resins used in these studies since the model parameters need to be estimated from experimental data. Moreover, Crawford and his coworkers neglected the effect of the material viscosity and the capillary forces. However, recent studies have suggested that the viscoelastic character of the resin may affect the bubble removal phenomenon in rotational molding (Kontopoulou, 1995, Kontopoulou *et al.*, 1997 (b)).

2.2.4 Heat transfer models and numerical simulations

Heat transfer is an important factor for the control of the molding cycle. However, it is difficult to model due to convection, conduction, and radiation, which are simultaneously involved, and also due to the complexity of the process (i.e., biaxial rotation, powder mixing, melting and coalescence, and the dynamic nature of the boundary conditions). Rao and Throne (1972) proposed the first heat transfer model for rotational molding. They made several assumptions with respect to the mold geometry, the powder flow, and the heat transfer mechanisms involved. In the same year, Throne also presented an analysis of the factors influencing cooling rate in rotational molding (Throne, 1972). Since these first models, several attempts have been made to predict the molding cycle. Progelhof and Throne (1976) extended the description of the fluid dynamics and heat transfer for liquid systems. Throne (1976) developed an alternate heat transfer model for powder rotating systems.

Experimental results obtained by Scott (Crawford and Scott, 1985, Scott, 1986) gave a clear insight on the heat transfer mechanisms involved in rotational molding.

Following this experimental study, Crawford and Nugent developed a numerical simulation of the rotational molding process (Crawford and Nugent, 1989). The output of the simulation are the temperature profiles through the mold and polymer and the contact time distribution of the polymer on the mold surface. Relatively good agreement was found between the numerical prediction and experimental results (Crawford and Nugent, 1989, Nugent *et al.*, 1992). Several improvements on the simulation have been made. Sun and Crawford (1993 (a) and (b)) considered internal heating and cooling. Xu and Crawford (1994) considered the temperature change of the air inside the mold during the molding cycle. All these simulations have been developed to give a tool in predicting the molding cycle given specific conditions and ultimately to help design new molding methods (Nugent, 1990, Nugent *et al.*, 1992, Xu, 1994, Sun and Crawford, 1993 (a) (b)).

At present, one commercial numerical simulation of the rotational molding process is available (Xu and Crawford, 1997). However, it presents the same limitations as all heat transfer models developed to predict the molding cycle: it is limited to simple mold geometry. Moreover, in all the models presented in the literature for rotational molding or any other process involving polymer sintering (Nelson *et al.* 1995), the sintering process is either neglected or determined empirically.

CHAPTER 3

EXPERIMENTAL WORK

3.1 Apparatus and procedure

The experimental apparatus consisted of a Mettler FP82 heat chamber, controlled with a central processor, Mettler FP80. A sectional view of the apparatus is presented in Figure 3.1. The sample, consisting of two particles of approximately equal size, was placed on a glass slide. The slide was then placed in a flat rectangular chamber formed by two metal plates. The chamber is built into a double-walled housing finished with mirrors. The temperature is measured using a platinum resistance sensor imbedded in the lower plate of the chamber. The recorded temperature for the sample is determined automatically from the measurement using a correction factor based on calibration. The accuracy of the temperature measurement in the furnace is ± 0.6°C in the range of 100 to 200°C. The sample was placed in the chamber at a temperature below the melting point of the polymer. The temperature was then set to the sintering conditions (steady state occurs within 15 to 20 seconds). An optical microscope was used to observe the sintering process. Because of the relatively large size of the sample (diameter ≥ 250 μm), transmittance illumination mode was used. Therefore, the sintering surface has to be transparent to allow measurements. The sintering sequence was recorded using time lapse photography.

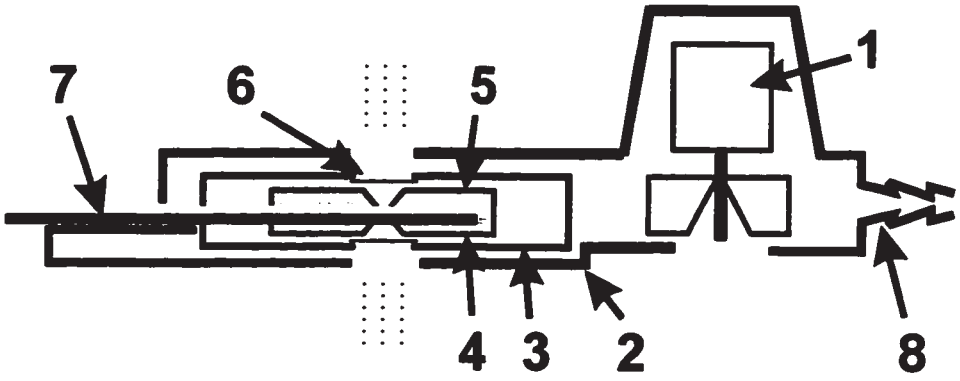

Figure 3.1 Sectional view of the hot stage Mettler FP82: **1** Fan, **2** Outer casing, **3** Inner casing, **4** Metal plate with heating wires and Pt100 temperature resistance, **5** Metal plate with heating wires, **6** Heat protection filter, **7** Slide, **8** Cooling connector.

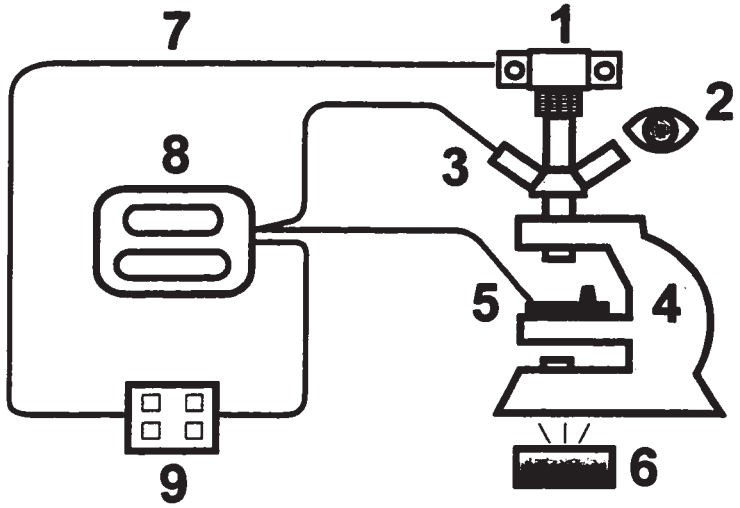

Figure 3.2 Schematic of apparatus used for polymer sintering experiments: **1** Camera, **2** Eye piece, **3** Photomonitor, **4** Microscope, **5** FP82 Hot stage, **6** Light source, **7** Connection cable to flash contact, **8** FP80 Control, **9** Hand set.

A schematic representation of the experimental setup is presented in Figure 3.2.

The sintering results shown in subsequent figures have been obtained by observations of at least two pairs of particles for each experimental condition (to assure reproducibility), and the numerical values for particle size and neck radius given are the averages. The neck diameter and the projected area of the particles on the pictures were measured using the image analysis software LECO 2001 (Leco Instruments, 1992) and SigmaScanPro (Jandel Scientific Software, 1992). The particle contour was idealized as schematically represented in Figure 3.3, and the particle radius was estimated from the measurements of the projected area of the particles and the diameter of the neck between the particles. The dimensionless sintering neck growth is calculated from measurement of the sintering neck radius y formed between the particles and the average radius of the two particles a (Figure 3.3).

Most of the experiments have been performed at constant temperature. However, to facilitate the comparison between resins with different melting points, a time-dependent sintering temperature has been programmed to simulate the rotational molding heating cycle for some experiments (Figure 3.4). The rate of increase of the sintering temperature was determined by linear regression of data obtained during the neck growth and fusion stages of the rotational molding cycle (Figure 3.4). A linear profile for the sintering temperature was used due to experimental limitations. Moreover, experimental results have shown that the temperature profile of the polymer melt during the heating cycle of rotational molding is nearly linear (Scott, 1986).

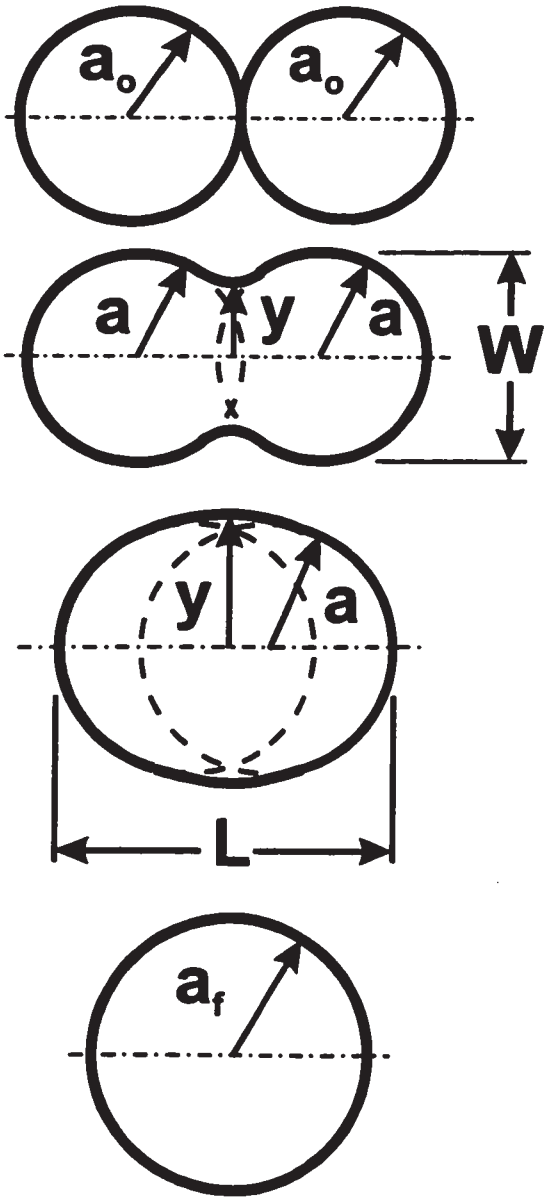

Figure 3.3 Schematic sintering sequence for two particles, where a, a_o, a_f, y, L, and W are the particle radius, initial particle radius, final particle radius, neck radius, length and width of the sintering particles (adapted from Rosenzweig and Narkis, 1980).

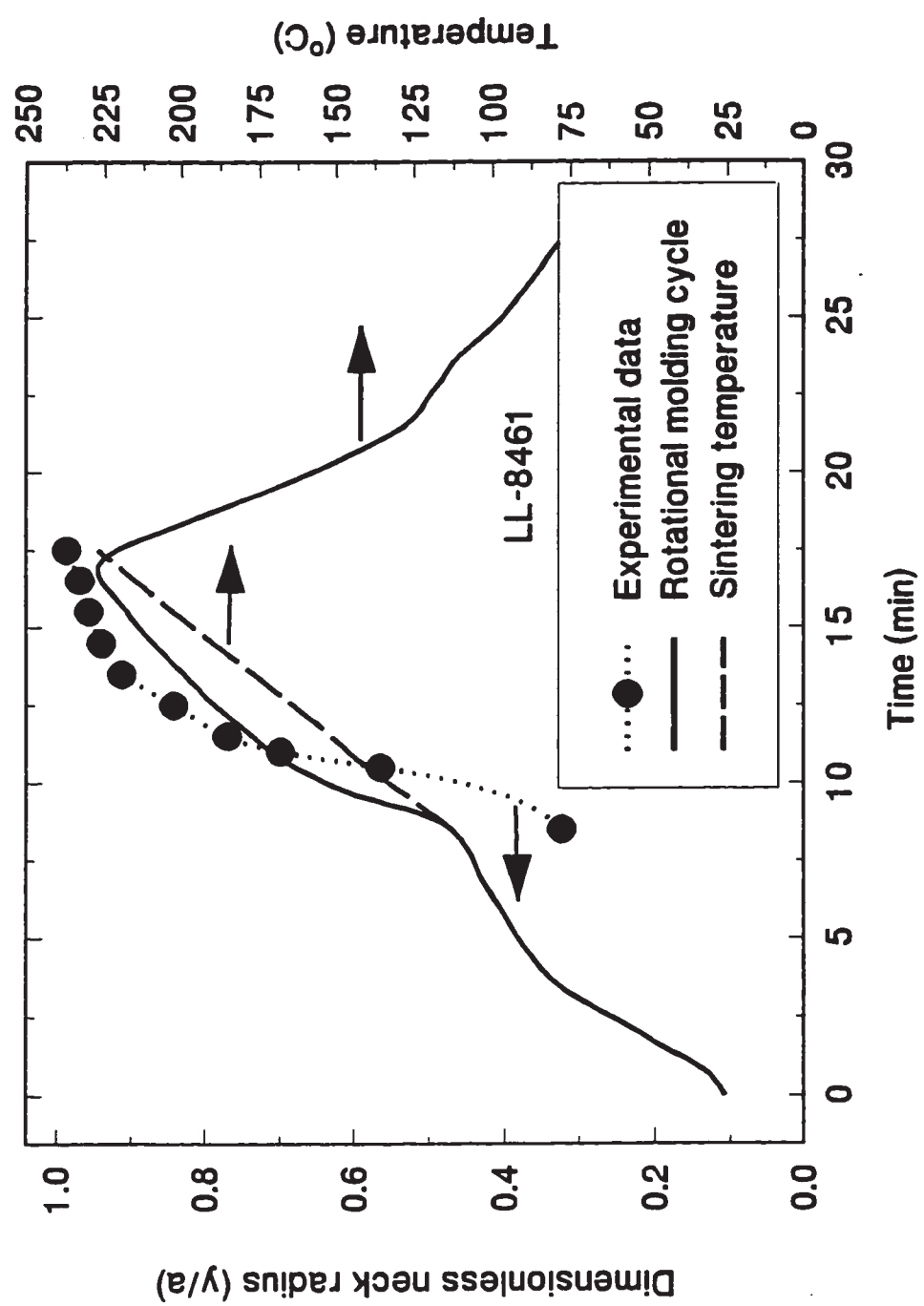

Figure 3.4 Sintering dimensionless neck growth for LL-8461 powder particles, sintering temperature profile and mold inside air temperature profile obtained during a rotational molding cycle.

The mold internal air temperature was obtained on a uniaxial rotating machine which has been described elsewhere (Bisaria *et al.*, 1994), and the molding conditions are described in Table 3.1.

3.2 Materials

The experiments were performed using the following rotational molding grade resins: high density polyethylene (HDPE), linear low density polyethylene (LLDPE), propylene ethylene copolymer (PP/PE), polycarbonate (PC), polyvinyl chloride (PVC), and ethylene butyl acrylate copolymer (EBA). One blow molding grade high density polyethylene (HDPE-BM) was also used. Table 3.2 presents a list of the resins used and the resin properties as reported by their suppliers. These resins were used in powder form, irregular particles (as received), and cylindrical form particles (produced in our lab by capillary extrusion of powder). The zero-shear viscosity for the resins, presented in Tables 3.3, 3.4 and 3.5, has been determined from viscosity measurements performed at very low shear rate using a Bohlin rotational rheometer. The thermal properties and the results from chemical analysis are presented in Table 3.6.

Polyethylene micropellet particles (HD-8660, LL-8460, LL-8555) produced by an underwater pelletizing method were also used. Micropellets are the latest development as an alternative which eliminates the need for powder grinding (pulverizing) for rotational molding. Micropelletization also offers the opportunity to melt compound during the product formation, whereas grinding does not.

Table 3.1 Rotational molding experiments on uniaxial rotating machine: molding conditions

Material	LL-8461	EBA-NCPE8019	PC-Makrolon	PVC-1
Mold type	Square*	Square*	Round†	Round†
Mold rotation speed (RPM)	4	4	4	4
Oven Temperature (°C)	404	406	508	405
Shot weight (kg)	0.1	0.1	0.05	0.05

* 0.095×0.095×0.1 m cube shaped mold made of 1.6 mm thick steel
† 0.096 m diameter and 0.102 m length cylindrical mold made of 2.7 mm thick aluminum pipe

Table 3.2 Materials

Name	Type	Trade name	Supplier	MFI (g/10 min)*	Density (kg/m^3)
HD-8661	HDPE	HD-8661	Esso Chemical Canada	2.0	942
LL-8461	LLDPE	LL-8461	Esso Chemical Canada	3.3	939
LL-8556	LLDPE	LL-8556	Esso Chemical Canada	5.6	935
PP-SC1355RM	PP/PE copolymer	SC13 55RM	Borealis	13.0 †	900
PP-MT4390HU	PP/PE copolymer	Petrothene MT 4390-HU	Millenium Petrochemical	20.0 †	900
PP-TR121	PP/PE copolymer	Petrothene PP TR121	Millenium Petrochemical	11.0 †	890
PC-Makrolon	PC	Makrolon 5303	Miles	11.0 ‡	1200
PVC-1	PVC	N.A.	Plast-O-Meric MP	N.A.	N.A.
EBA-NCPE8019	EBA	NCPE 8019	Borealis	7.5	924
HDPE-BM	HDPE	N.A.	Esso Chemical Canada	0.3	960

* Measured at 190°C
† Measured at 230°C
‡ Measured at 300°C
N.A. Not available

Table 3.3 Zero-shear viscosity for polyethylene resins

Resin	Viscosity (Pa.s)		
	at 170°C	at 180°C	at 190°C
HD-8661	8539	8308	8058
LL-8461	3333	2110	1535
LL-8556	1962	1040	945
EBA-NCPE8019	3301	N.A.	2524
HDPE-BM	50000	N.A.	N.A.

N.A. Not available

Table 3.4 Zero-shear viscosity for polypropylene resins

Resin	Viscosity (Pa.s)		
	at 190°C	at 210°C	at 230°C
PP-SC1355RM	2654	1879	1067
PP-MT4390HU	1639	1026	674
PP-TR121	3424	2208	1388

Table 3.5 Zero-shear viscosity for polycarbonate and polyvinyl chloride resins

Resin	Viscosity (Pa.s)					
	at 170°C	at 180°C	at 190°C	at 200°C	at 220°C	at 235°C
PC-Makrolon	N.A.	N.A.	N.A.	67811	15723	7853
PVC-1	86142	23036	4885	N.A.	N.A.	N.A.

N.A. Not available

Table 3.6 Thermal properties and composition of the resins

Resin	Copolymer content (% mole)	Melting Temperature (°C)	Crystallinity (%)
HD-8661	N.A.	120.0	50.3
LL-8461	N.A.	120.0	42.0
LL-8556	N.A.	118.0	41.5
PP-SC1355RM	11.0	164.4	47.6
PP-MT4390HU	14.6	164.8	40.8
PP-TR121	16.7	164.1	40.3
PC-Makrolon	N.A.	148.6*	N.A.
PVC-1	N.A.	120.0* 174.0	N.A.
EBA-NCPE8019	17.0	98.0	10.4
HDPE-BM	N.A.	123.0	65.7

N.A. Not applicable
* Glass transition temperature

The compositions of the micropellet resins HD-8660, LL-8460 and LL-8555 are the same as their respective powder resin HD-8661, LL-8461 and LL-8556. However, micropellet and powder resins have different thermal and shear histories, both of which may play an important role in rotational molding performance.

The cylindrical particle size varied from 300 to 800 μm. As received, the powder and micropellet particles ranged in size from 75 to 600 μm and from 800 to 900 μm, respectively. However, for sintering experiments, the powder particle size distribution was narrowed between 250 to 600 μm using sieve analysis.

3.3 Results and discussion

The sintering experiments were conducted above the melting points of the resins used. The initial particle size and contact is measured at temperatures below the resin melting point for semi-crystalline resins and below the glass transition temperature for amorphous resins. The results shown start at 30 seconds because at shorter times the temperature of the system could not be stabilized at the desired sintering temperature. The coalescence is considered completed when the dimensionless neck radius y/a is equal to 1. For powder resins, the standard deviation of the dimensionless neck radius can get as high as 0.07. However, for sintering times larger than 30 seconds the standard deviation of the dimensionless neck radius measurement lies between 0.01 and 0.03. Fluctuations in the results are principally due to variations in the particle size and shape. The reproducibility of experimental results was good for all resins used in this study except for resin PP-TR121. The result fluctuations for resin PP-TR121 are illustrated

in Figure 3.5. For each temperature, the sintering conditions were held constant and the particle size did not vary significantly. The high variance in the results obtained with resin PP-TR121 could be due to a non-uniform distribution of the copolymer.

3.3.1 Effects of polymer properties

Varying the average particle diameter and keeping a constant size ratio between the two particles, experiments were performed with resins presented in Table 3.1. It is of primary importance to determine the extent to which the particle size affects the sintering rate for further comparisons. Mathematical models based on purely viscous flow mechanism (Frenkel, 1945, Hopper, 1984, 1989, 1990) predict an increase in sintering rate that is proportional to the decrease in particle size. This result is expected since in those models, the energy dissipated by viscous flow, the resistance to the coalescence, is only balanced by the work from surface tension force, the driving force of the sintering process. The viscous dissipation occurs over the volume of the sintering particles, while the surface tension is only acting on the surface of the sintering system.

Results for the resin LL-8556 show that the sintering rate is not significantly affected by a reduction of the particle size except in the beginning of the coalescence (Figure 3.6). The effect of the particle size on the initial sintering rate is more pronounced for the resin LL-8461 as shown in Figure 3.7.

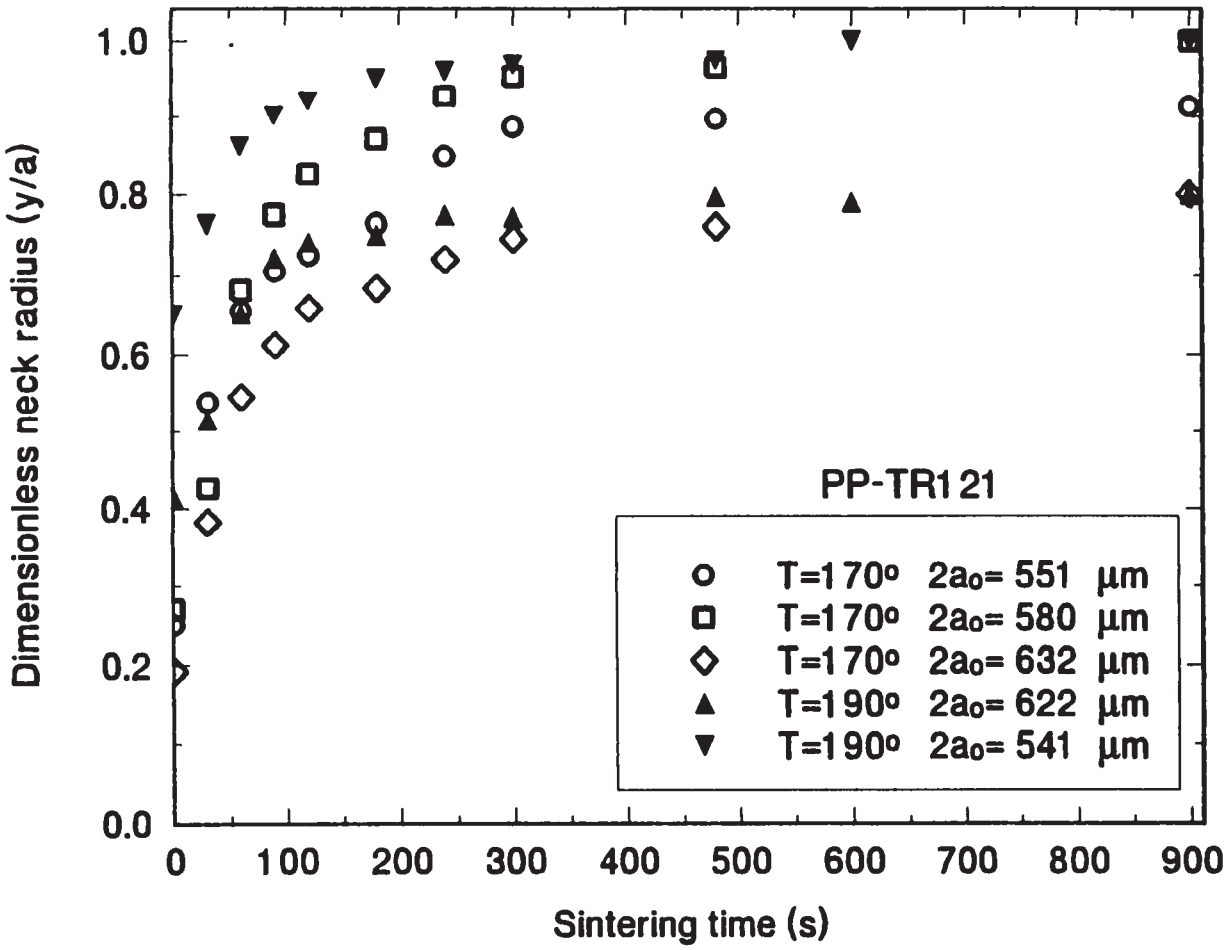

Figure 3.5 Sintering dimensionless neck growth (unprocessed data) of PP-TR121 powder particles at170°C and 190°C.

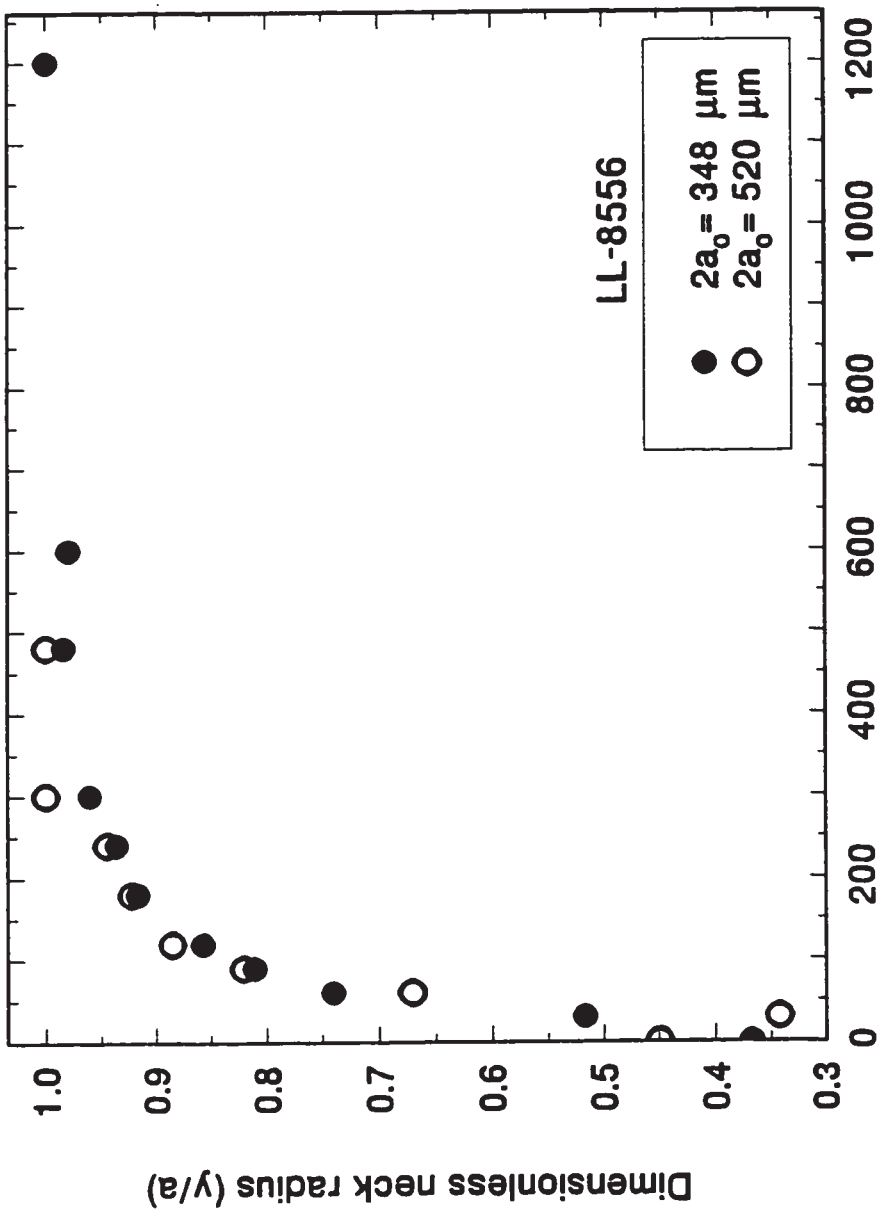

Figure 3.6 Sintering dimensionless neck growth for LL-8556 powder particles at 130°C.

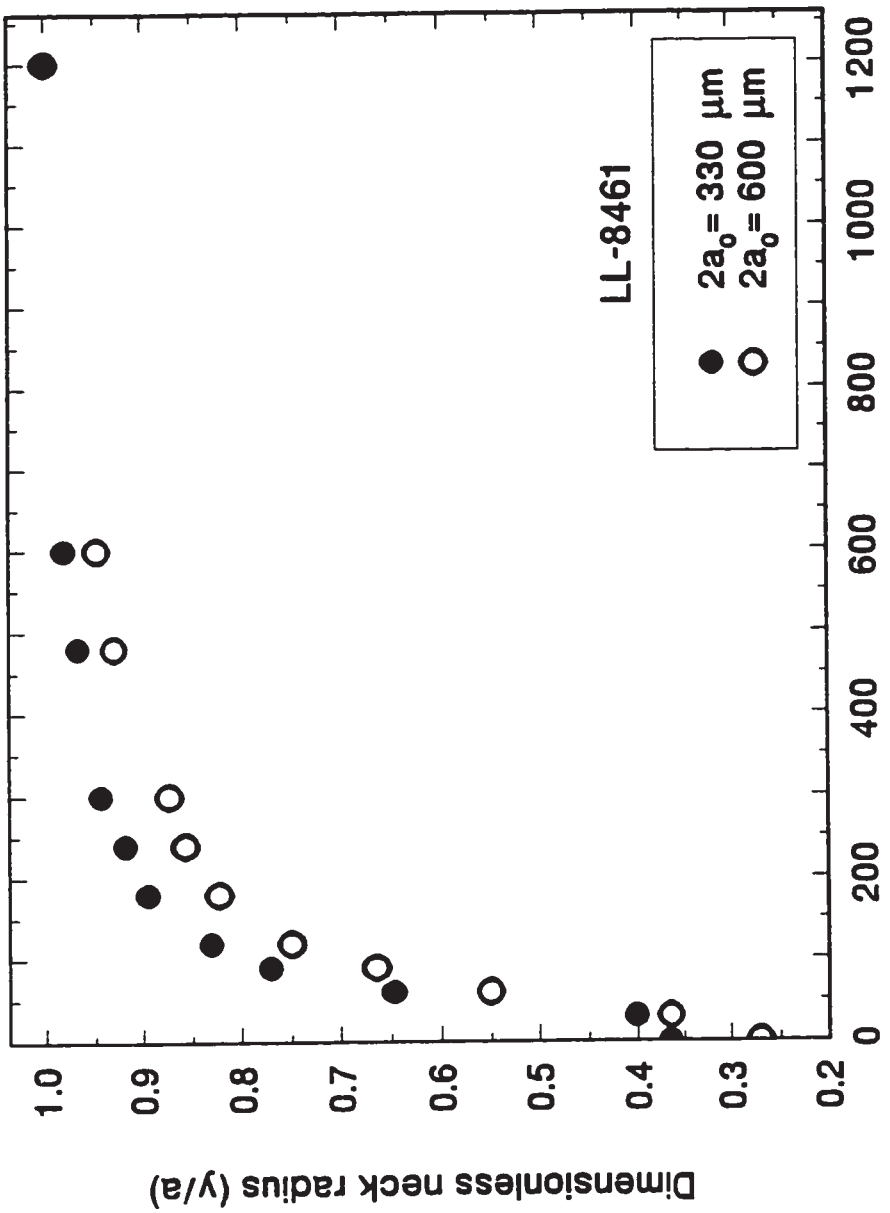

Figure 3.7 Sintering dimensionless neck growth for LL-8461 powder particles at 130°C.

For resins HD-8661 and PP-SC1355RM, it was found that the sintering rate and the time required to complete the coalescence were substantially dependent on the particle size (Figures 3.8 and 3.9). The results for HD-8661 and PP-SC1355RM appear to agree fully with the prediction of the mathematical models, but for the case of LL-8556 there is hardly any evidence of dependence of sintering rate on particle size. It is envisioned that forces other than purely viscous forces may be important in the sintering system.

Figure 3.10 shows the sintering times for the resins LL-8556 and HD-8661, in powder form and for identical sintering conditions (130°C). It was reported (Table 3.2) that the resin HD-8661 has a higher viscosity than resin LL-8556. The sintering times (Figure 3.10) are compared for these two resins and for two sizes of particles (352 ± 4 μm and 524 ± 4 μm). As expected, the sintering rate was found to increase when the zero shear viscosity decreases. It appears that the effect of the viscosity on the sintering rate is enhanced as the particle size increases for these resins.

Observations from rotational molding experiments have been reported for the polypropylene copolymers. Although the viscosity of resin PP-TR121 is within acceptable range for polypropylene, rotationally molded parts produced with this resin have a high porosity (Kontopoulou, 1995). Moreover, it was shown that although resin PP-MT4390HU has a lower viscosity than resin PP-SC1355RM, it produces rotationally molded parts with higher bubble content (Kontopoulou, 1995, Kontopoulou, 1997 (a)). This result has been correlated with the polyethylene content of the copolymer, which is believed to affect the elasticity of the resin (Kontopoulou, 1995).

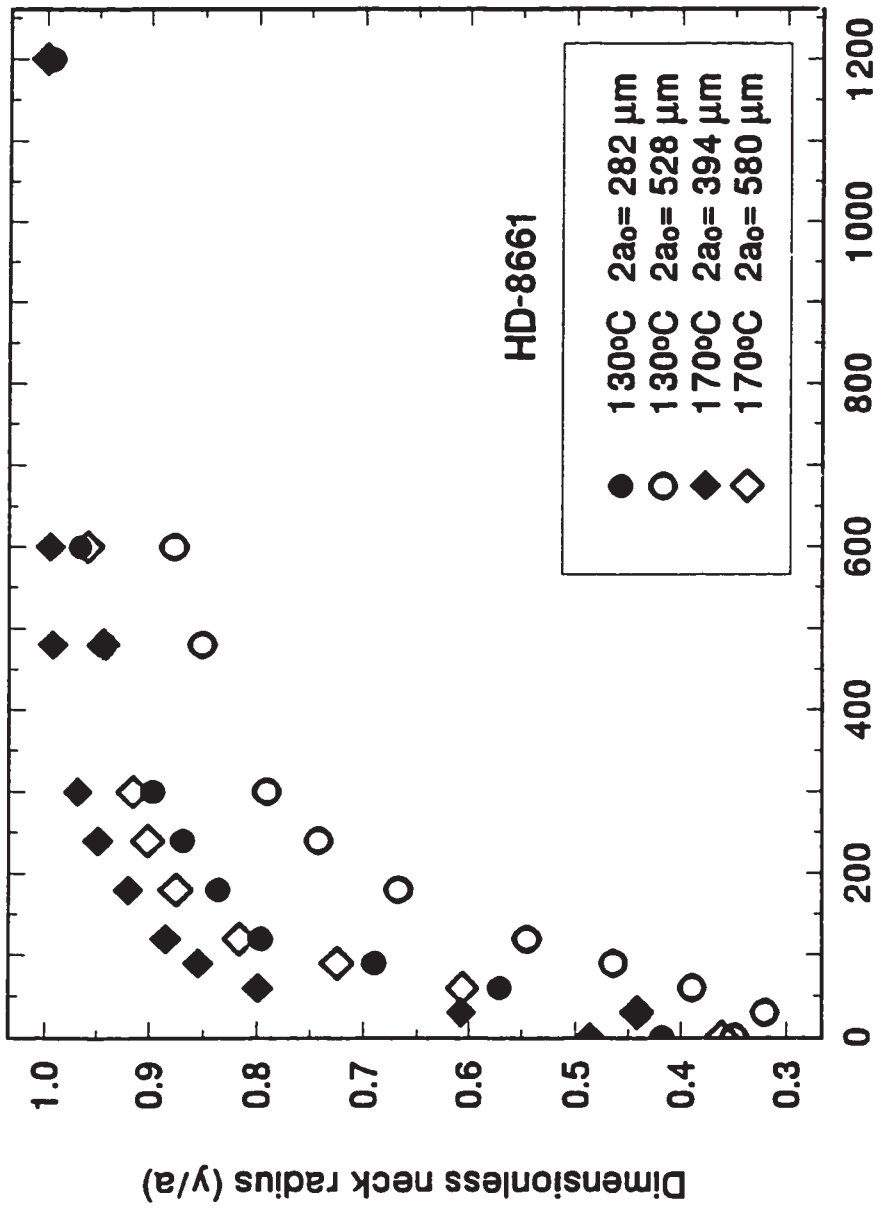

Figure 3.8 Sintering dimensionless neck growth for HD-8661 powder particles at 130°C and 170°C.

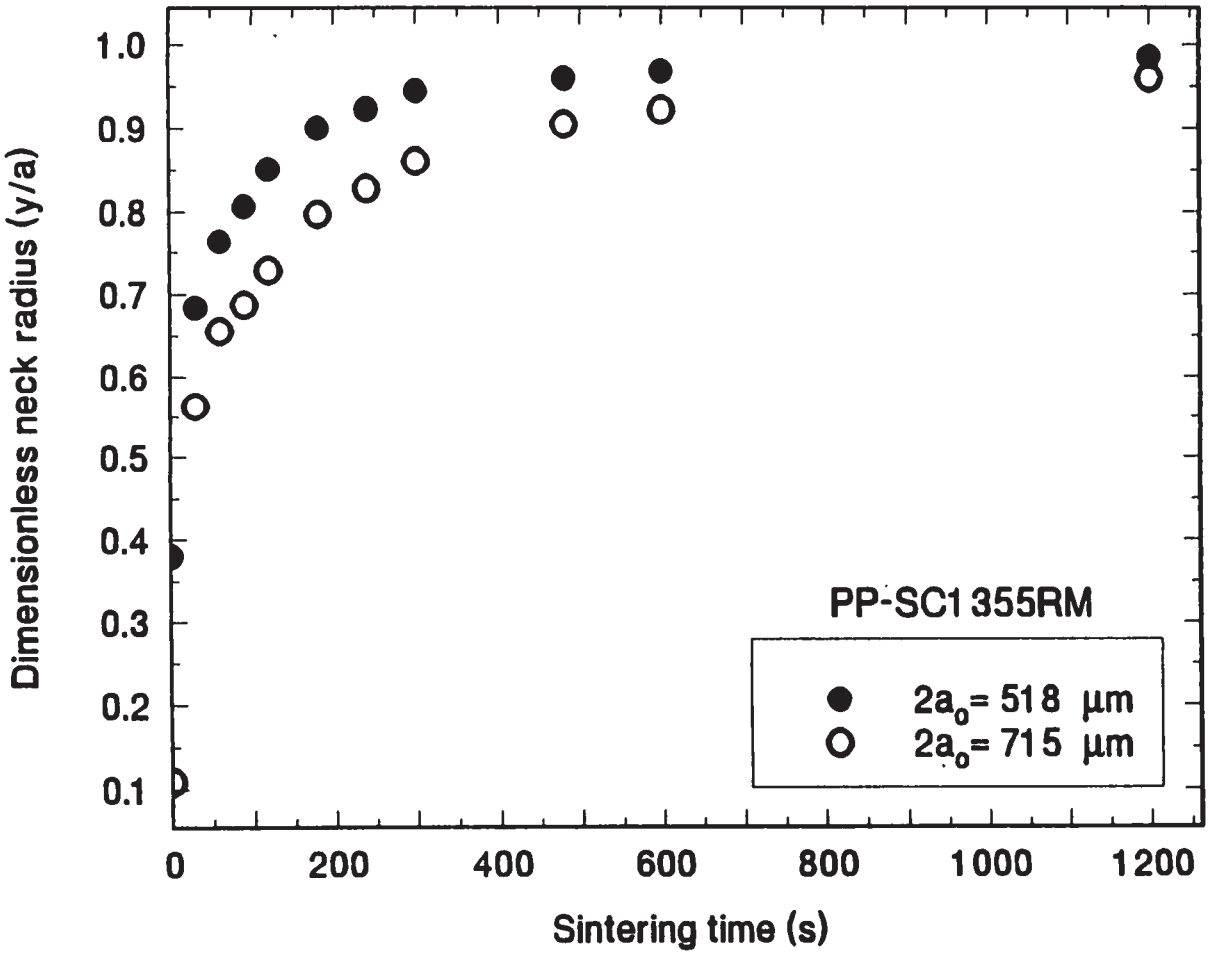

Figure 3.9 Sintering dimensionless neck growth for PP-SC1355RM cylindrical particles at 190°C.

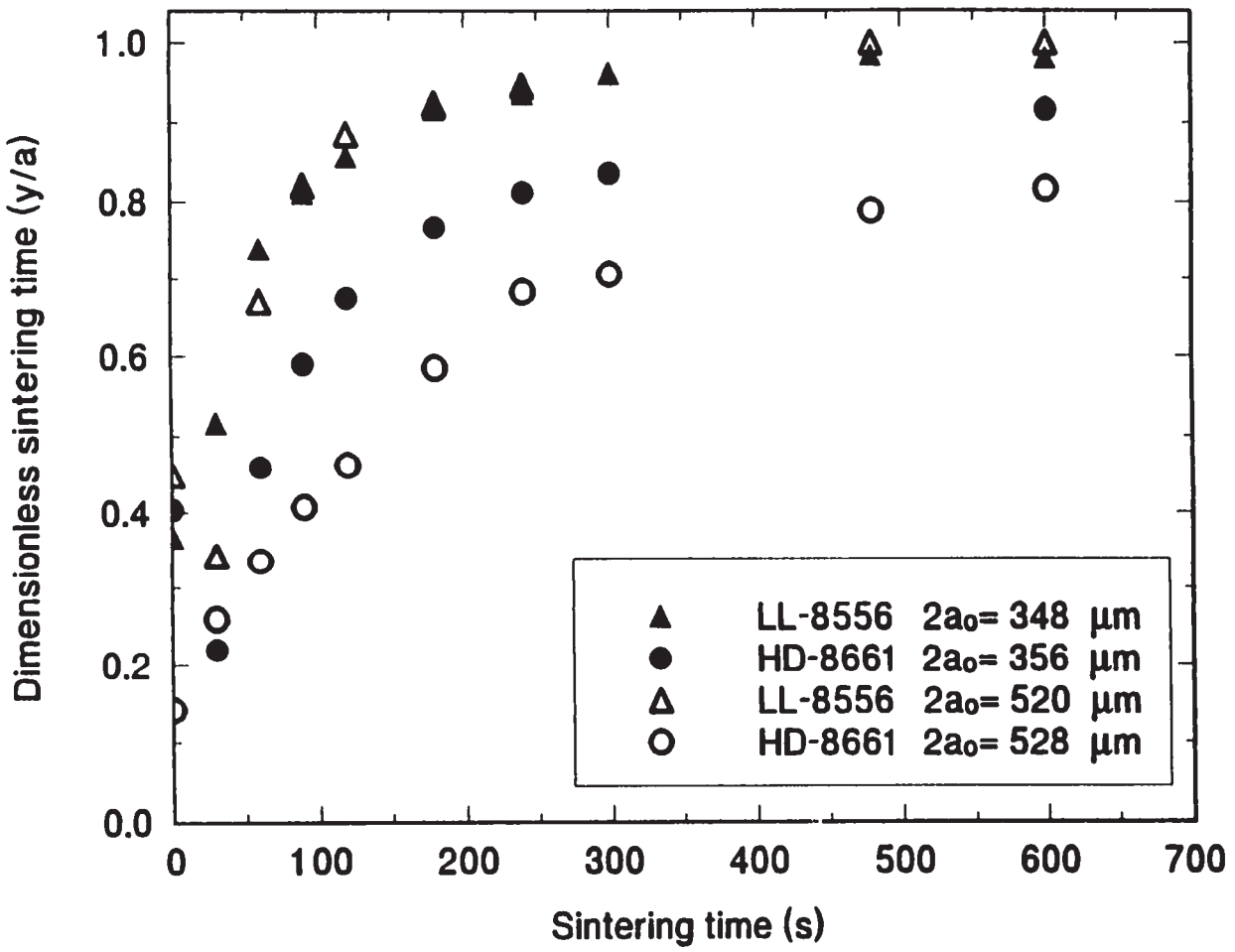

Figure 3.10 Sintering dimensionless neck growth for resins LL-8561 and HD-8661 powder particles at 130°C.

The elastic character of a resin is mostly related with its molecular weight distribution and the molecular architecture (Tuminello, 1990). The high variability of the sintering results obtained with resin PP-TR121 (Figure 3.5) corroborates the observations from the rotational molding experiments. However, as shown in Figure 3.11, no significant difference in the sintering neck growth is observed for resins PP-SC1355RM and PP-MT4390HU. Figure 3.12 presents the sintering sequence for resin PP-MT4390HU. The interface between the particles, represented by the shadow seen between the two particles, vanishes only in the very late stage of sintering. A similar observation has been reported for resin PP-TR121 (Kontopoulou, 1995). The long time required for the interface to vanish could be due to a slow molecular inter-diffusion at the interface between the particles, and this phenomenon would be consistent with observations in rotational molding experiments.

The sintering sequences for resins HD-8661 and HDPE-BM (both at 170°C) are presented in Figures 3.13 and 3.14, respectively. In the case of resin HD-8661, as the polymer melts, the surfaces of the particles become smooth and the contours become circular, and the coalescence is completed after 600 seconds. This description represents a typical sintering sequence for rotational molding grade resin. However, in the case of resin HDPE-BM, which has a very high viscosity (50000 Pa.s at 170°C), as the particles melt, the change in their shape is significant but does not lead to the formation of circular particle contours. The deformations of the particles as they melt may be due to some stress release.

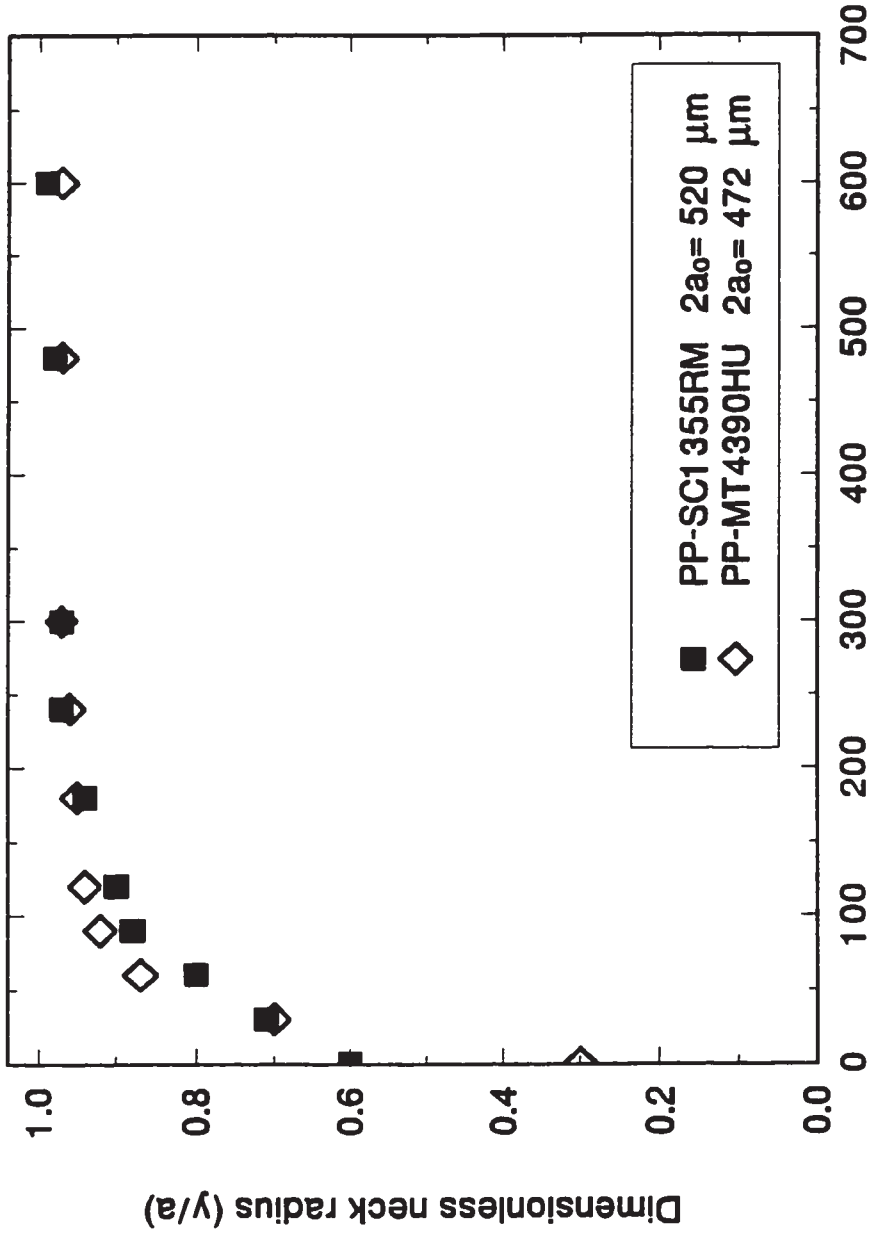

Figure 3.11 Sintering dimensionless neck growth for resins PP-SC1355RM and PP-MT4390HU powder particles at 190°C.

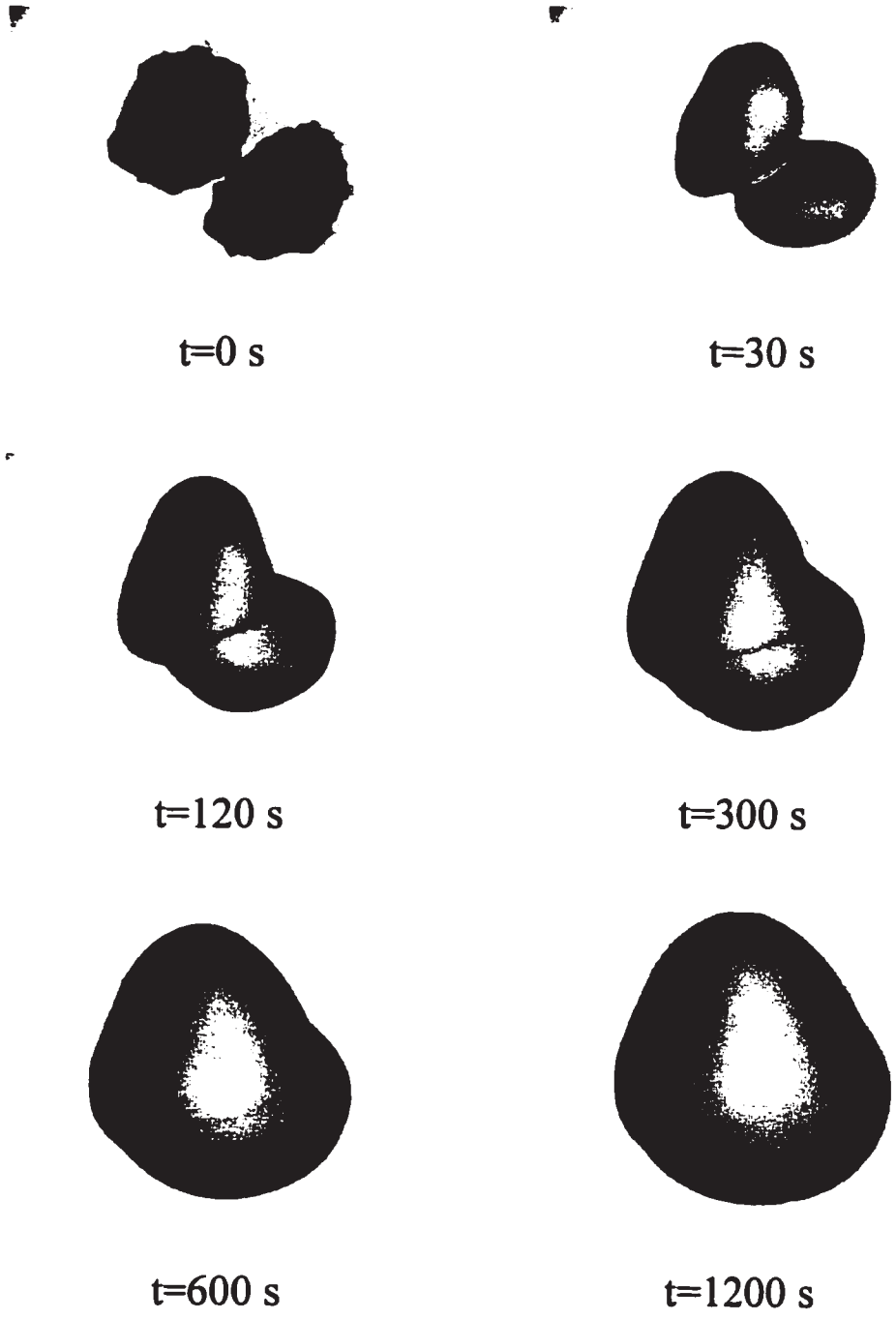

Figure 3.12 Sintering sequence for PP-MT4390HU powder particles at 190°C.

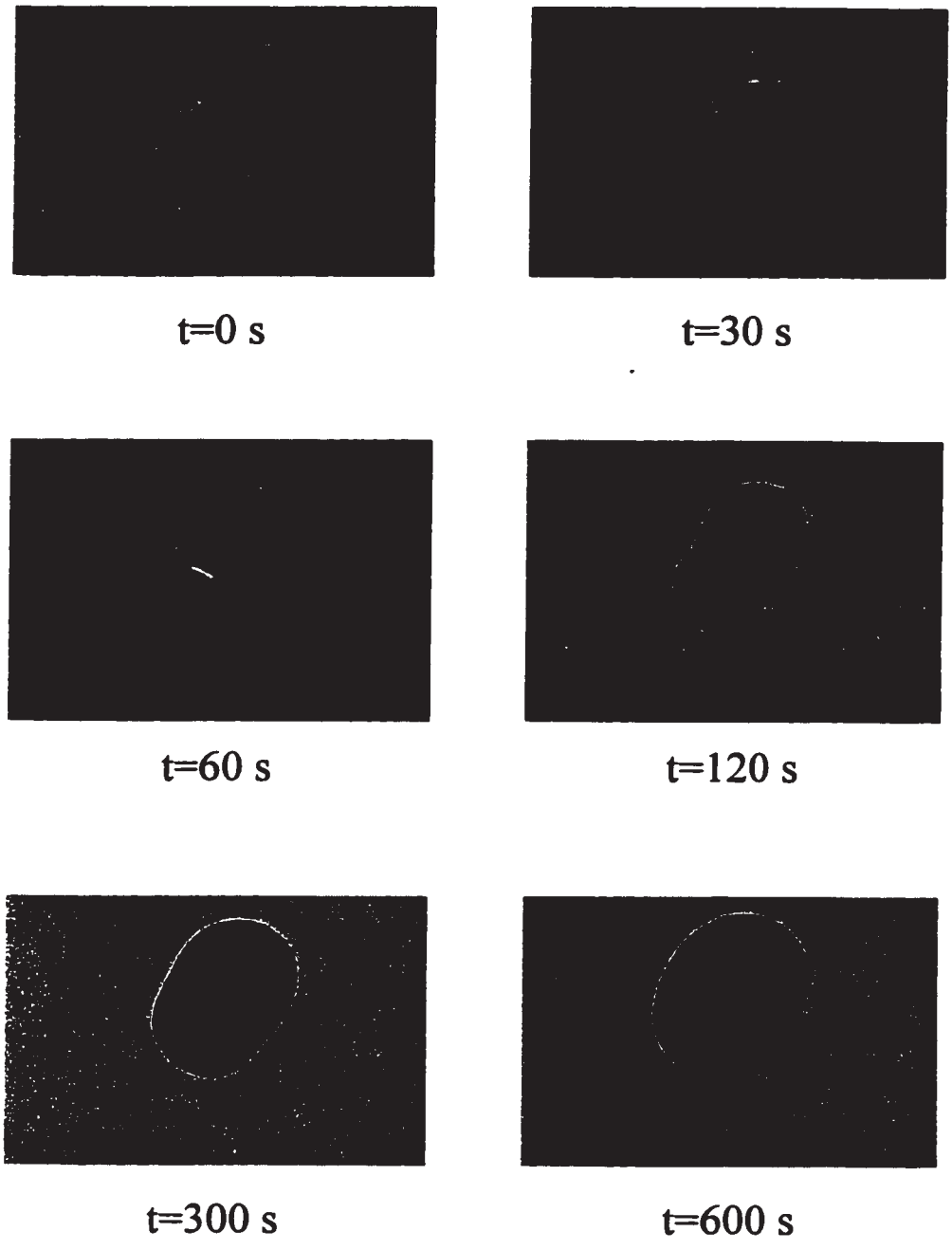

Figure 3.13 Sintering sequence for HD-8661 powder particles at 170°C.

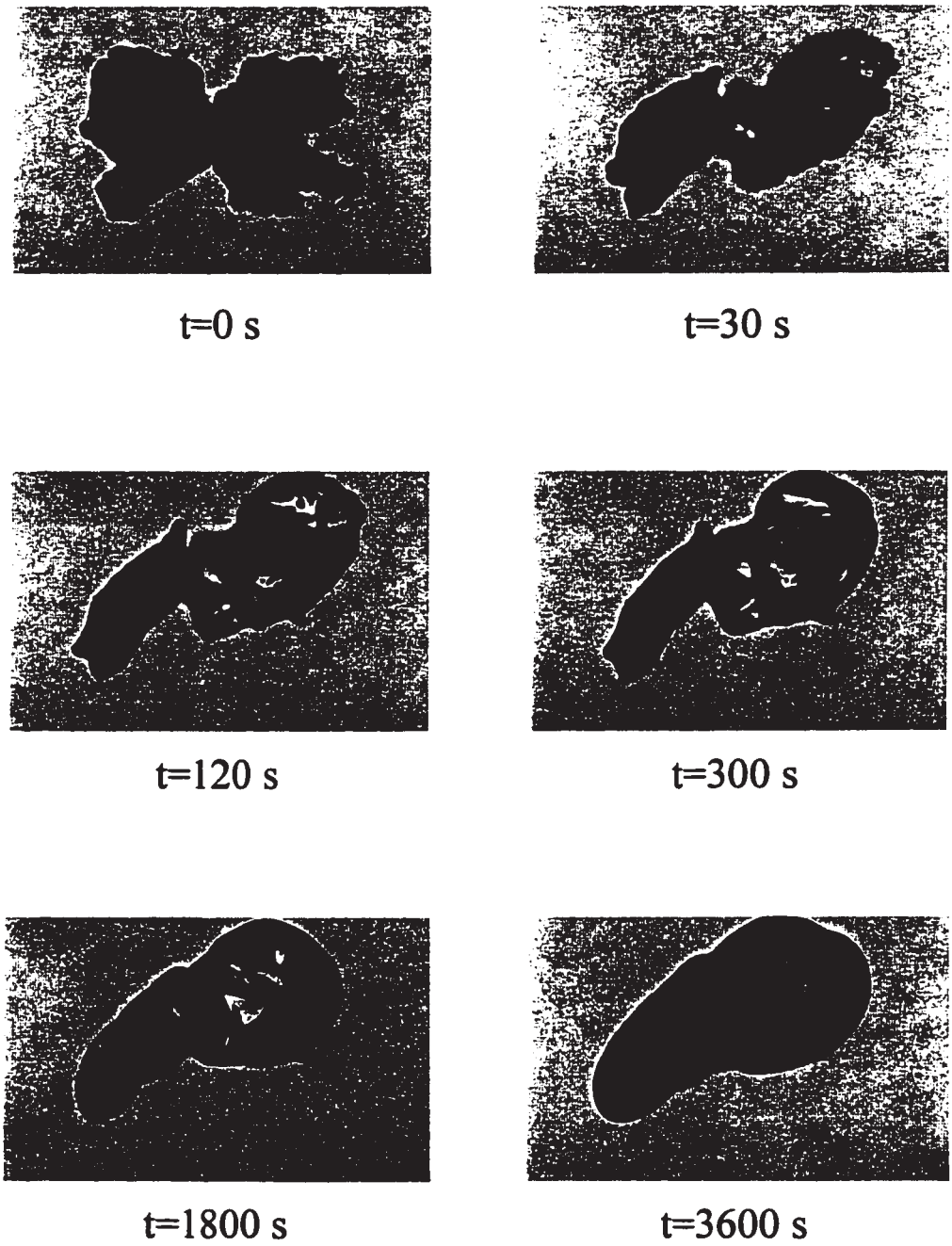

Figure 3.14 Sintering sequence for HDPE-BM powder particles at 170°C.

The sintering rate for this blow molding resin is extremely low, and the particles coalesce very slowly as confirmed also by extremely underfused (porous) rotationally molded parts which were obtained in a parallel study of the rotomoldability of this resin in a uniaxial machine (Bisaria *et al.*, 1994).

The sintering neck growth for the ethylene butyl acrylate resin has been studied. Figure 3.15 presents the results obtained with resins EBA-NCPE8019 and LL-8461. The sintering temperature profile was identical for both resins and is presented in Figure 3.4. It can be seen that resin EBA-NCPE8019 sinters at a lower rate than resin LL-8461, although it has similar viscosity (Table 3.2). As for the polypropylene copolymer resins used in this study, rheological measurements have shown that for resin EBA-NCPE8019, a longer time is required for the stress to relax in a stress relaxation experiment than for resin LL-8461 (Kontopoulou *et al.*, 1997 (b)). This result suggests that the increased melt elasticity due to the presence of the copolymer may affect the sintering rate.

The sintering of amorphous polymers, polycarbonate and polyvinyl chloride, have been considered. Figures 3.16 and 3.17 present the sintering neck growth for resins PC-Makrolon and PVC-1, respectively. The coalescence of the PC-Makrolon starts only after a delay of a few minutes during the heating cycle (Figure 3.16). The viscosity of both PVC-1 and PC-Makrolon resins is highly temperature dependent. The sharp increase in the sintering rate for the PC-Makrolon resin occurs when the sintering temperature reaches 225°C. At this temperature the viscosity of the material has dropped below 15000 Pa.s (Table 3.4).

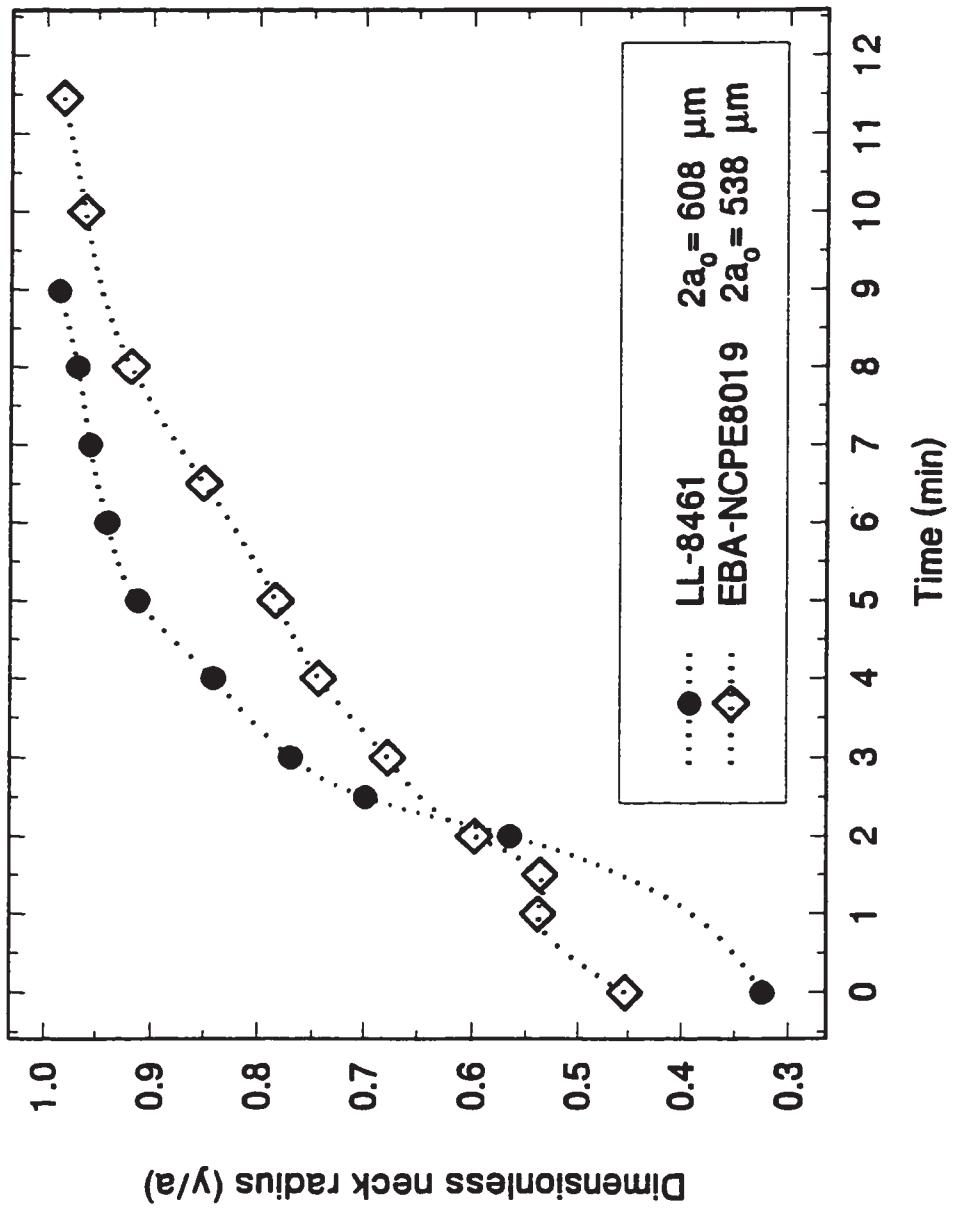

Figure 3.15 Sintering dimensionless neck growth for resins LL-8461 and EBA-NCPE8019 powder particles with an initial sintering temperature T_o=111°C and a rate of temperature increase dT/dt=11°C/min.

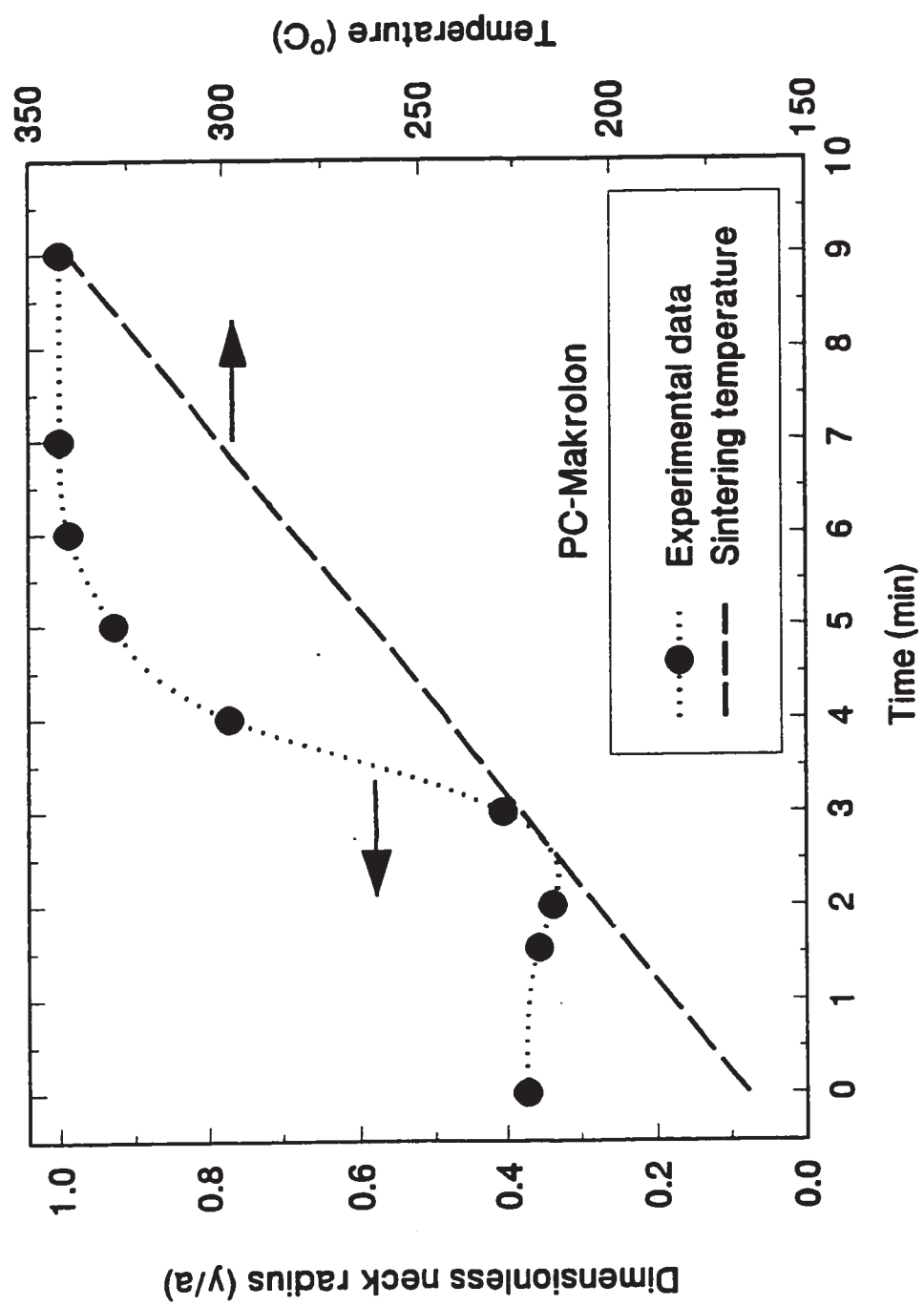

Figure 3.16 Sintering dimensionless neck growth for resin PC-Makrolon powder particles with an initial sintering temperature $T_o = 165°C$ and a rate of temperature increase $dT/dt = 19.4°C/min$.

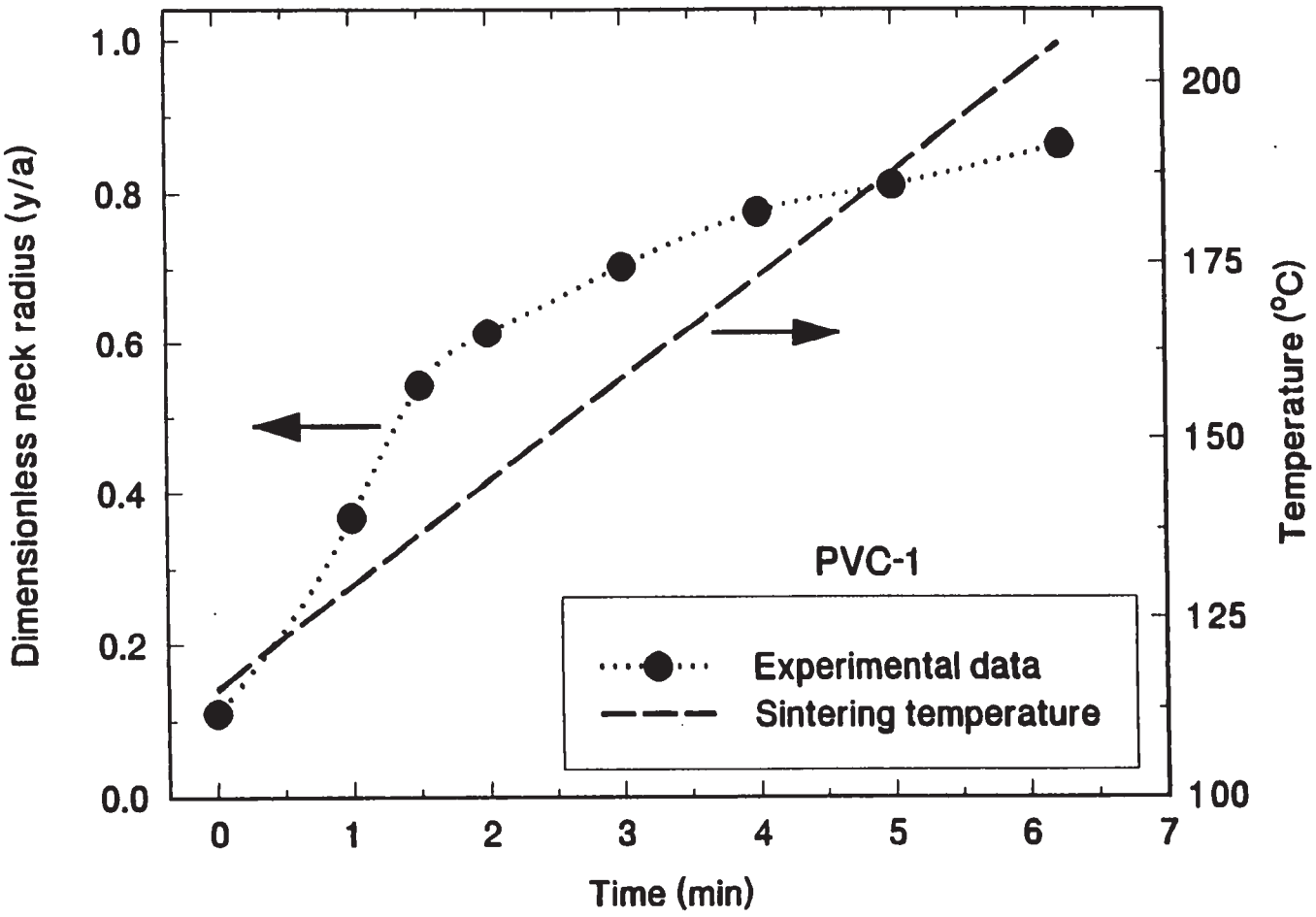

Figure 3.17 Sintering dimensionless neck growth for resin PVC-1 powder particles with an initial temperature $T_o = 115°C$ and a rate of temperature increase $dT/dt = 14.5°C/min$.

Figure 3.17 shows that PVC-1 resin sinters steadily at temperatures below 170°C, although the resin viscosity is higher than 80000 Pa.s (Table 3.4). The enhanced sinterability of PVC-1 resin could not be explained on the basis of surface tension forces counteracted by viscosity, unless special additives were included by the supplier. It is unknown whether any surface modifier was included. However, it has been shown that low energy additives, such as fluorocarbons used as plasticizer for PVC resins, greatly lower the surface tension of polymer melt (Jarvis *et al.*, 1964). Further investigations would require measurements of the surface tension.

The delay observed in the neck growth of the PC-Makrolon resin probably affects the final porosity of the rotationally molded parts. It is suggested that in the heating cycle, the powder particles of the PC-Makrolon resin will have time to adhere to each other, and air will be trapped in the melt before a significant neck growth occurs between the particles. Rotational molding experiments showed that molded parts from PC-Makrolon resin have a higher bubble content than those from PVC-1 resin (Kontopoulou *et al.*, 1997 (b)).

3.3.2 Effects of surface conditioning

Experiments have been performed on three different surfaces: (i) glass, (ii) glass covered with a thin layer of mineral oil, and (iii) glass covered with a polymeric film. Adhesion forces may arise between the sintering particles and the sintering surface. The effect of surface conditioning was investigated to evaluate the importance of these forces on the sintering rate.

In most of the mathematical representations of the sintering process the adhesion forces are neglected. In an attempt to minimize the adhesion and to promote slippage between the sintering particles and the glass surface, a thin layer of mineral oil was applied to the glass surface. Oil has been used by several authors as a lubricant in different applications such as compressing flow and squeezing flow of polymer melts, as reviewed by Macosko (1994). Resins PP-SC1355RM and EBA-NCPE8019 are used to evaluate the effect of adhesion forces on the sintering rate. Figures 3.18 and 3.19 show no significant difference between the sintering rate measured with a glass surface and a glass surface covered with mineral oil for resins PP-SC1355RM and EBA-NCPE8019, respectively. Teflon surface and glass surface covered with mold release agent were used and similar results were observed.

In rotational molding, molded parts are a few millimeters thick, while the particle diameter varies from 100 to 600 microns. Therefore, most of the particles sinter on a polymeric surface during the rotational molding process. To simulate this situation, powder particle sintering has been performed on a glass surface covered with a thin film of polymer. Adhesive bonding between the sintering particles may be greater on a polymeric surface than on a glass surface due to molecular diffusion at the interface. Figure 3.20 shows that small particles sinter at a lower rate on a polymeric surface than on a glass surface for resin LL-8461. .This effect vanishes for large particles (Figure 3.20). However, as presented in Figure 3.21, there is no significant difference between the sintering results obtained with a glass surface and a polymeric surface for resin HD-8661.

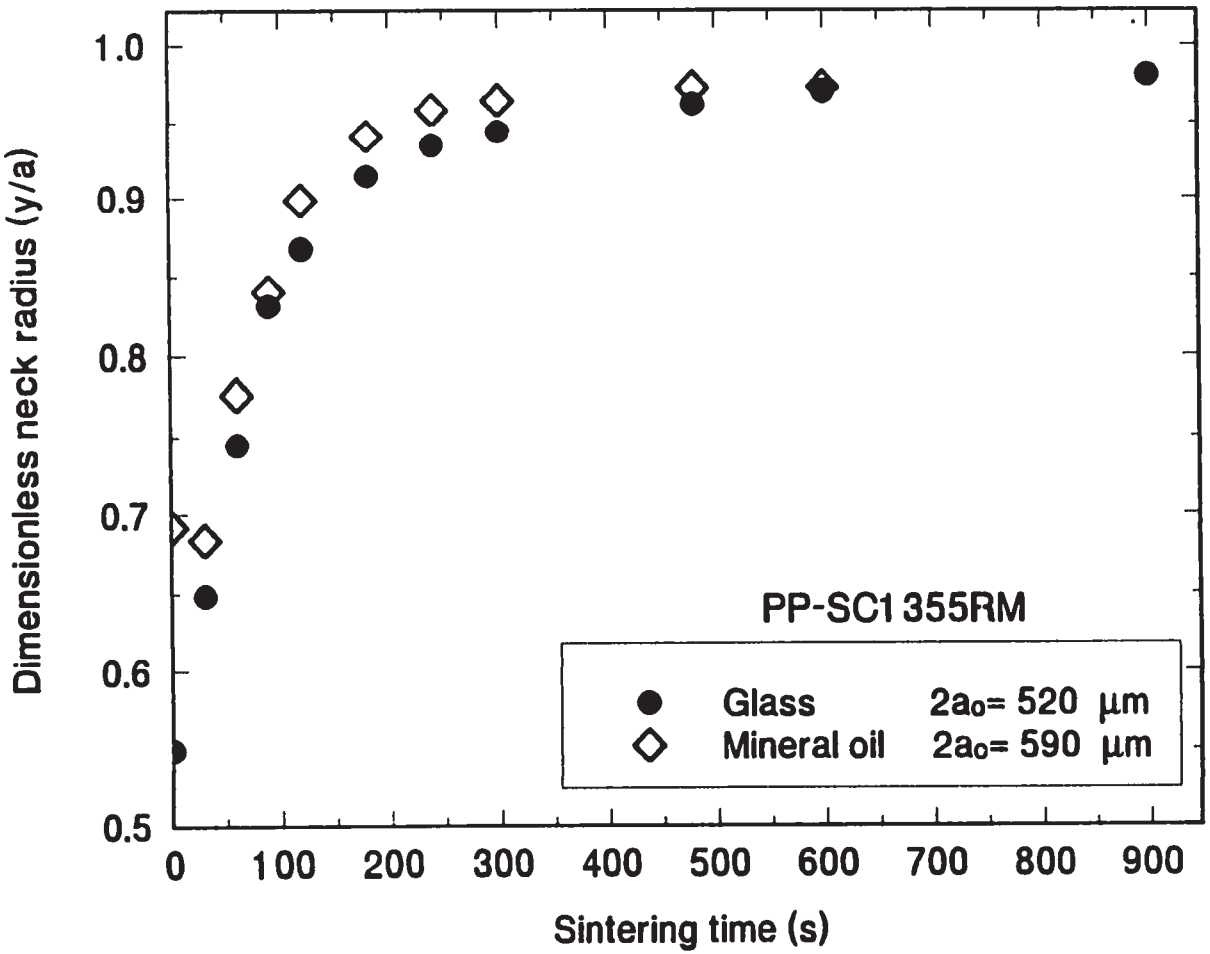

Figure 3.18 Sintering of PP-SC1355RM powder particles on a glass surface and glass surface covered with thin film of mineral oil, at 190°C .

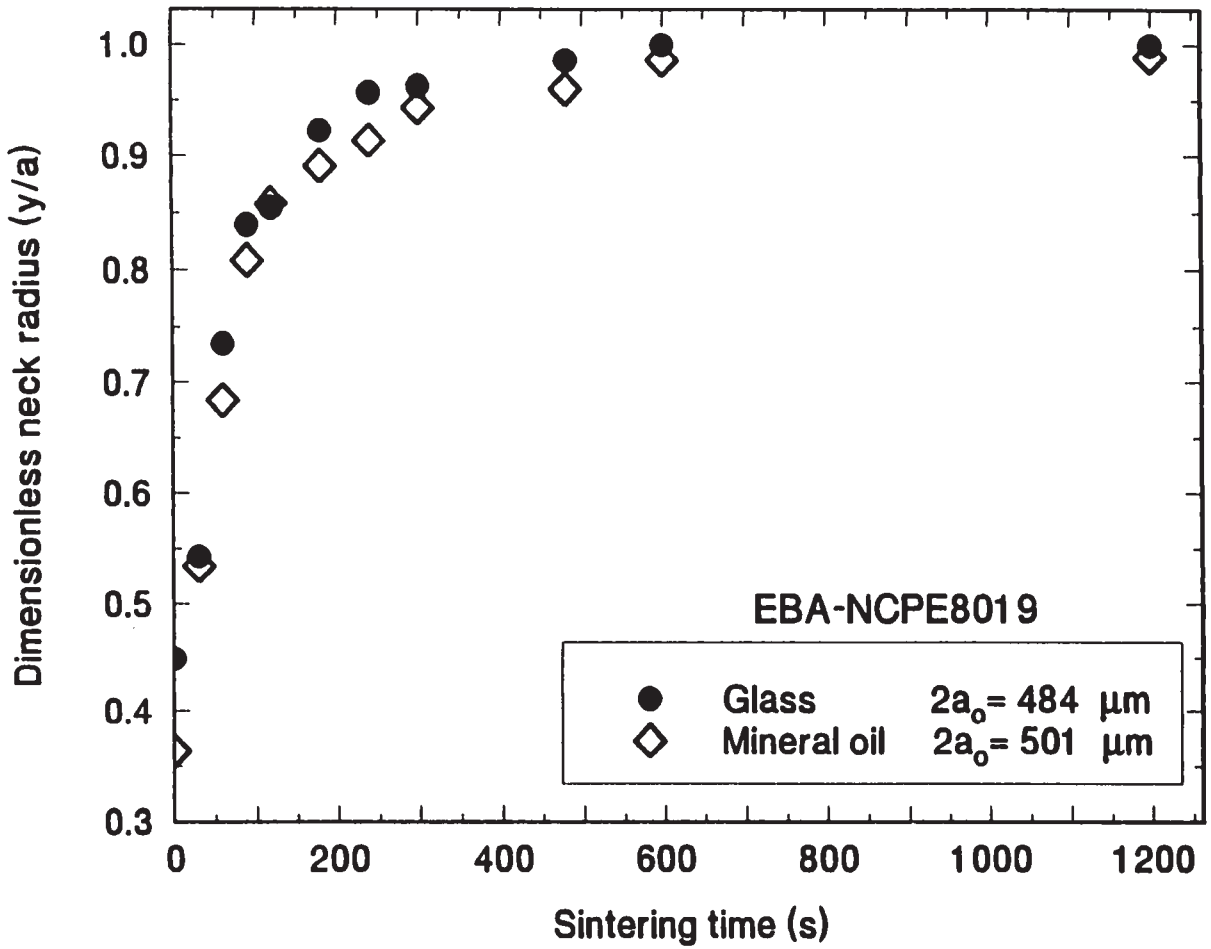

Figure 3.19 Sintering of EBA-NCP8019 powder particles on a glass surface and glass surface covered with thin layer of mineral oil, at 170°C.

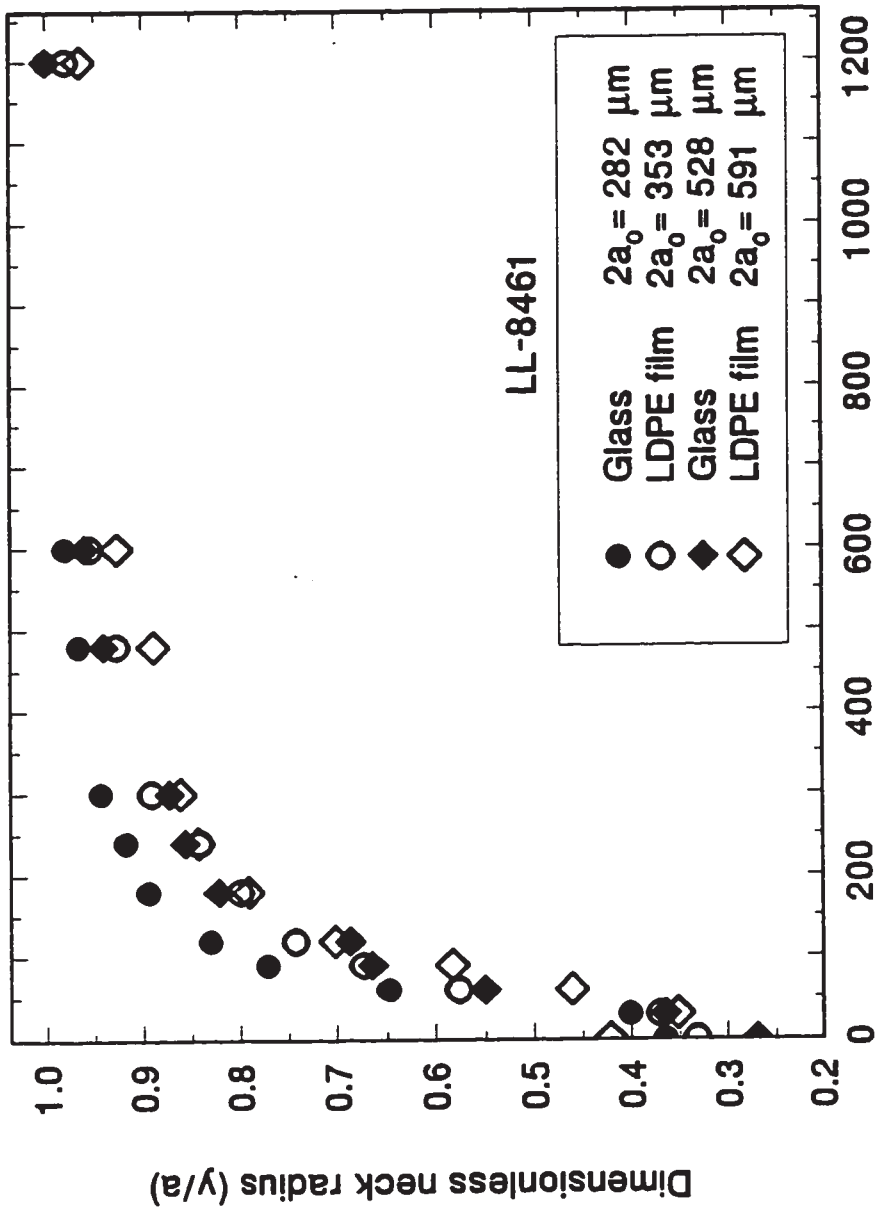

Figure 3.20 Sintering of LL-8461 powder particles on glass surface and on LDPE film surface, at 130°C.

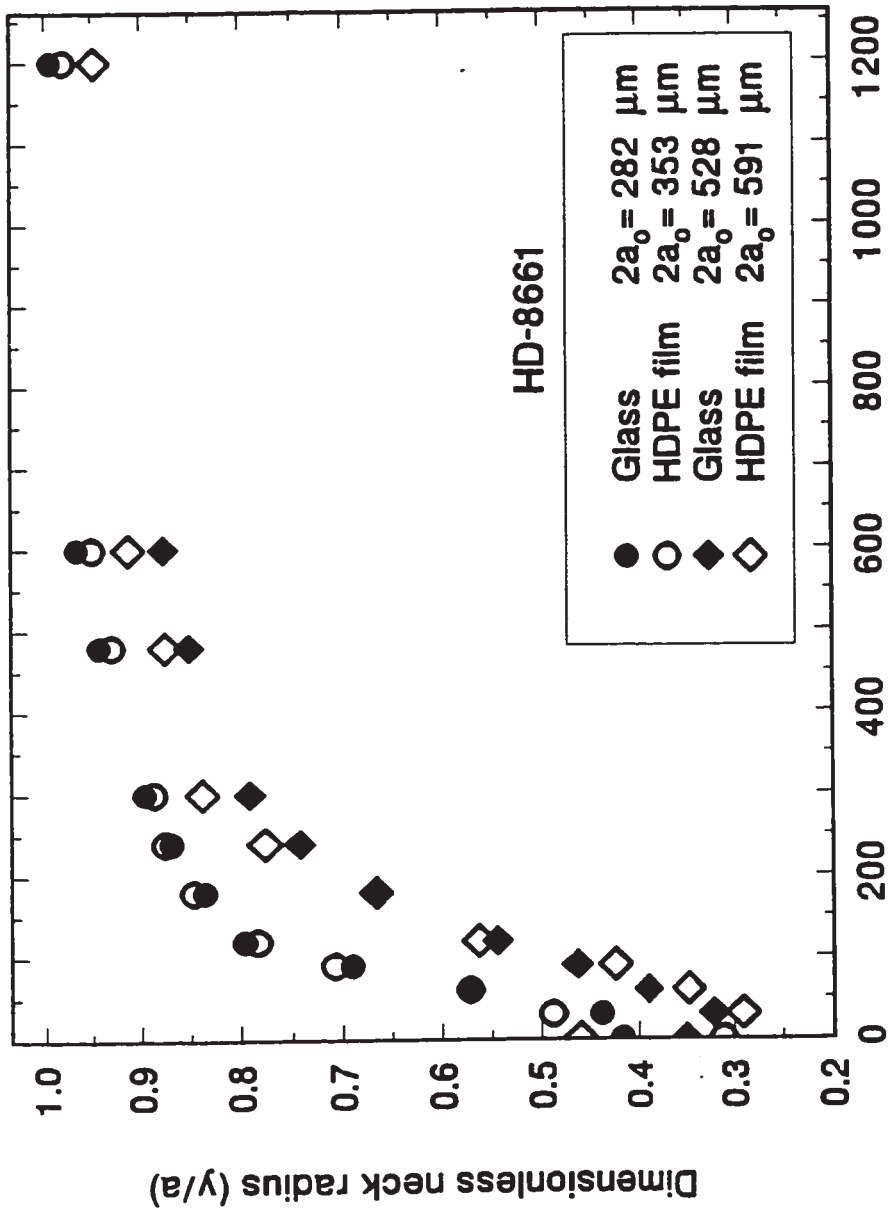

Figure 3.21 Sintering of HD-8661 powder particles on glass surface and on HDPE film surface, at 130°C.

3.3.3 Effects of particle geometry

Commercial rotational molding powders are produced by pulverizing (grinding) polymer pellets. Powder particles have irregular shapes and a particle size distribution. For comparison purposes, powder particles are represented as simple geometric shapes. In the current work, the effect of particle geometry has been studied with two LLDPE resins (LL-8461, LL-8556), one HDPE resin (HD-8661), and one polypropylene copolymer (PP-SC1355RM). For all resins used, it was found that powder and cylindrical particles of comparable diameter sinter in a similar way except in the beginning of the coalescence for resins LL-8461 and HD-8661 (Figures 3.22 to 3.25). It is shown in Figures 3.23 and 3.24 that in the first 200 seconds the cylindrical particles coalesce somewhat faster than the powder particles. This phenomenon is probably due to the differences in the shear and thermal histories between the powder and cylindrical particles rather than the difference in the particle geometry. It is expected that the theoretical sintering models developed for cylindrical particles may also be applicable to powder.

The micropellet particles supplied by Esso Chemical Canada are geometrically very similar to the regular cylindrical particles produced in our laboratories. Due to their regular geometry, micropellets have better flow properties than powder particles. This characteristic has a significant effect on the thickness uniformity of molded parts and the mold filling for complex geometry (Takács *et al.*, 1996). Experimental results for powder and cylinder resin LL-8556 and micropellet resin LL-8555 are presented in Figure 3.26.

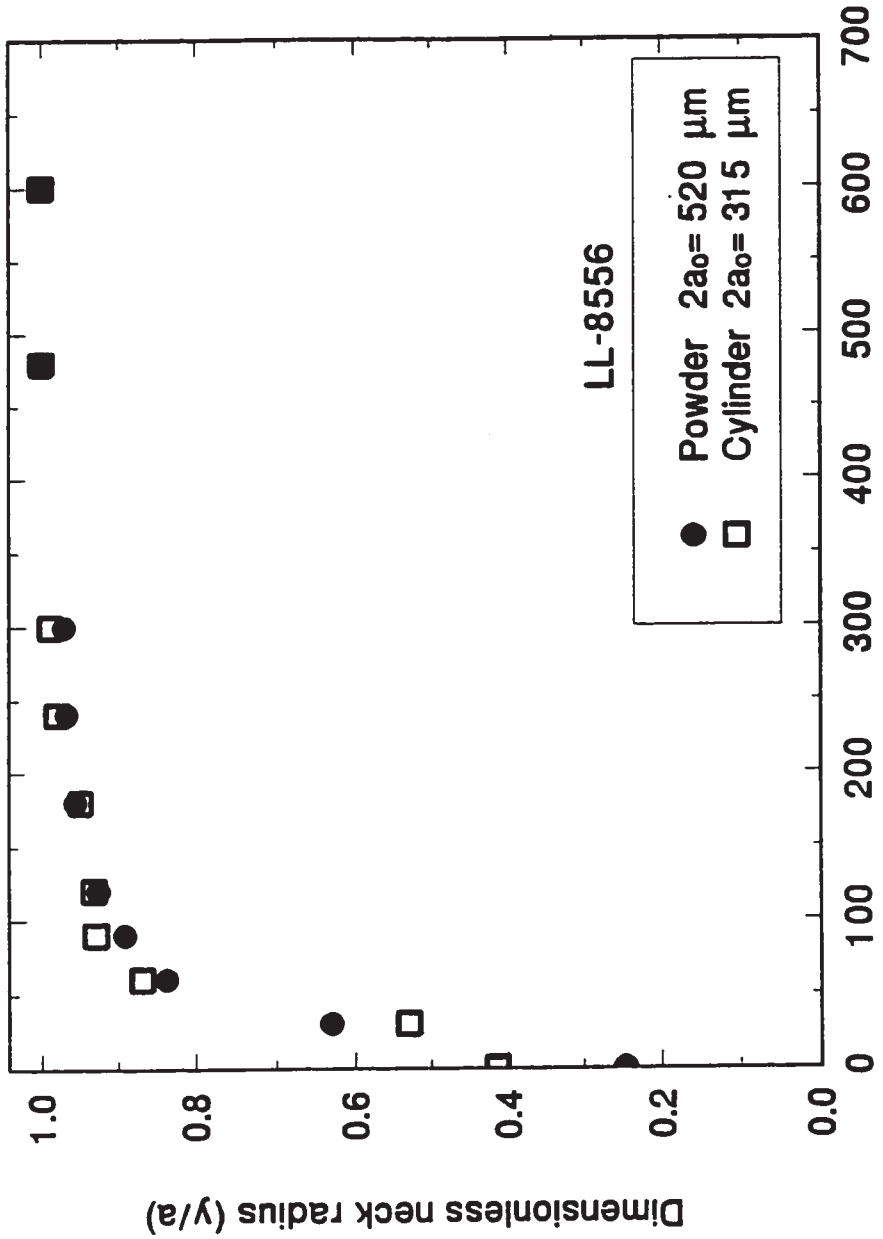

Figure 3.22 Sintering of LL-8556 powder and cylindrical particles at 130°C.

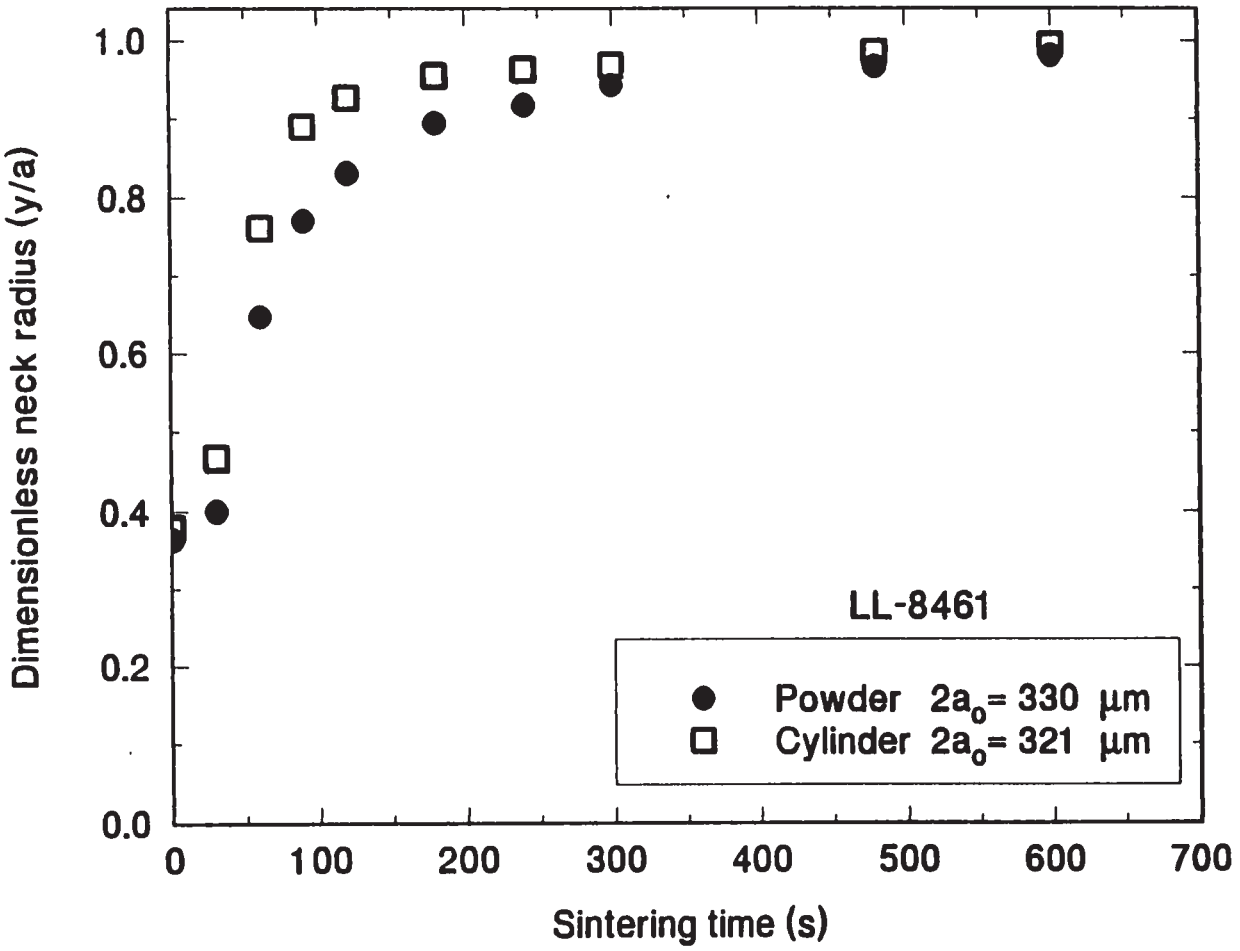

Figure 3.23 Sintering of LL-8461 powder and cylindrical particles at 130°C.

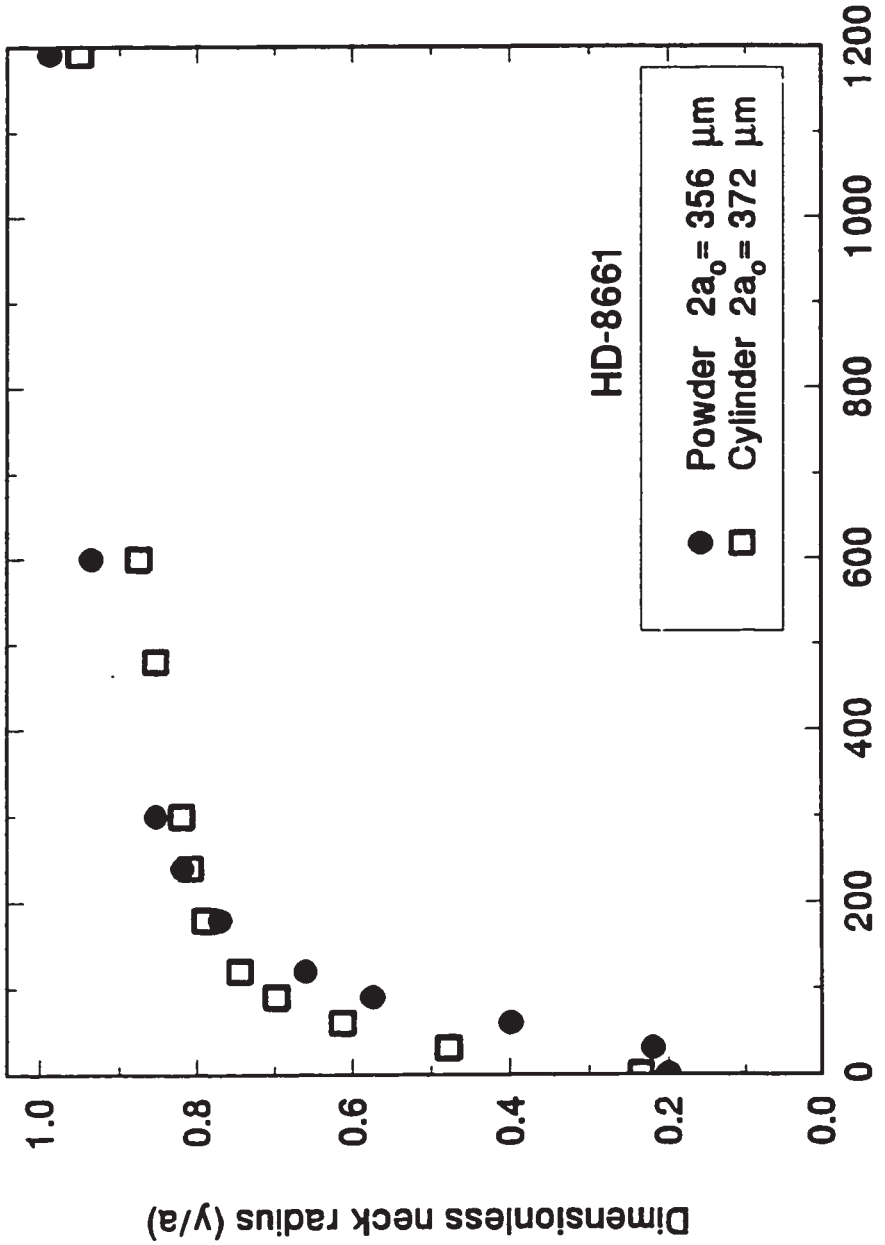

Figure 3.24 Sintering of HD-8661 powder and cylincrical particles at 130°C.

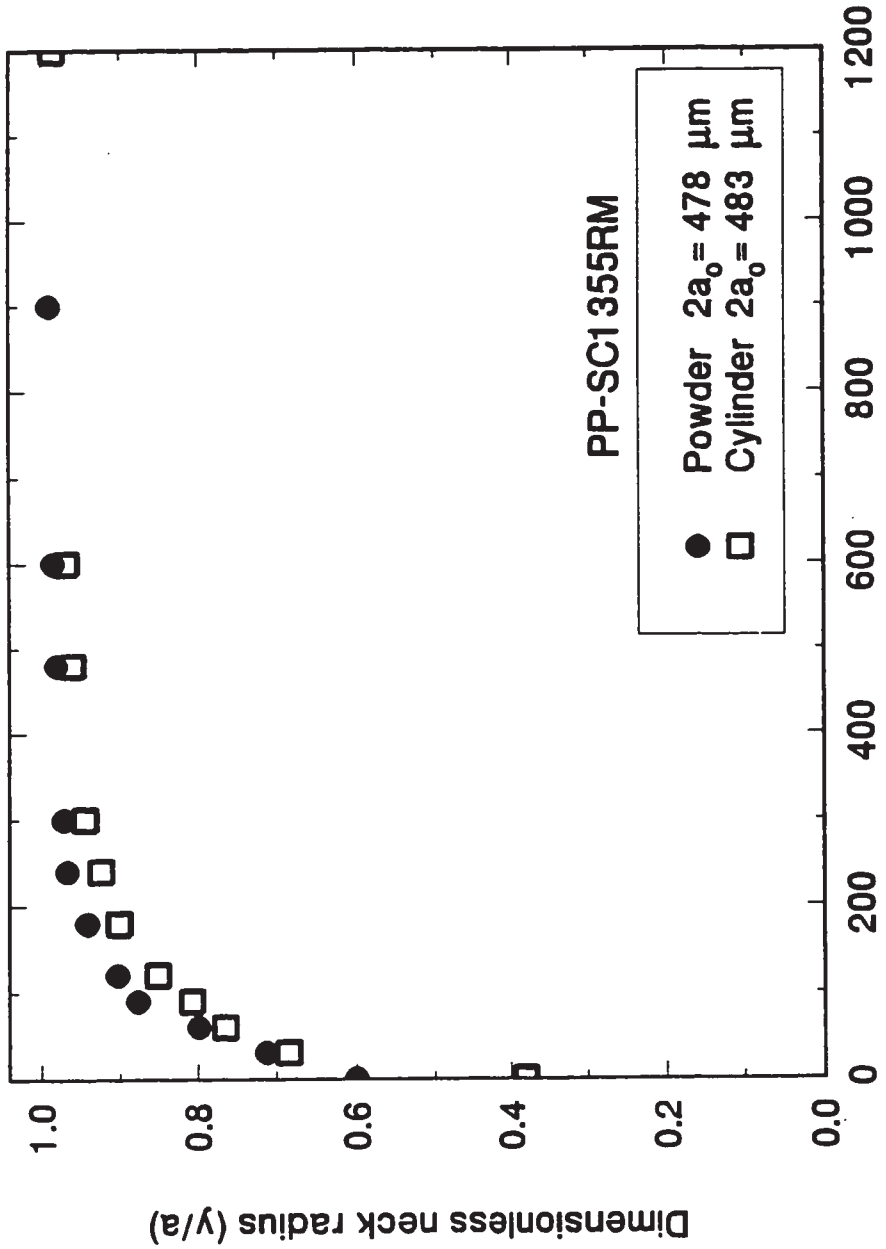

Figure 3.25 Sintering of PP-SC1355RM powder and cylindrical particles at 190°C.

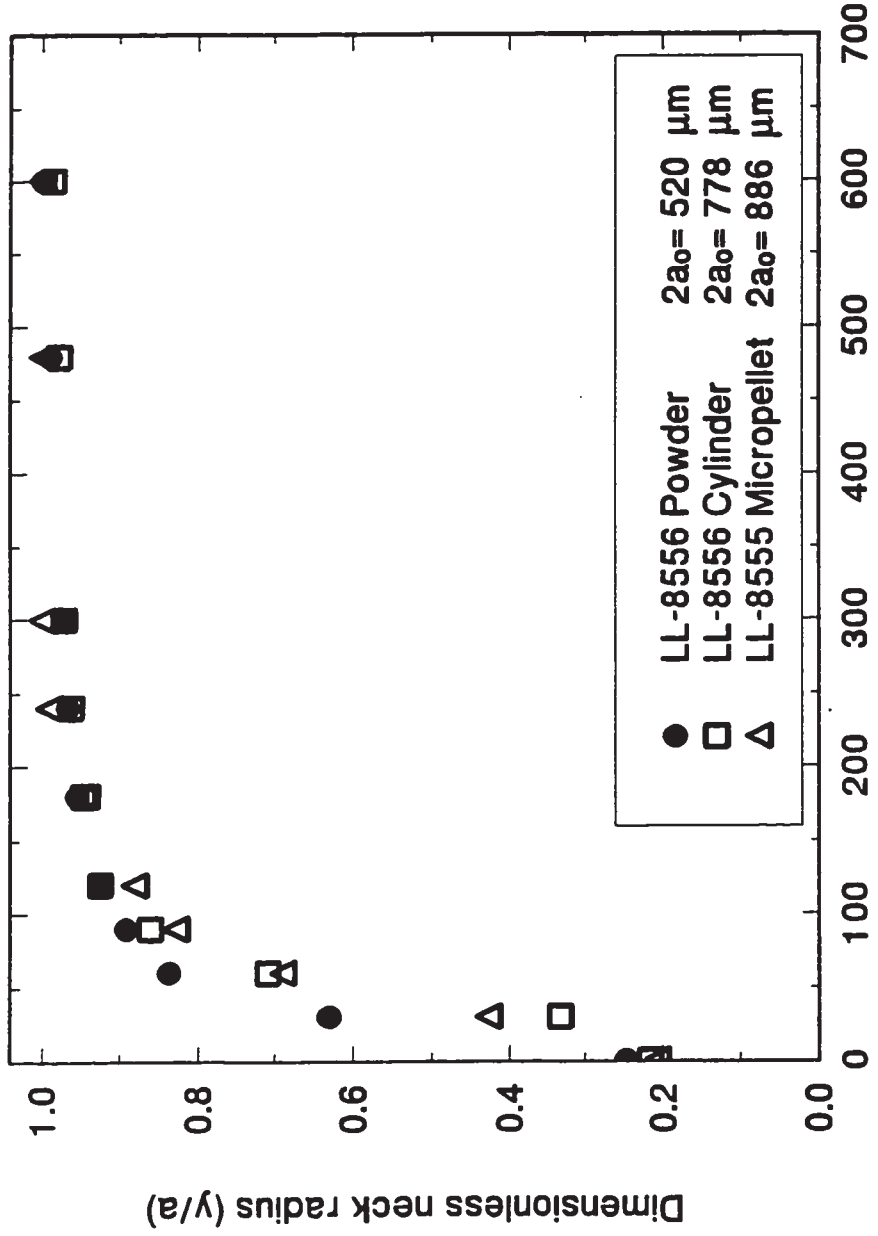

Figure 3.26 Sintering of LL-8556 as powder, cylindrical particles and of LL-8555 micropellet particles at 150°C.

It is shown that micropellets sinter at a similar rate as powder and cylinder particles despite some differences in particle size. However, the sintering rate of cylinder resin HD-8661 is significantly lower than that of micropellet resin HD-8660, as shown in Figure 3.27. The sintering sequence for micropellet resin HD-8660 is presented in Figure 3.28, and the pictures reveal a strong deformation of the HD-8660 particles in the early stage of coalescence. Based on this observation, it is suggested that some stress is being released as the particles melt. Rotational molding experiments have shown that parts produced with micropellets contain more and larger bubbles than those molded from powder (Takács *et al.*, 1996). The bubbles formed during the coalescence of micropellets are larger than those from powder particles due to the large size of micropellets. Moreover, rheological measurements have shown that micropellet resins have higher viscosity, storage modulus and loss modulus than their respective powder resins (Takács *et al*, 1996). It is suspected that the shear and thermal conditions experienced by the polymer during micropelletization are severe and may affect the resin properties. Using a commercial finite element package called POLYCAD® (Vlachopoulos *et al.*, 1992) numerical simulation of the melt flow through a die under typical micropelletization conditions have been performed . The temperature and shear stress profiles at the exit of the die are presented in Figure 3.29 and 3.30. The temperature maximum near the wall is due to viscous dissipation. The numerical results show that the shear stress and melt temperature are high enough to induce thermooxidative degradation such as chain scission and crosslinking (Hinsken *et al.*, 1991), which can cause some changes in the molecular structure of the polymer.

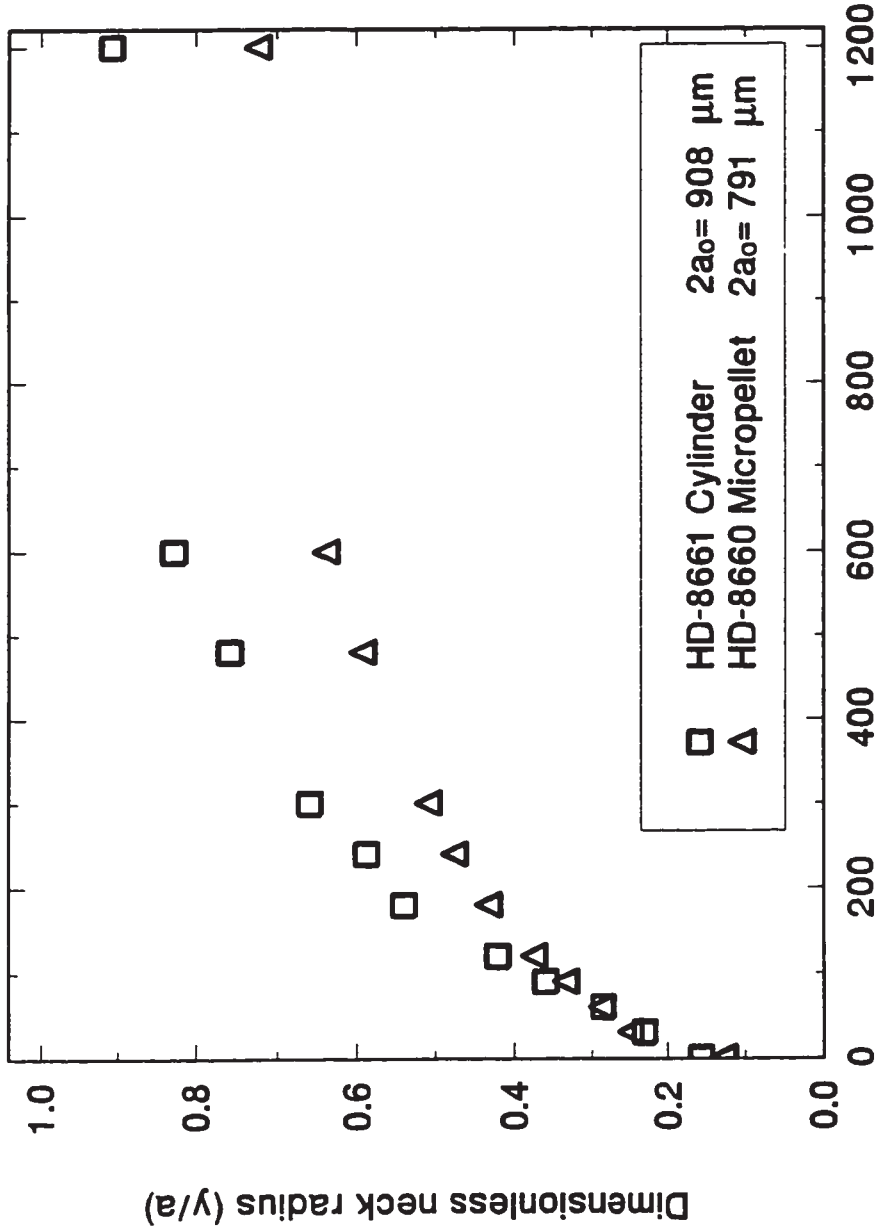

Figure 3.27 Sintering of HD-8661 as cylindrical particles and HD-8660 micropellet particles at 130°C.

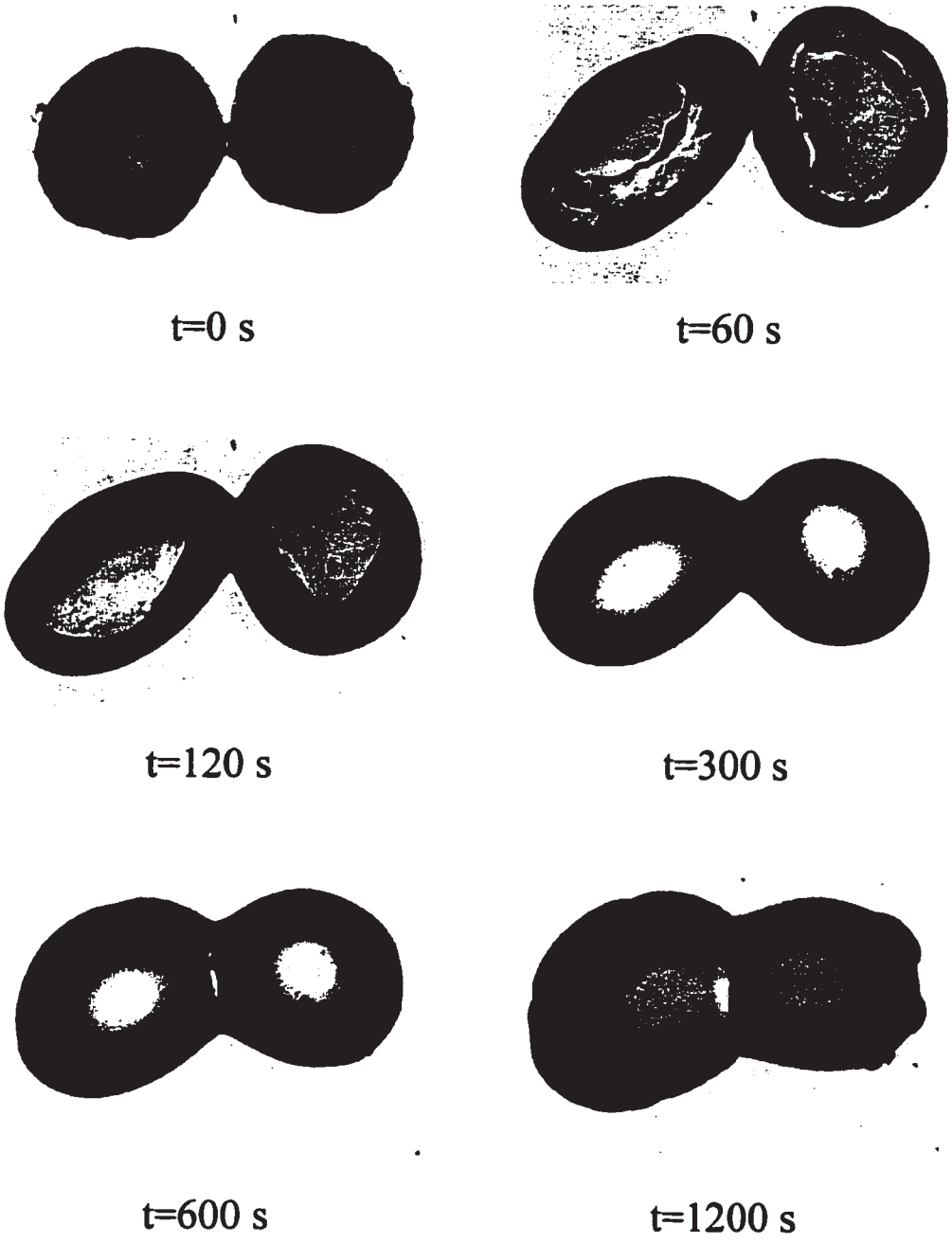

Figure 3.28 Sintering sequence for HD-8660 micropellet particles at 130°C.

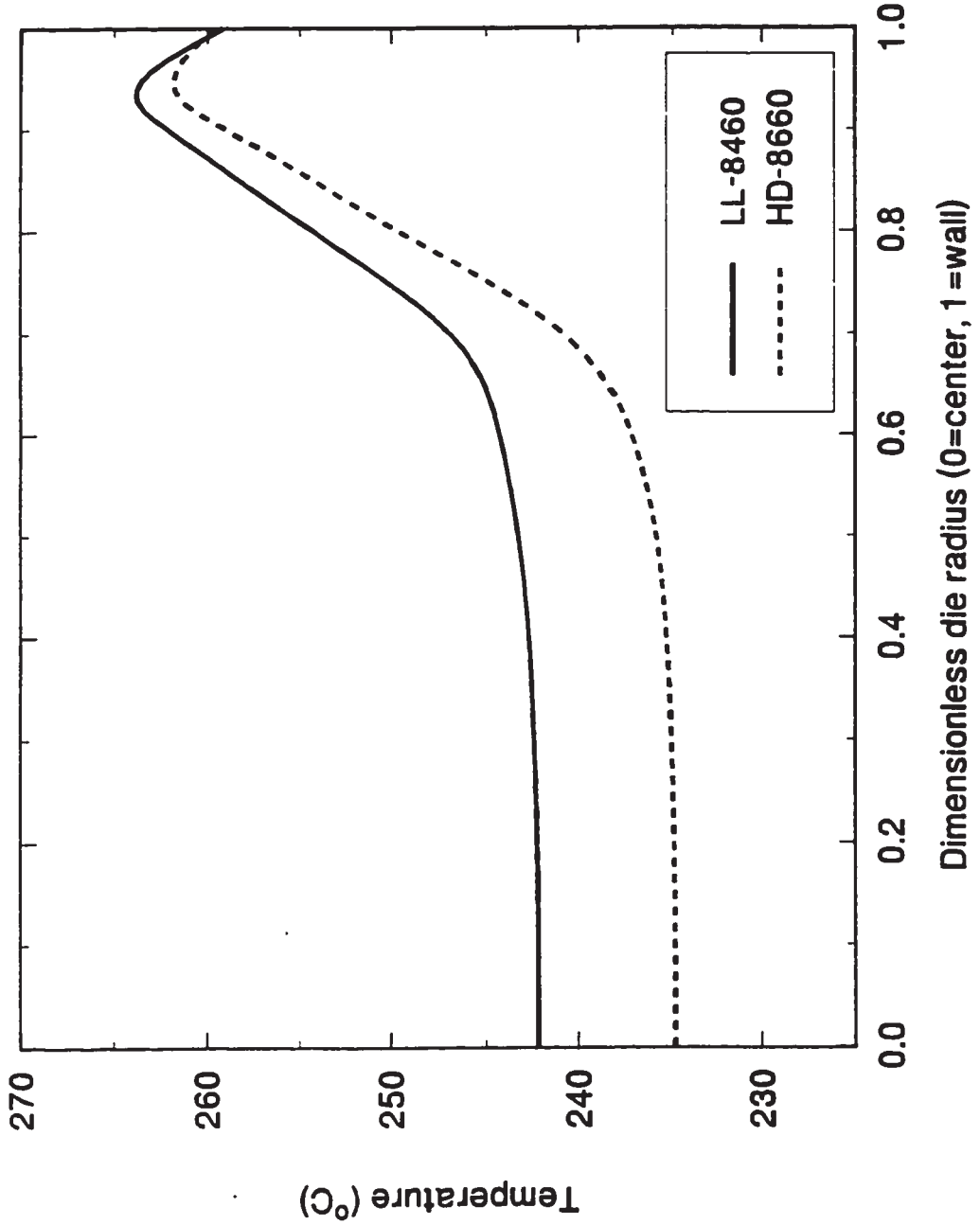

Figure 3.29 Numerical predictions of the melt temperature profile at the lips of a typical micropelletizing die for resins LL-8460 and HD-8660.

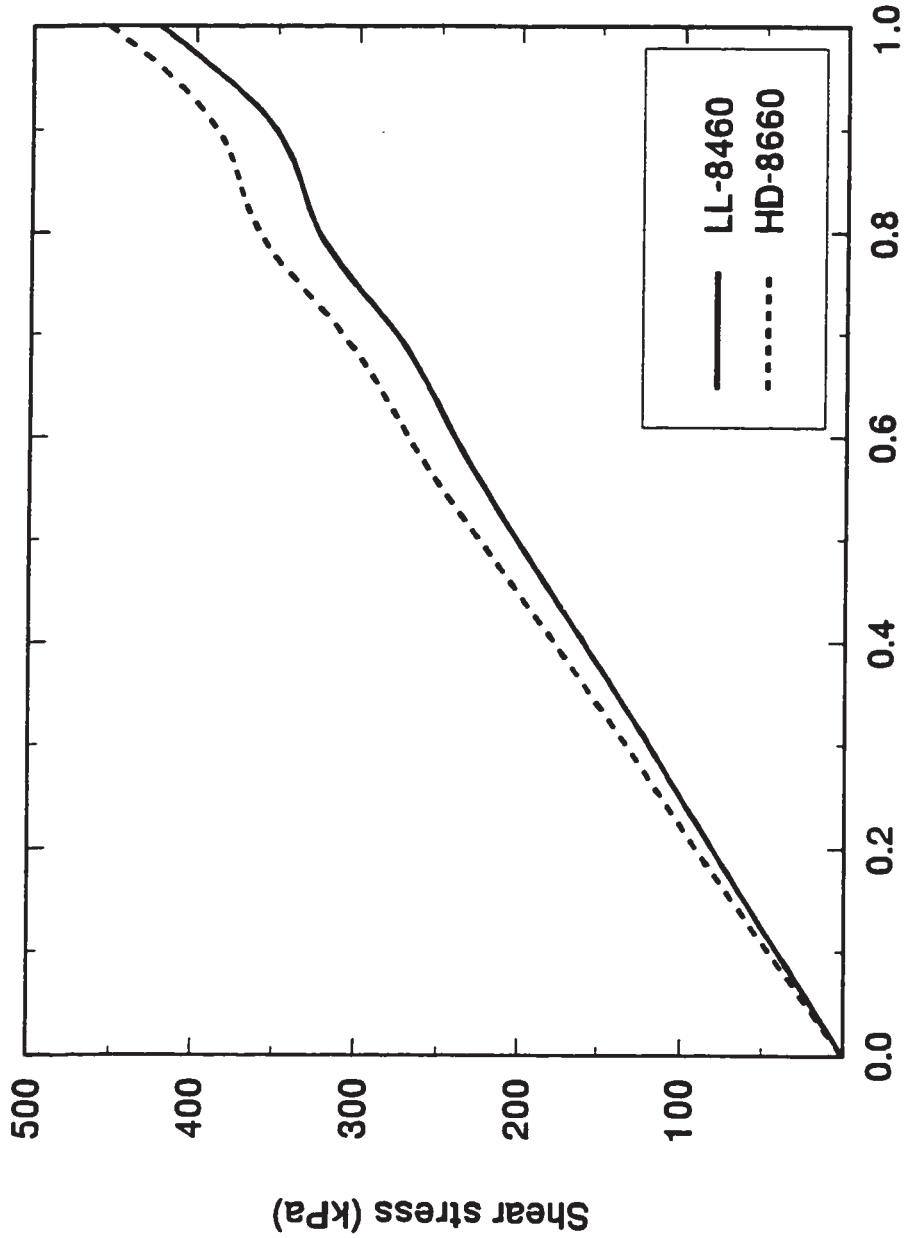

Figure 3.30 Numerical predictions of the shear stress at the lips of a typical micropelletizing die for resins LL-8460 and HD-8660.

3.4 Summary

The experiments were conducted using pairs of particles with amorphous and semi-crystalline polymers. It was found that the effect of viscosity on the sintering rate is significant. Faster coalescence occurs when the molecular weight and the viscosity of the resin are low. One PVC resin was found to sinter faster than expected. The viscosity and surface tension are not sufficient to describe the coalescence behavior of the copolymers used in this study. In some cases, there is evidence that the presence of a copolymer may affect the sintering process.

The effect of particle geometry on the sintering rate has been investigated. It was found that powder particles sinter at approximately the same rate as cylindrical particles. This result has led to the study of the rotomoldability of micropellets. For some resins, micropellet particles are found to sinter at a lower rate than powder. An examination of the processing conditions in the production of micropellets revealed that they are quite severe and they probably affect the material properties of the resin.

Adhesion between the sintering particles and the sintering surface arises due to mechanical interlocking, chemical bonding, and due to physical and electrostatic forces (Wu, 1982). However, it has been shown that the effect of surface conditioning on the sintering rate is relatively unimportant in most of the cases studied.

CHAPTER 4

MATHEMATICAL MODELING OF VISCOUS SINTERING

The models proposed by Frenkel (1945) for the sintering of two spheres and by Hopper (1984, 1990, 1991) for the sintering of two cylinders, as well as results obtained from numerical simulations, are briefly presented and discussed in this chapter. A modification of Frenkel's model is proposed, and the predictions are compared to experimental data.

4.1 Frenkel's model and Eshelby's correction for coalescence of two spheres

Assuming Newtonian viscous flow under the action of surface tension, Frenkel (1945) proposed a simple model for the sintering of two equal size spheres. In the same paper Frenkel also discussed the problem of closing a spherical cavity in an infinite homogeneous viscous body, the time required for sintering of two spherical droplets, and the rate of rounding an initially non-spherical amorphous body.

Frenkel's model is based on the balance of the work of surface tension and the viscous dissipation. All other forces, including gravity or applied pressure, are neglected. The shape of two spheres evolves as shown in Figure 4.1.

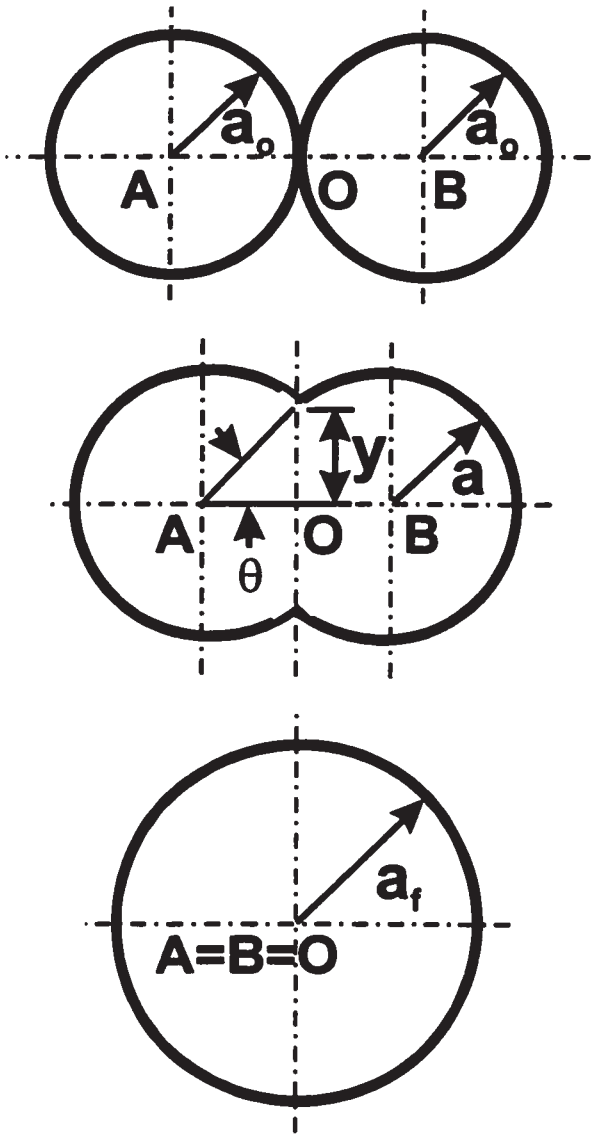

Figure 4.1 Schematic diagram of shape evolution.

At time $t=0$, two equal sized spheres of radius a_o, centered at points A and B, have only one contact point O. At time t, both centers have moved towards point O, and a shape of two intersecting spheres of radius $a(t)$ has been created. The angle of the intersection and the radius of the neck are denoted by $\theta(t)$ and $y(t)$, respectively. In the final stage, only one sphere of radius a_f remains, and all three points A, B and O coincide. The model is limited to small values of the sintering angle $\theta(t)$, assuming the particle radius to be constant $a(t)=a_o$. The work of surface tension is calculated based on the total change of surface area rather than on curvature change, and the surface tension is assumed to be constant.

In Frenkel's model development it is assumed *a priori* that the geometry of the two particles is represented as a series of geometrical domains described by one parameter θ. It is also assumed that the flow is essentially extensional and that the change of domain fully describes this flow (Figure 4.2). Hence, the parameter θ describes fully the flow situation. In the model development, Frenkel considered only the velocity component in x direction (Figure 4.2) and thereby violated the continuity equation. Eshelby (1949) proposed a correction describing the flow field as follows

$$\nabla u = \begin{matrix} -2\dot{\epsilon} & 0 & 0 \\ 0 & \dot{\epsilon} & 0 \\ 0 & 0 & \dot{\epsilon} \end{matrix} \qquad (4.1)$$

where ∇u and $\dot{\epsilon}$ are the velocity gradient and the strain rate. The strain rate is assumed to be constant throughout the complete sintering system and is defined arbitrarily.

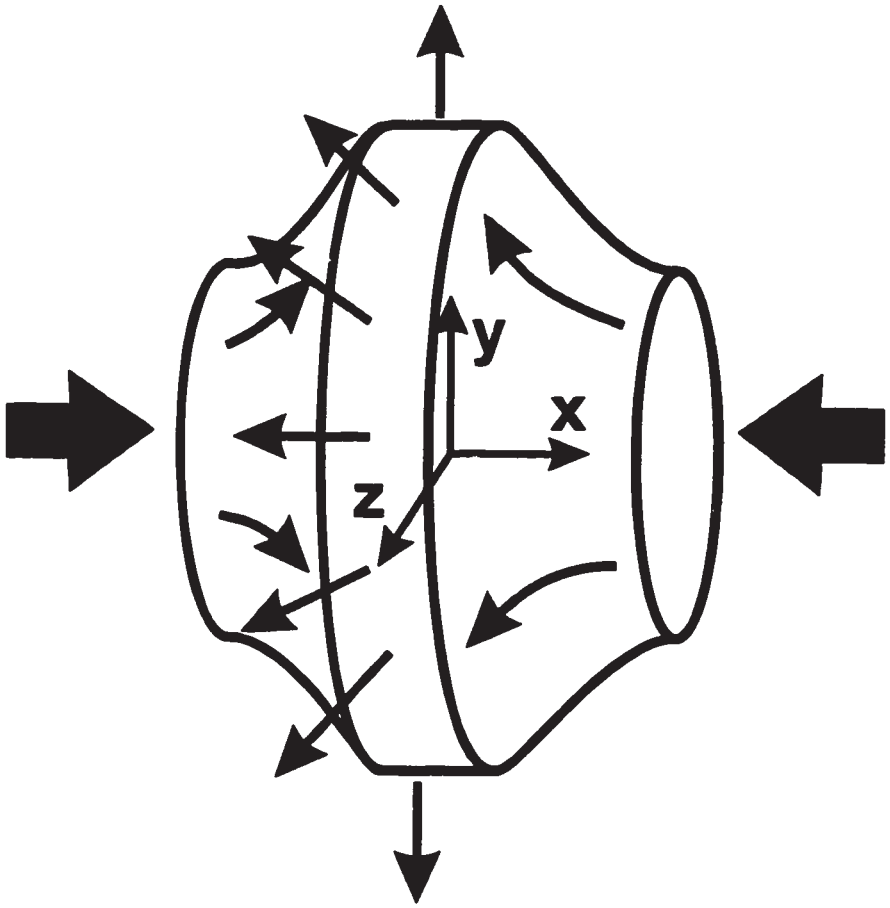

Figure 4.2 Extensional flow.

These approximations for the flow field and for the strain rate do not allow one to study the effect of particle rearrangements and the formation of new contacts in a packing of particles on the sintering rate. Frenkel's model can be expressed as

$$\frac{y}{a} = \left(\frac{3}{2} \frac{t\,\Gamma}{\eta a_o} \right)^{1/2} \tag{2.1}$$

Applying the correction proposed by Eshelby (1949) results in the following equation

$$\frac{y}{a} = \left(\frac{t\,\Gamma}{\eta a_o} \right)^{1/2} \tag{2.2}$$

In both Equations (2.1) and (2.2) the particle radius a is assumed to be constant and equal to a_o.

Frenkel's model has been used by many as a benchmark to describe the kinetics of Newtonian sintering. In spite of its simplicity, the model gives insight on the effect of material properties and particle size on the coalescence rate. One can use Frenkel's methodology to predict the sintering rate. However, its limitations should not be overlooked. Its applicability to real sintering systems is questionable.

4.2 Hopper's model for coalescence of two cylinders

Hopper (1984, 1990, 1991) resolved the problems related to viscous flow induced by capillarity. The methodology used by Hopper is based on the use of the Kolosoff-Muskhelishvili equation and complex function theory. Conformal mapping techniques

are used to solve Stokes equations. Moreover, the solutions depend on guessing appropriate mapping functions. Difficulties arise when complex problems are faced, as discussed by Hopper (1990). The results and the mathematical analysis for the sintering of two equal size cylinders have been presented by Hopper (1984, 1990). Hopper also demonstrated his technique by solving several examples involving viscous flow induced by capillarity (1990, 1991). The shape of the cylinders is described in terms of a mapping variable φ:

$$\frac{W}{a_f} = (1+\varphi)^2 \varphi^{-1/2} (1+\varphi^2)^{-1/2} \tag{4.2}$$

$$\frac{y}{a_f} = (1-\varphi)(1+\varphi^2)^{-1/2} \tag{2.3}$$

where W, a_f, y are the maximum width of the sintering cylinder, the final radius of the cylinder and the sintering neck radius. The shape evolution is related to the material properties and described as a function of time through the mapping function φ

$$\frac{t\,\Gamma}{\eta a_f} = \frac{\pi}{4} \int_{\varphi^2}^{1} [\beta (1+\beta)^{1/2} K(\beta)]^{-1} d\beta \tag{2.4}$$

where

$$K(\beta) = \int_0^1 [(1-\chi^2)(1-\beta\chi^2)]^{-1/2} d\chi \tag{2.5}$$

Hopper also presented the solution for the coalescence of a cylinder on a semi-

infinite slab (1990, 1991). After some corrections (Hopper, 1992), he found his solution to be in general agreement with the numerical results obtained by Kuiken (1990). Hopper (1992) investigated the effect of the initial diameter ratio of the cylinders on the coalescence rate. He compared the results obtained for the sintering of two equal sized cylinders (diameter ratio equal to 1) with those for the coalescence of a cylinder on a plane surface (diameter ratio equal to ∞) and concluded that the coalescence rate depends weakly upon the initial diameter ratio (Hopper, 1992). Hopper (1993) further extended his method for the sintering of two cylinders of varying initial diameter ratio.

Results presented by Hopper are limited for Newtonian flow and two dimensional problems. His method has the advantage that no flow field approximation is required. Although the solutions presented by Hopper are not affected by any shape evolution estimations, the appropriate shape evolution has to be presumed. Although Hopper's techniques do not provide insight into the flow field, they provide a description for the complete process for sintering of two cylinders.

4.3 Numerical simulations of sintering

Numerical simulation of viscous sintering has first been considered by Ross *et al.* (1981) who used finite element formulation to model the late stage of coalescence of an infinite line of cylinders. Different formulations have been developed since Ross and his coworkers began to study the effect of particle rearrangement, particle size, packing and composition on the sintering rate and densification kinetics.

Jagota and Dawson (1988 (a)) presented a numerical solution for the coalescence of two spheres using a finite element formulation. Based on this result, they showed that the velocity field in the sintering system is similar to that assumed by Frenkel (Jagota and Dawson, 1990). Moreover, they found that the deformations of the sintering particles are localized in a small region near the neck (Jagota and Dawson, 1990). This finding was later confirmed by Martínez-Herrera and Derby (1995). The simulation developed by Jagota and Dawson has served to describe the densification of powder packing (Jagota and Dawson, 1988 (b), Jagota *et al.*, 1988), to describe the densification of composite packing (Jagota and Scherer, 1993, 1995), and to analyze the sintering kinetics of coated particles (Jagota, 1994).

Van de Vorst *et al.* (1992) modeled the sintering process applying the boundary element method. They followed the approach proposed earlier by Kuiken (1990). The use of the boundary element method facilitates the remeshing and reduces the dimensionality of the problems being treated (Van de Vorst, 1994). Results obtained using the boundary element method are in general agreement with the results obtained using the finite element method for the coalescence of two spheres (Van de Vorst, 1994). Additionally, both Van de Vorst (1994) and Martínez-Herrera and Derby (1994) showed that their numerical predictions for the coalescence of two cylinders were very close to Hopper's model predictions.

Numerical simulations have been used to study the rearrangement of particles as well as the density change during sintering (Van de Vorst, 1993, 1994, Martínez-Herrera and Derby, 1995). Van de Vorst (1993, 1994) found his numerical results to be in

relatively good agreement with the experimental observations reported by Exner and Petzow (1975) for the shape evolution of multiple particles. Experimental and numerical results have shown that the total density of the sintering system is affected by the initial positioning of the particles (Exner and Petzow, 1975, Van de Vorst, 1994, Martínez-Herrera and Derby, 1995). However, numerical results presented by Van de Vorst (1994) showed that the neck growth between particles in a packing of particles can be described reasonably well with a model developed for the coalescence of two particles.

4.4 A modification of Frenkel's model

One of the objectives of the present work is to develop a sintering model which describes the complete sintering process of two spherical particles. The emphasis of this work is on the development of a simple but a general model which could be further adapted in simulating industrial processes, in which sintering is involved, such as rotational molding. The approach is similar to that of Frenkel (1945) and Eshelby (1949) but goes beyond the description of the initial stages. Similar simplifications are used in order to reduce the number of parameters in the model. However, unlike in Frenkel's model, the variation of the particle radius with time in the coalescence process is here considered. The contour of the sintering particles is idealized as presented in Figure 4.1. The following relation for $a(t)$ versus $\theta(t)$ is obtained from the conservation of mass with the assumption of a constant density

$$a(t) = a_o\left(\frac{4}{(1+\cos(\theta(t)))^2(2-\cos(\theta(t)))}\right)^{1/3} \qquad (4.3)$$

For simplicity, the functions $\theta(t)$, $a(t)$, and $y(t)$ will be subsequently denoted θ, a, and y. Thus, the total surface of particles varies with the angle θ according to the following formula

$$S = 4\pi a^2(1+\cos(\theta)) = \frac{8\pi a_o^2 2^{1/3}}{(1+\cos(\theta))^{1/3}(2-\cos(\theta))^{2/3}} \tag{4.4}$$

Whereas Frenkel assumed the particle radius to be constant (i.e., $a(t)=a_o$) and made an approximation for small angles (i.e., $\cos(\theta)=1-\theta^2/2$).

The work of viscous forces W_v for a Newtonian fluid can be expressed as

$$W_v = \iiint_V (\tau : D)\, dV \tag{4.5}$$

where V is the volume of the sintering system. D is the deformation tensor:

$$D = 1/2\,(\nabla u + (\nabla u)^T) \tag{4.6}$$

and for Newtonian fluid the extra-stress tensor can be defined as follows

$$\tau = 2\eta D \tag{4.7}$$

Following Eshelby, the flow field is assumed to be extensional (Equation 4.1) and consequently

$$W_v = \iiint_V 12\,\eta\dot{\epsilon}^2\, dV \tag{4.8}$$

Following Frenkel, the strain rate $\dot{\epsilon}$ is assumed to be constant throughout the complete domain and is approximated by

$$-2\dot{\epsilon} = \frac{\partial u_x(A)}{\partial x} \approx \frac{u_x(A) - u_x(O)}{a} \tag{4.9}$$

where $u_x(A)$ is the velocity with which point A moves towards point O (Figure 4.1). The term $u_x(O)$ is the velocity of the fluid at the plane of contact of the two particles and is equal to zero. The term $u_x(A)$ is defined as follows

$$u_x(A) = \frac{d}{dt}(a\cos(\theta)) = -\frac{2^{5/3} a_o \sin(\theta)}{(1+\cos(\theta))^{5/3}(2-\cos(\theta))^{4/3}}\theta' \tag{4.10}$$

where $d\theta/dt$ is denoted as θ'. Consequently,

$$-2\dot{\epsilon} = \frac{u_x(A)}{a} = -\frac{2\sin(\theta)}{(1+\cos(\theta))(2-\cos(\theta))}\theta' \tag{4.11}$$

which leads to the formula for dissipated energy

$$W_v = \frac{32\pi a_o^3 \eta(1-\cos(\theta))}{(1+\cos(\theta))(2-\cos(\theta))^2}(\theta')^2 \tag{4.12}$$

The work of surface tension W_s is defined as

$$W_s = -\Gamma\frac{dS}{dt} \tag{4.13}$$

where Γ is the coefficient of surface tension and S is the surface of the sintering system. Applying the chain rule on Equation (4.4) the term dS/dt can be derived

$$\frac{dS}{dt} = \frac{dS}{d\theta}\frac{d\theta}{dt} = -\frac{8\pi a_o^2 2^{1/3}\cos(\theta)\sin(\theta)}{(1+\cos(\theta))^{4/3}(2-\cos(\theta))^{5/3}}\theta' \tag{4.14}$$

and the expression for the work of surface tension becomes

$$W_s = \Gamma\frac{8\pi a_o^2 2^{1/3}\cos(\theta)\sin(\theta)}{(1+\cos(\theta))^{4/3}(2-\cos(\theta))^{5/3}}\theta' \tag{4.15}$$

Under the assumption that θ' is always positive, and by equating the work of surface tension to the viscous dissipation we obtain

$$\theta' = \frac{\Gamma}{a_o\eta}\frac{2^{-5/3}\cos(\theta)\sin(\theta)(2-\cos(\theta))^{1/3}}{(1-\cos(\theta))(1+\cos(\theta))^{1/3}} \tag{4.16}$$

with the initial condition

$$\theta(0) = \theta_o = 0 \tag{4.17}$$

Equation (4.16) has a trivial solution $\theta=0$. It is singular near zero, and a special numerical treatment is necessary to solve it. There is a unique solution to Equation (4.14) since its right hand side is locally Lipschitz continuous in θ. For $\theta\to 0$, the following approximations are made: $sin(\theta)=\theta$ and $(1-cos(\theta))=\theta^2/2$ respectively. Hence, the asymptotic behavior of Equation (4.16) is

$$\theta' = \frac{1}{2}\frac{\Gamma}{\eta a_o\theta} \tag{4.18}$$

Considering that $\theta > 0$ and applying the initial condition (Equation 4.17), the solution of Equation (4.18) is,

$$\theta(t) = \left(\frac{t\,\Gamma}{\eta a_o} \right)^{1/2} \tag{4.19}$$

which corresponds to the Frenkel-Eshelby model. Thus, a solution for $\theta(t)$ is obtained solving Equation (4.16) numerically using an automatic step size Runge-Kutta-Fehlberg integration method (Burden and Faires, 1985). To overcome numerical instabilities when $\theta = 0$, the initial boundary condition is fixed at a time value slightly different than zero, and the corresponding value of θ_o is determined from Equation (4.19). Once a solution for the evolution of the sintering angle with time is obtained, the evolution of the neck radius with time can easily be derived

$$\frac{y}{a} = \sin(\theta) \tag{4.20}$$

$$\frac{y}{a_o} = \sin(\theta) \left(\frac{4}{(1+\cos(\theta))^2 (2-\cos(\theta))} \right)^{1/3} \tag{4.21}$$

$$\frac{y}{a_f} = \sin(\theta) \left(\frac{2}{(1+\cos(\theta))^2 (2-\cos(\theta))} \right)^{1/3} \tag{4.22}$$

Numerical results of the present modified-Frenkel model are presented in Table 4.1. The initial condition was set at the value for dimensionless time $t\Gamma/\eta a_o$=0.0001 instead of zero and from Equation (4.17) θ_o=0.01.

4.3 Critique of the various models and comparison with experimental results

A comparison between the Frenkel-Eshelby model and the present model predictions is shown in Figure 4.3. It can be seen that the model predictions are asymptotically identical in the early stage of sintering (i.e., $y/a<0.4$), where the approximation of constant particle radius is valid. This result is expected since the asymptotic behavior of the present model is the same as the Frenkel-Eshelby model. Figure 4.4 presents a comparison of the present modified-Frenkel model predictions and the numerical results obtained by Jagota and Dawson (1988) using the finite element method, and the numerical results obtained by Van de Vorst (1994) using a boundary element method. The present modified-Frenkel model predictions are in general agreement with the numerical results for the coalescence of two spheres (Jagota and Dawson, 1988, Van de Vorst, 1994) (Figure 4.4). The differences in the predictions may be principally attributed to the flow approximation used in the development of the modified model, specifically in the evaluation of the strain rate. The geometrical assumption of a sharp neck contour may also contribute to the differences observed between the present model predictions and numerical results (Jagota and Dawson, 1988, Van de Vorst, 1994).

Table 4.1 Modified-Frenkel model predictions

$t\Gamma/\eta a_o$	y/a	y/a_o	y/a_f
0.0001	0.010000	0.010000	0.007937
0.01	0.097878	0.097878	0.077686
0.02	0.139593	0.139597	0.110798
0.03	0.171268	0.171279	0.135944
0.04	0.198362	0.198382	0.157456
0.05	0.220972	0.221008	0.175414
0.06	0.241943	0.241998	0.192074
0.07	0.260895	0.260976	0.207136
0.08	0.278646	0.278758	0.221250
0.09	0.294891	0.295040	0.234173
0.10	0.310862	0.311052	0.246882
0.20	0.427368	0.418399	0.340021
0.30	0.506011	0.508688	0.403746
0.40	0.573609	0.580672	0.460880
0.50	0.624233	0.631857	0.501506
0.60	0.672070	0.682755	0.541903
0.70	0.706200	0.720951	0.572219
0.80	0.740330	0.759148	0.602536
0.90	0.766581	0.790120	0.627119
1.00	0.791024	0.819434	0.650385
2.00	0.924121	1.007575	0.799713
4.00	0.987195	1.159200	0.920058
6.00	0.997642	1.216684	0.965682
8.00	0.999528	1.240669	0.984719

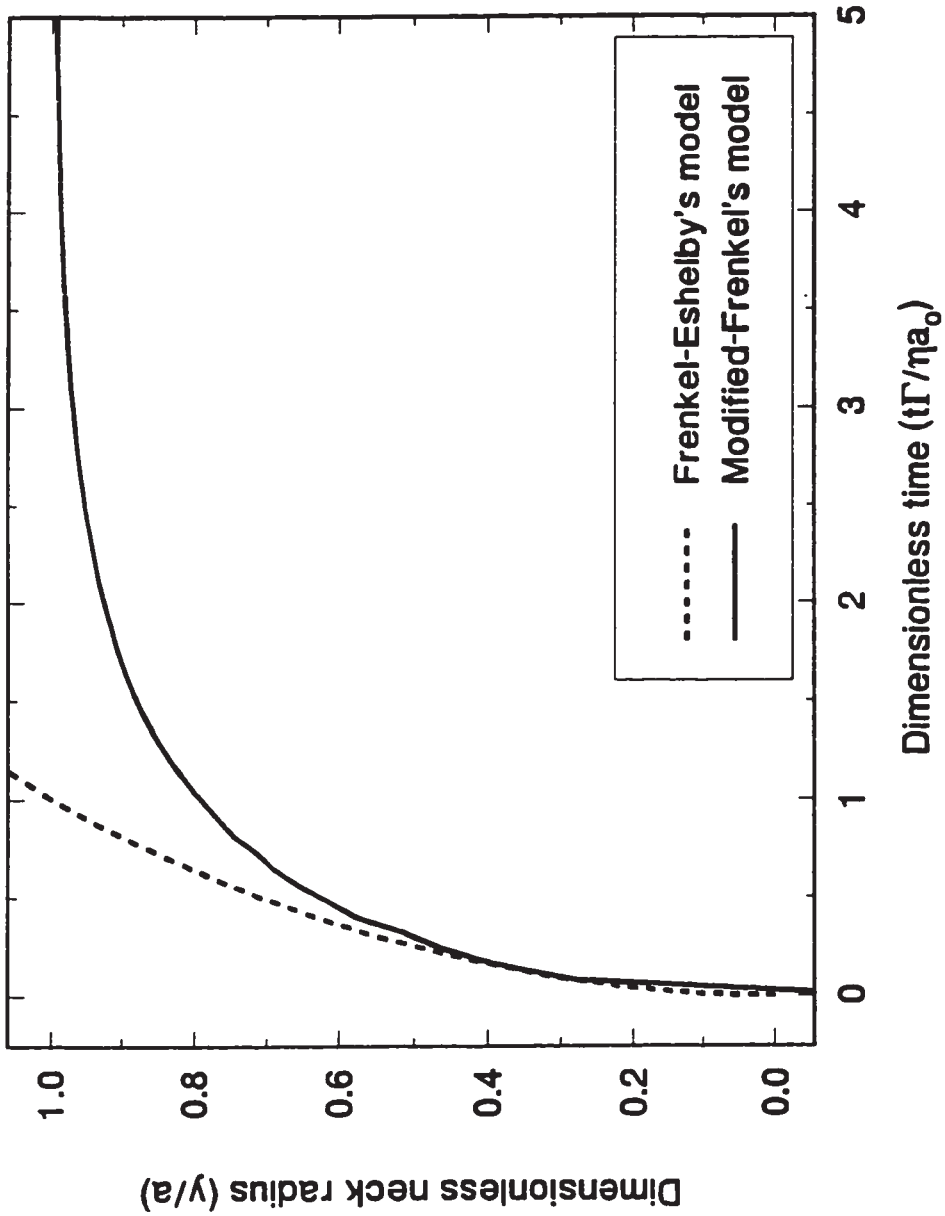

Figure 4.3 Comparison of the modified-Frenkel model with the Frenkel-Eshelby model.

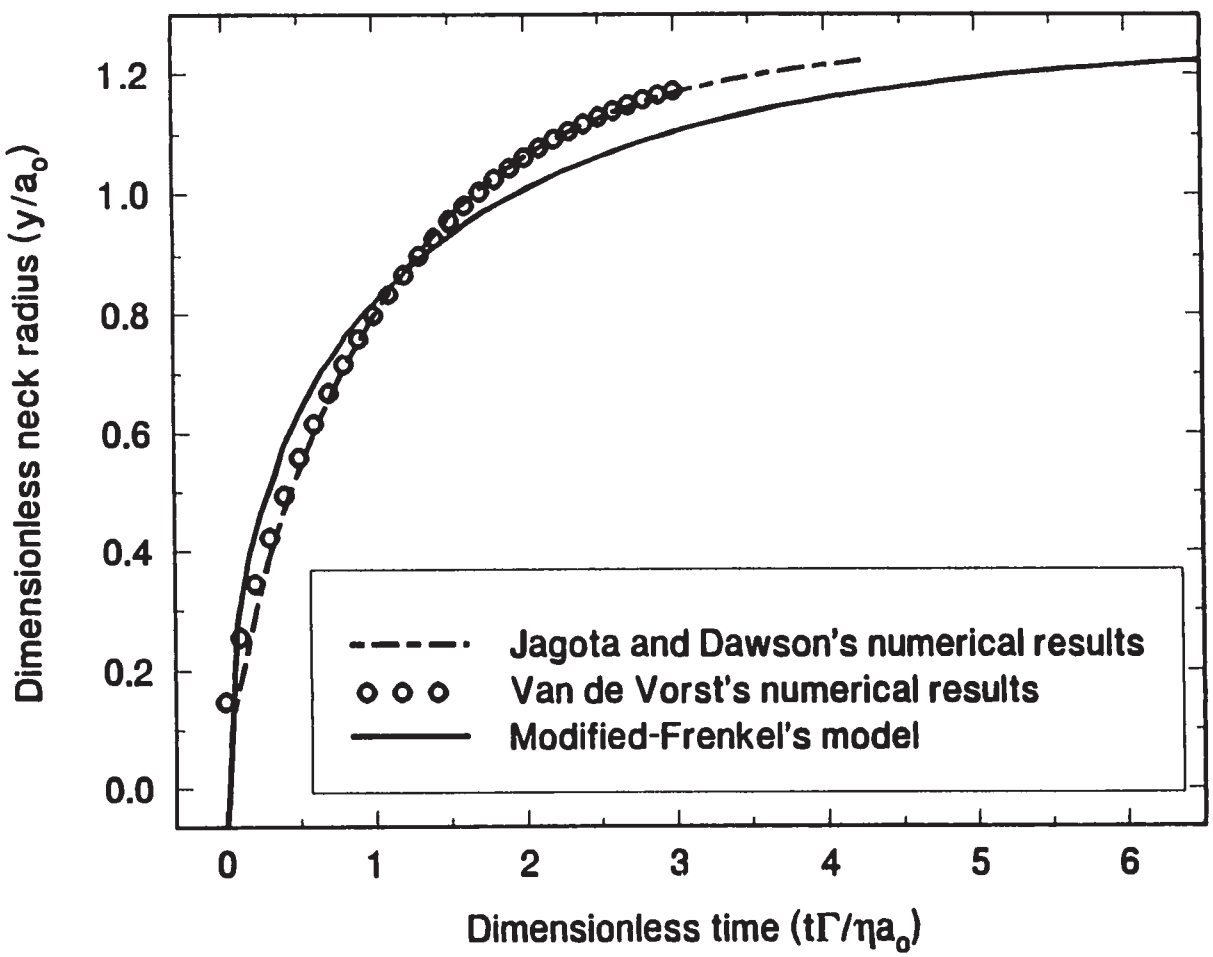

Figure 4.4 Comparison of the modified-Frenkel model predictions with numerical results presented by Jagota and Dawson (1988), and numerical results presented by Van de Vorst (1994).

The present model makes possible the use of constitutive equations other than Newtonian equations. It also has the advantage of being simple enough to enable inclusion into more general formulations of industrial processes, such as rotational molding or powder coating.

Experimental sintering results for all resins used in the present study have been compared with the theoretical predictions using Frenkel's model (Equation 2.1), Frenkel-Eshelby's model (Equation 2.2), results reported by Hopper (1984) and the modified-Frenkel model (Table 4.1). Although numerical results for sintering have been reported in the literature (Jagota and Dawson, 1988, Van de Vorst, 1994), only analytical solutions have been considered since there is not much difference between the numerical results and the modified-Frenkel model (Figure 4.4). Hopper (1984) reported results for y/a_f as a function of the dimensionless time $t\Gamma/\eta a_f$. To facilitate the comparison with available experimental results, Hopper's model predictions have been transformed to be in the form of y/a as a function of $t\Gamma/\eta a_o$. The value of a/a_f is approximated as the ratio between the maximum width W and the final diameter of the sintering particles $2a_f$ (Equation 4.2). For the experimental results, a dimensionless sintering time was calculated using the material property data (viscosity and surface tension) and using the value of the initial particle radius a_o.

The viscosity and the surface tension data are needed for the mathematical models. The zero-shear viscosity values presented in Tables 3.3, 3.4, and 3.5 are used. The surface tension is the driving force in the sintering process. A number of authors have reported surface tension data for linear polyethylene and polypropylene in the

literature. The surface tension of hydrocarbon polymers obtained by direct measurement on melts and liquids, as tabulated by Wu (1982), ranges from 0.02 to 0.04 N/m, in the temperature range of 20 to 180°C. For linear polyethylene with a weight average molecular weight of 67000, Wu (1982) reported the surface tension to be 0.0288 N/m (140°C) with a temperature dependence $d\Gamma/dT$ of -5.7×10^{-5} N/m°C. This value for the surface tension was used for resin HD-8661, for which the weight average molecular weight is 88000, and was also used for the LLDPE resins (LL-8556 and LL-8461) and for the blow-molding resin (HDPE-BM). Wu (1982) reported the surface tension of an atactic and isotactic polypropylenes to be 0.0231 N/m (140°C) with a temperature dependence $d\Gamma/dT$ of -5.6×10^{-5} N/m°C. Hata and Kasemura (1980) have indicated that the effect of tacticity of the surface tension is negligibly small. The surface tension values of the copolymers used in this study were calculated using a linear relation (Rastogi and St.Pierre, 1969)

$$\Gamma = x_1\Gamma_1 + x_2\Gamma_2 \tag{4.23}$$

where x_1, x_2 and Γ_1 and Γ_2 are the mole fraction and the surface tension of each component of the copolymers, respectively. The surface tension of resins PP-SC1355RM and PP-MT4390HU was calculated based on the data reported by Wu (1982) and Roe (1968). The surface tension of resin EBA-NCPE8019 is estimated based on data reported by Wu (1982) for poly(n-butyl acrylate) (Γ=0.0225 N/m at 180°C with $d\Gamma/dt=-7.0\times10^{-5}$ N/m°C) and by Wu (1982) for polyethylene. The surface tension of the polycarbonate and polyvinyl chloride melts was determined from data obtained for

solid polymers. The effect of glass transition on the surface tension is small (Wu, 1982). The temperature dependence of the surface tension can be accurately fitted with the Guggenheim equation (1945) and extrapolated to the solid range (Wu, 1982). However, a linear relation is generally sufficiently accurate over an ordinary temperature range (0°C to 200°C) (Wu, 1982). Based on data presented by Wu (1971), the surface tension of polyvinyl chloride was estimated to be 0.0363 N/m at 170°C. The surface tension of the polycarbonate resin is approximated to be equal to the dispersion component of solid surface tension (Petke and Ray, 1969). Based on data presented by Petke and Ray (1969), the polycarbonate surface tension was determined to be 0.0375 N/m at 200°C and 0.0354 N/m at 235°C.

Sintering experiments were conducted at 170°C with resin HD-8661. Results presented in Figure 4.5 show that both Hopper's model and the modified-Frenkel model are in good agreement with the experimental data. The sintering experiments at 130°C for resin LL-8556 and LL-8461 were also used to evaluate the models. Unfortunately, viscosity measurements could not be carried out at 130°C with our equipment. Viscosity data were correlated by an Arrhenius expression from 190°C to 170°C and then extrapolated down to 130°C. Sintering results are illustrated in Figures 4.6 and 4.7. As observed for resin HD-8661, the predictions of Hopper's model and of the modified-Frenkel model are in very good agreement with the experimental data for resins in the early stage of sintering but they underestimate somewhat the time required for the completion of the coalescence. This observation is more noticeable for small particles of resin LL-8556 (Figure 4.7).

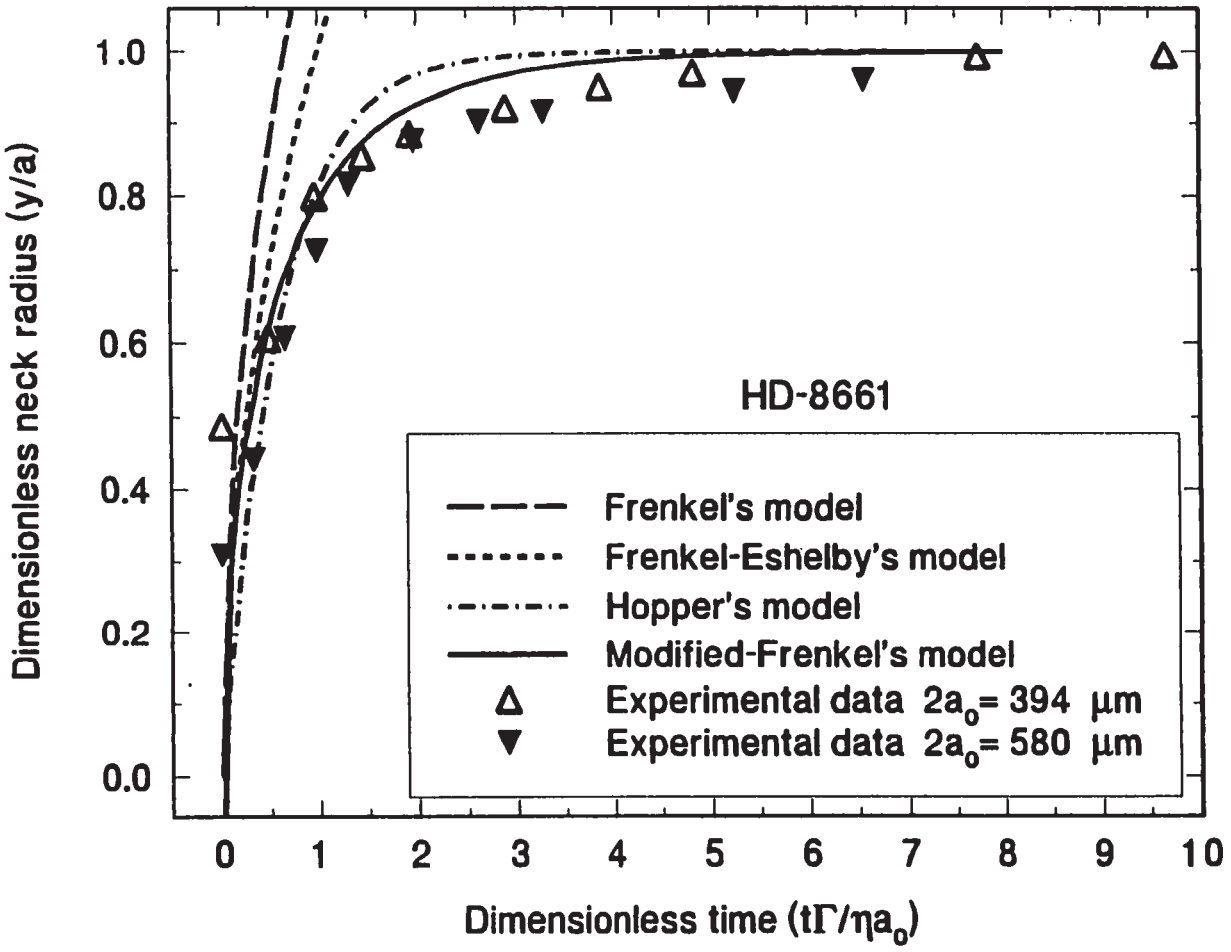

Figure 4.5 Comparison of the modified-Frenkel model with theoretical model predictions, and experimental data obtained with resin HD-8661 powder particles at 170°C.

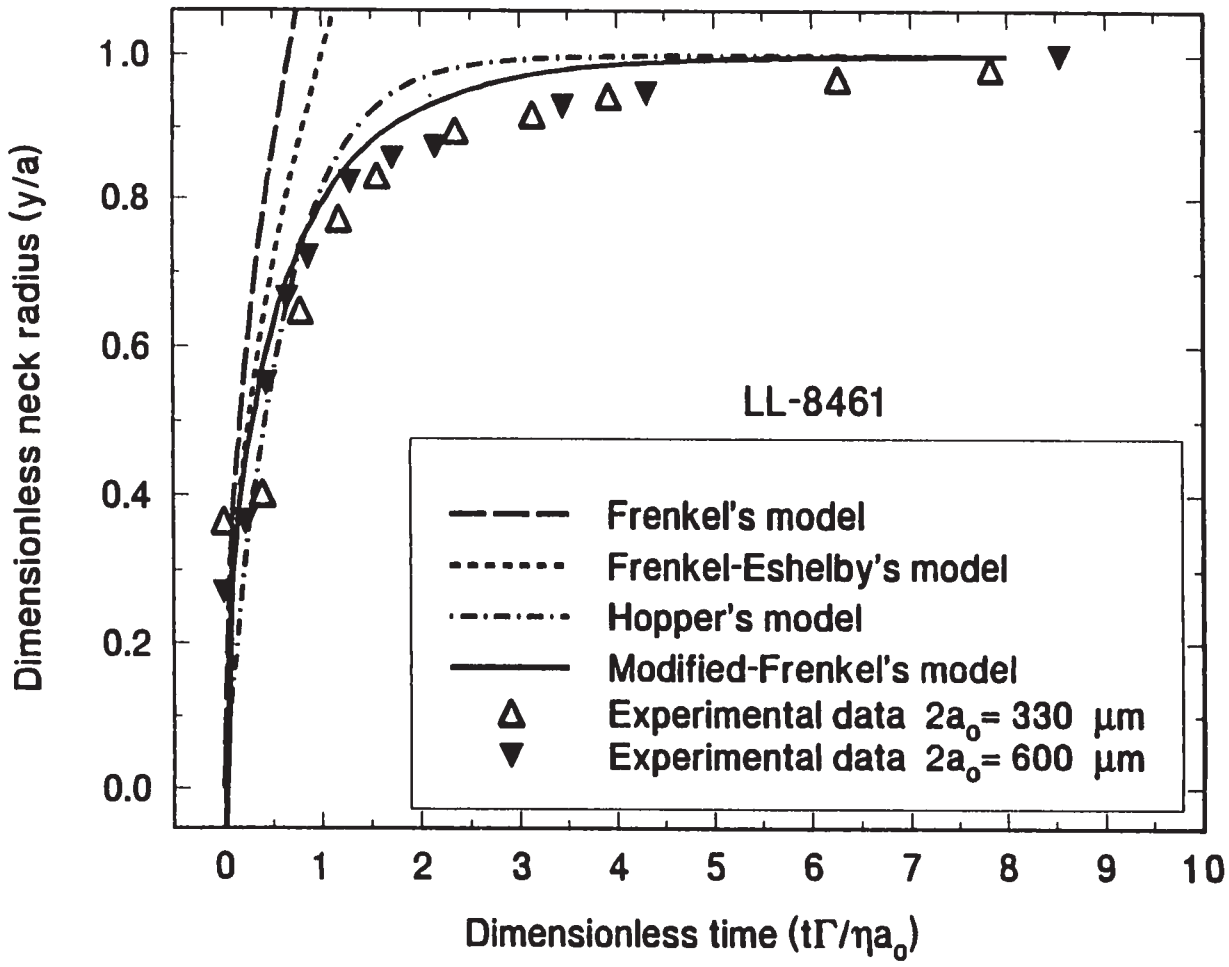

Figure 4.6 Comparison of the modified-Frenkel model with theoretical model predictions, and experimental data obtained with resin LL-8461 powder particles at 130°C.

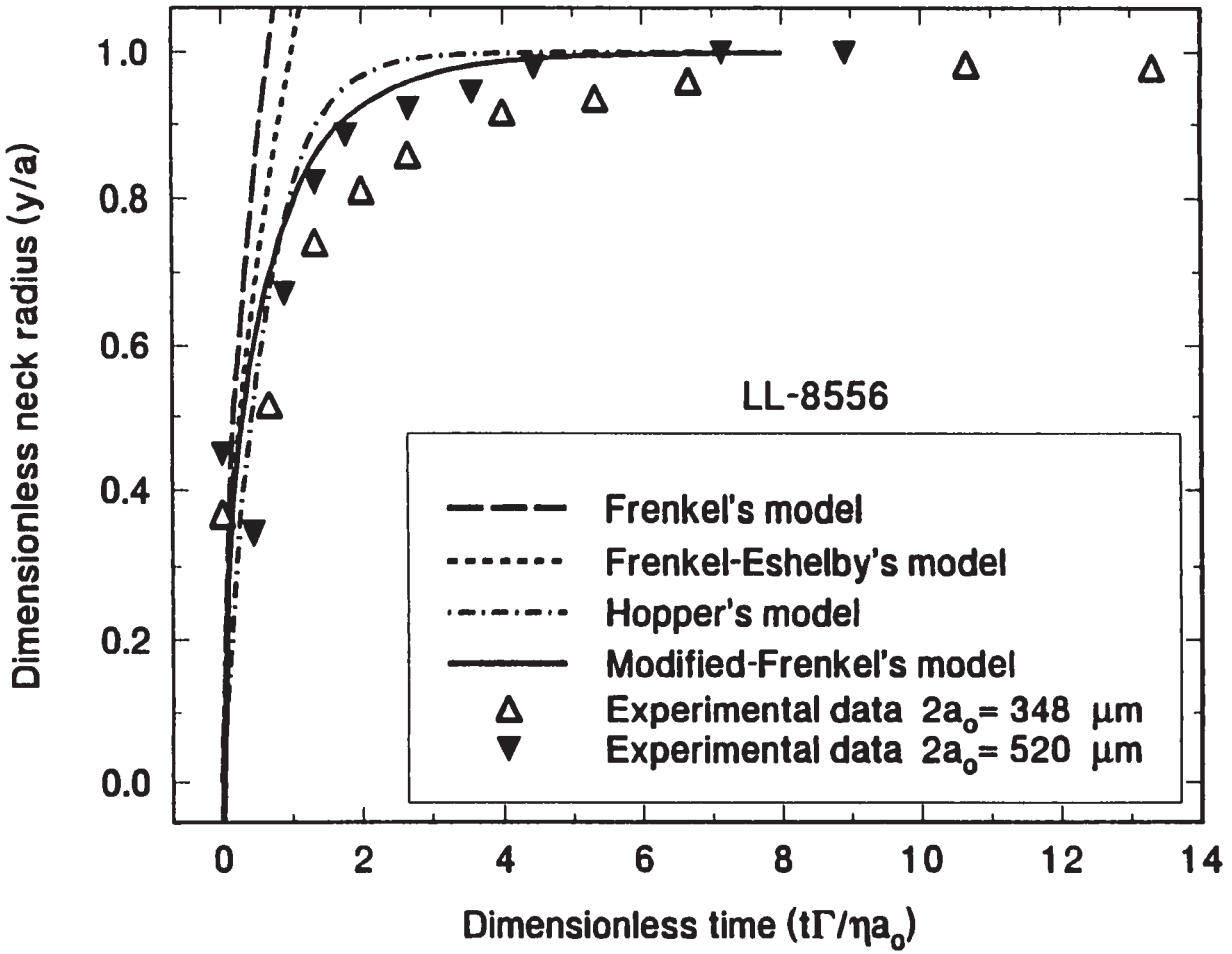

Figure 4.7 Comparison of the modified-Frenkel model with theoretical model predictions, and experimental data obtained with resin LL-8556 powder particles at 130°C.

In the case of resin LL-8556, the adhesion forces are probably not negligible when small particles are used in the experiment, as explained in section 3.3 (Figures 3.20). The effect of the adhesion of the particles on the sintering surface would result in a reduction of the coalescence rate. The theoretical models were developed without taking into account the adhesion forces between the particles and the sintering surface. However, for all other experiments using rotational molding grade polyethylene, it can be seen that both models are in good agreement with the experimental results, and the experimental trend is better represented by the modified-Frenkel model (Figure 4.8). The coalescence rates predicted with the Frenkel and the Frenkel-Eshelby models are higher than that experimentally observed. A reason for the difference between the mathematical models is the assumption used in Frenkel's development that the particle radius is constant, an assumption which is satisfactory only when $y/a < 0.3$.

The sintering sequence for the resin HDPE-BM is presented in Figure 3.14. The neck growth between these particles can hardly be quantified since the geometry of the particles is highly irregular. It can be observed that even after 3600 seconds, the coalescence of the two particles ($a_o \approx 300$ μm) in Hopper's model and in the modified-Frenkel model predict that the coalescence should be 99% completed after 2023 and 2768 seconds, respectively. Calculations revealed that both Hopper's model and the modified-Frenkel model failed to predict the sintering behavior for resin HDPE-BM.

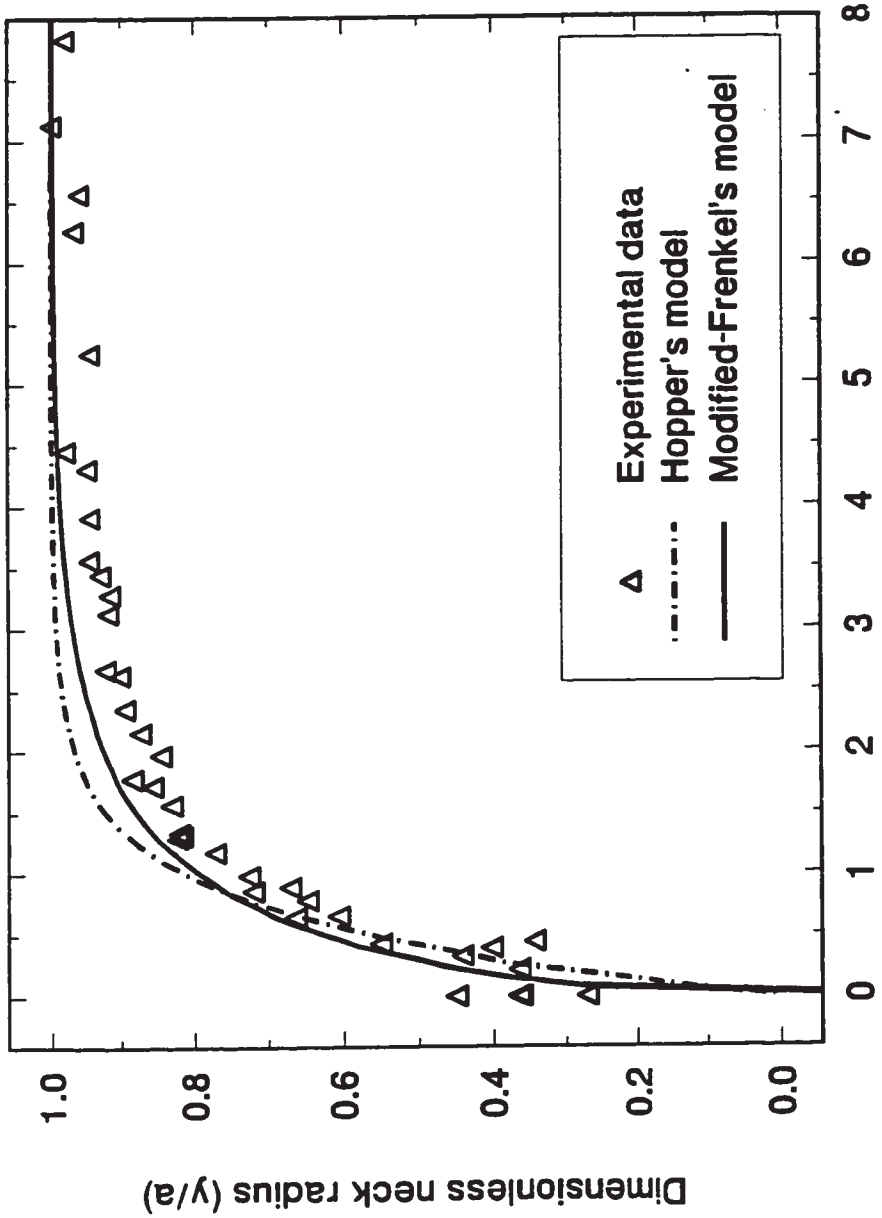

Figure 4.8 Comparison of the modified-Frenkel model predictions with Hopper's model (1984), and experimental data obtained with rotational molding grade polyethylene resins.

The predictions of the modified-Frenkel model and the model proposed by Hopper have been compared with experimental results obtained with the polypropylene copolymer resins, PP-SC1355RM, PP-MT4390HU, (Figure 4.9), and with the polyethylene copolymer EBA-NCPE8019 (Figure 4.10). Figures 4.9 and 4.10 show that both theoretical models overestimate the sintering rate for these three resins.

It is possible that the surface tension of the polypropylene copolymers has been overestimated. Wu (1982) reported that depending on the degree of polymerization, the surface tension of a block copolymer is practically equal to that of the lower energy component. However, in the case of the resins PP-SC1355RM, PP-MT4390HU, and EBA-NCPE8019, the difference in the values used for the surface tension of the two components was not sufficient to explain the failure of the theoretical model. This finding supports the hypothesis that properties other than viscosity and surface tension may be important in polymer sintering.

Figure 4.11 presents the comparison between the experimental results obtained with the polycarbonate resin and the theoretical models. It can be seen that the Hopper model predictions are in good agreement with the experimental results obtained at a sintering temperature of 200°C, while the modified-Frenkel model slightly underestimates the sintering rate. However, both Hopper's model and the modified-Frenkel model overestimate the sintering rate for the results obtained at 235°C. Sintering results obtained with the polyvinyl chloride resin have also been compared with Hopper's model and the modified-Frenkel model. In Figure 4.12, it can be seen that both models underestimate the sintering rate obtained experimentally.

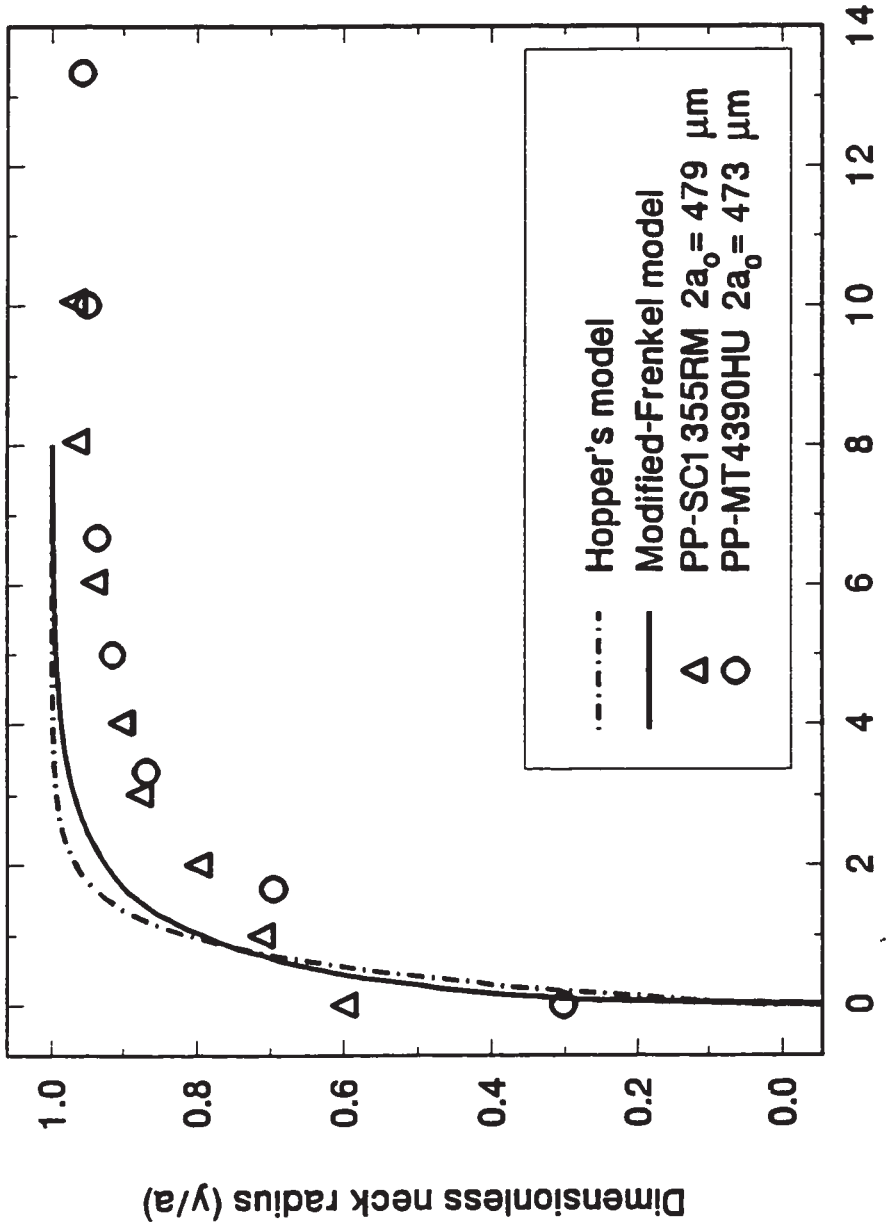

Figure 4.9 Comparison of the modified-Frenkel model predictions with Hopper's model (1984), and experimental data obtained with resins PP-SC1355RM and PP-MT4390HU powder particles at 190°C.

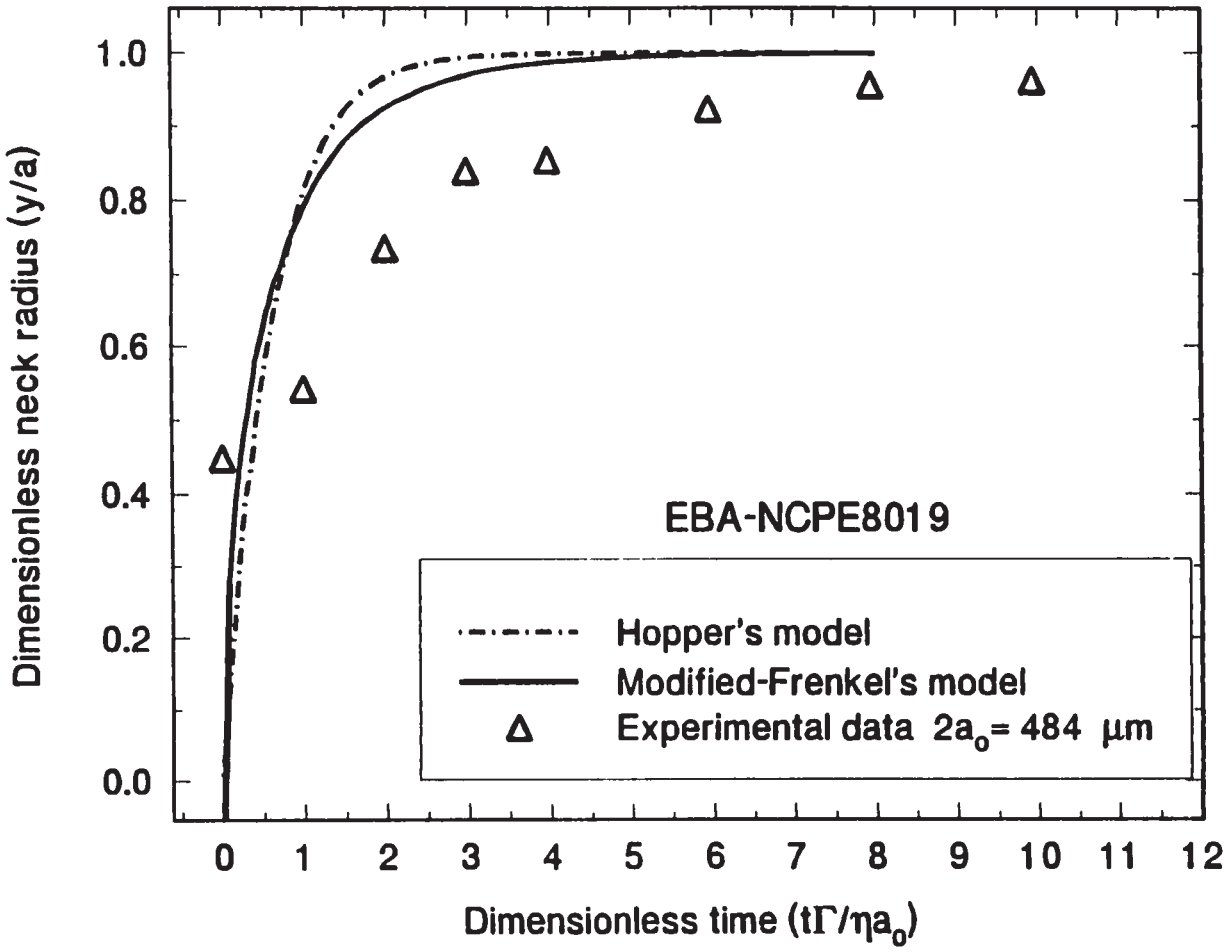

Figure 4.10 Comparison of the modified-Frenkel model predictions with Hopper's model (1984), and experimental data obtained with resin EBA-NCPE8019 powder particles at 170°C.

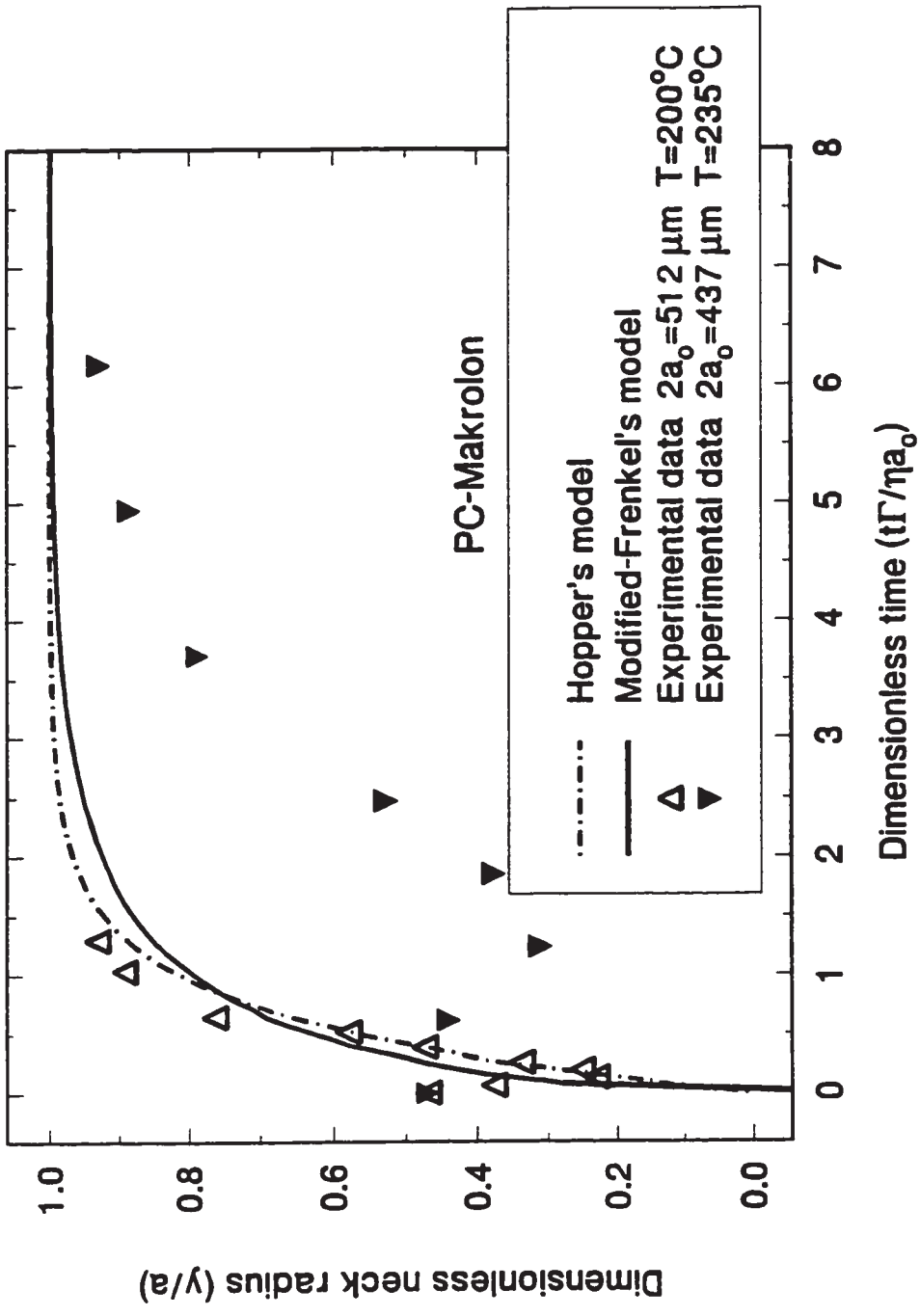

Figure 4.11 Comparison of the modified-Frenkel model predictions with Hopper's model (1984), and experimental data obtained with resin PC-Makrolon powder particles at 200°C and 235°C.

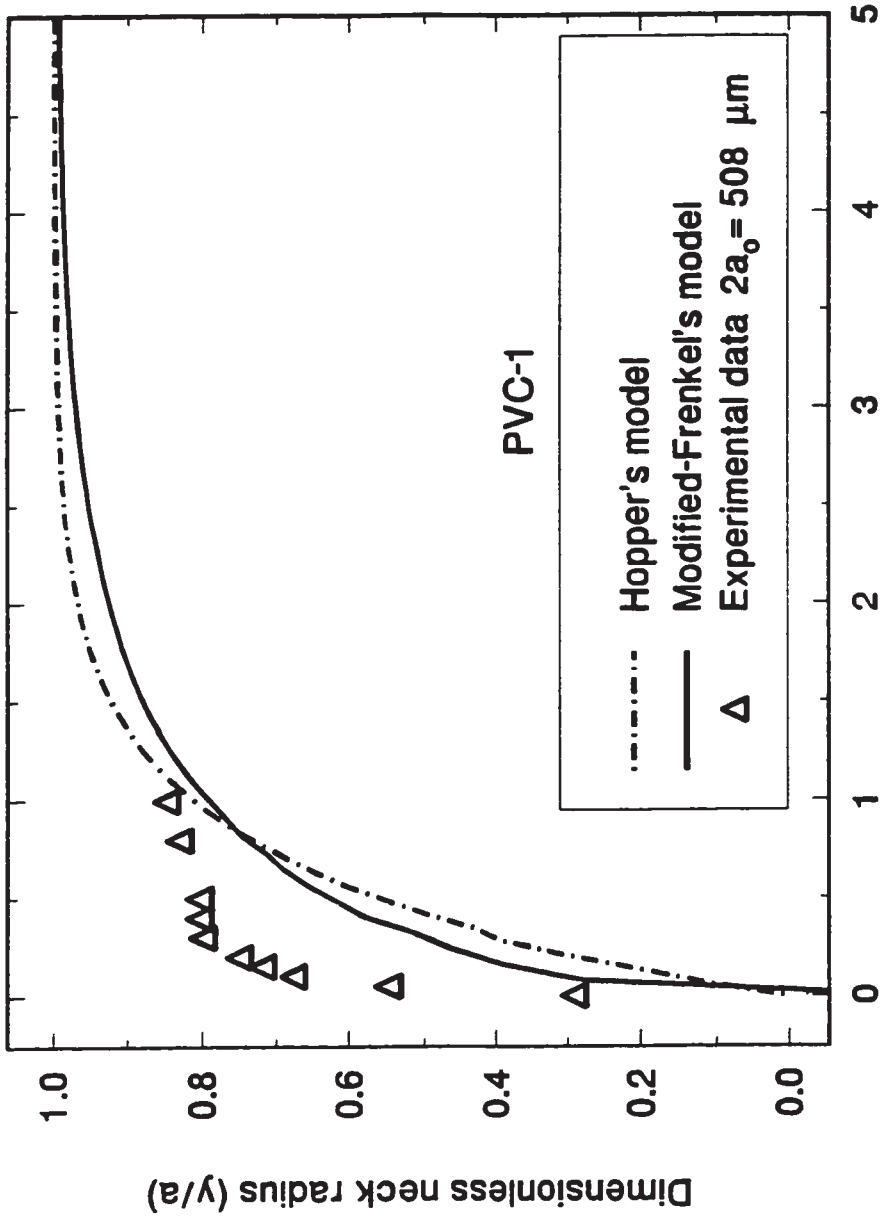

Figure 4.12 Comparison of the modified-Frenkel model predictions with Hopper's model (1984), and experimental data obtained with resin PVC-1 powder particles at 170°C.

This trend is similar to that obtained by Mazur and Plazek (1994) with acrylic resins. One should be cautious when drawing conclusions from these observations with the polycarbonate and the polyvinyl chloride resins. The value of the surface tension for the polycarbonate has been determined based on several assumptions (Petke and Ray, 1969). Also, it is probable that surfactants or other surface modifiers have been used in the manufacturing of the polyvinyl chloride resin. To investigate this possibility, accurate measurements of the surface tension of these resins would be necessary

4.4 Summary

A model for the coalescence of two equal sized spheres of Newtonian fluid has been proposed in the present study. The approach is similar to that of Frenkel, but the model describes the complete coalescence process. The resulting model predictions are relatively close to the other analytical and numerical solutions presented in the literature for the coalescence of spheres and cylinders. The main advantage of the present model over other analytical or numerical solutions for sintering is that the mathematical theory is simple enough to enable possible generalizations with considerations of other constitutive behavior or with inclusion into more general formulations of industrial processes, such as rotational molding or powder coating.

Experimental results obtained for the sintering of powder particles have been compared with the available theoretical models and with the proposed model. The predictions of both Frenkel and Frenkel-Eshelby models are significantly different from the experimental data. However, Hopper's model and the modified-Frenkel model

predictions are surprisingly close to most of our measurements. Based on comparisons with results obtained with a blow molding polyethylene resin, with polypropylene copolymers, and with a polyethylene copolymer, it was found that the Newtonian models predict faster coalescence than was observed experimentally. This result suggests that factors other than surface tension and viscosity play a role in the sintering of polymer particles. Experimental results obtained with polycarbonate and polyvinyl chloride appear to sinter at a faster rate than the Newtonian model predictions. This result was regarded with caution since some of the material properties used in this comparison are considered uncertain.

CHAPTER 5

VISCOELASTIC CONSIDERATIONS IN MODELING THE SINTERING PROCESS

5.1 Introduction

It has been suggested that the viscoelastic character of polymers play an important role in the sintering process (Lontz, 1964, Mazur and Plazek, 1994). Sintering experiments have also shown that resins that have high melt elasticity sinter slowly, as discussed in Chapter 3. In this particular case, the melt elasticity was defined as the resin's capacity of storing energy. Viscoelasticity may be related to the effects associated with non-linear time-dependent properties (Bird *et al.*, 1987). Under constant deformation or constant stress, viscoelastic material response may combine liquidlike or solidlike characteristics (Ferry, 1970).

As opposed to Newtonian fluids, polymers show some strain hardening in elongational flow, as reviewed by Meissner (1987). For polymer melts, the extensional viscosity is sensitive to the molecular structure, to the molecular weight distribution, and to the processing history (Macosko, 1994, Tzoganakis *et al*, 1989, Maxwell, 1995). The elongational viscosity is in general better represented by using viscoelastic constitutive equations (Tanner, 1988).

A fluid with a large extensional viscosity will show a high resistance to coalescence since the flow involved in the sintering is essentially extensional.

The sintering process can be viewed as a creep flow (Mazur, 1995). The sintering system is submitted to some stress induced by the surface curvature. A balance of normal and tangential forces at the surface of the sintering system can be written as follows:

$$\vec{n}\cdot(\vec{n}\cdot\tau^*) + P^* + \kappa = 0 \tag{5.1}$$

$$\vec{t}\cdot(\vec{n}\cdot\tau^*) = 0 \tag{5.2}$$

where $\vec{n}$, and $\vec{t}$ are the unit vectors normal and tangent to the surface, τ^* and P^* are the dimensionless stress tensor and pressure in the gas phase, respectively, and κ is the surface curvature (Martínez-Herrera and Derby, 1994). It has been thermodynamically demonstrated that the curvature at the neck of sintering of two particles causes stresses (Kuczynski, 1972).

Mazur and Plazek (1994) have suggested that the sintering particles undergo some elastic deformation due to the stresses induced by the surface curvature. Based on this assumption a resin with a higher elasticity will sinter at a faster rate than a purely viscous one. This finding was used to interpret the results that Mazur and Plazek (1994) obtained for the sintering of acrylic resins. However, it is not entirely obvious how to use this explanation to interpret the results obtained in the current study with the copolymer resins. The copolymer resins were found to have a higher elasticity than their

homopolymers counterparts (Kontopoulou *et al.*, 1997 (b)) while Newtonian sintering models predict a faster sintering rate than measured with these resins.

Another way to explain the role of viscoelasticity in polymer sintering is to consider the resin elasticity as its storage capacity (Ferry, 1970). A resin with a high energy storage capacity requires longer time for stresses to relax in stress relaxation experiment and requires longer time to deform in creep experiments. Based on this conjecture, it would be expected that a resin with high elasticity would sinter more slowly than a pure viscous material.

5.2 A viscoelastic model based on Frenkel's approach

The approach is based on the formulation proposed in Chapter 4 for the modified-Frenkel model, which describes the coalescence of two equal sized spheres. The convected Maxwell constitutive equation is used to introduce viscoelastic behavior in the description of the sintering process. The Maxwell constitutive equation is limited to the region of linear viscoelasticity. However, it is used by many authors in the simulation of complex problems because of its simplicity, and the results obtained give a good background for non-linear viscoelastic phenomena (Bird *et al*, 1987).

Generally, the upper convected Maxwell model (UCM) is used rather than the lower convected Maxwell model (LCM). The UCM can be derived from Rouse molecular theory and gives a more realistic prediction for the normal stresses in shear flow than the LCM (Larson, 1988). However, since the nature of the flow in sintering is essentially extensional, both UCM and LCM will be considered in the present study.

The convected Maxwell can be written as follows (Joseph, 1990):

$$\lambda \frac{\delta \tau}{\delta t} + \tau = 2\eta D \tag{5.3}$$

In Equation (5.3), the term λ is defined as a relaxation time and the term $\delta\tau/\delta t$ represents a general form of the invariant derivative of the extra-stress tensor:

$$\frac{\delta \tau}{\delta t} = \frac{D\tau}{Dt} - \omega \cdot \tau + \omega \cdot \tau - \alpha(D \cdot \tau + \tau \cdot D) \tag{5.4}$$

where $D\tau/Dt$ is the substantial derivative of the stress tensor and ω is the rotational tensor (Joseph, 1990). Equation (5.4) corresponds to the upper, lower and corotational derivatives for values α equal to -1, 1 and 0, respectively.

The flow field in the sintering system is defined to be extensional and the rotational tensor ω in Equation (5.4) is therefore equal to zero. Assuming quasi-steady state flow as a first approximation:

$$\tau + \lambda\alpha(D \cdot \tau + \tau \cdot D) = 2\eta D \tag{5.5}$$

the principal components of the extra-stress tensor can be defined as

$$\tau_{xx} = \frac{-4\eta\dot{\epsilon}}{1 - 4\alpha\lambda\dot{\epsilon}} \tag{5.6}$$

$$\tau_{yy} = \tau_{zz} = \frac{2\eta\dot{\epsilon}}{1 + 2\alpha\lambda\dot{\epsilon}} \tag{5.7}$$

Thus, the work of viscous forces W_v can be expressed as

$$W_v = \iiint_V \tau : D dV = \frac{32\pi a_o^3 \eta \dot{\epsilon}^2}{(1-4\alpha\lambda\dot{\epsilon})(1+2\alpha\lambda\dot{\epsilon})} \tag{5.8}$$

For the initial stage of sintering ($a=a_o$) the strain rate and the work of the surface tension can be defined as follows, as proposed by Frenkel (1945) and Eshelby (1949):

$$\dot{\epsilon} = \frac{1}{4}(\theta^2)' \tag{5.9}$$

$$W_s = \Gamma 2\pi a_o^2 (\theta^2)' \tag{5.10}$$

where $(\theta^2)'$ is defined as $\partial\theta^2/\partial t$. The energy dissipated by viscous flow is balanced by the energy from the reduction of the surface. After some manipulations, a quadratic expression in term of $(\theta^2)'$ is obtained, and with the assumption that $(\theta^2)'$ is always positive:

$$\theta^2 = t\ \frac{-\alpha\lambda - 2\frac{\eta a_o}{\Gamma} + \left[(3\alpha\lambda)^2 + 4\alpha\lambda\frac{\eta a_o}{\Gamma} + 4\left(\frac{\eta a_o}{\Gamma}\right)^2\right]^{1/2}}{2(\alpha\lambda)^2} \tag{5.11}$$

Equation (5.11) is based on the assumption that the particle radius is constant. Therefore for small value, θ^2 can be approximated as $(y/a)^2$.

Without the assumption that $a=a_o$, a non-linear differential equation is obtained by equating the energy dissipated by viscous flow, as described with Equation (5.8) with the work of surface tension (Equation 4.15):

$$8(\alpha\lambda K_1\theta')^2 + \left(2\alpha\lambda K_1 + \frac{\eta a_o}{\Gamma}\frac{K_1^2}{K_2}\right)\theta' - 1 = 0 \qquad (5.12)$$

where

$$K_1 = \frac{\sin(\theta)}{(1+\cos(\theta))(2-\cos(\theta))} \qquad (5.13)$$

$$K_2 = \frac{2^{-5/3}\cos(\theta)\sin(\theta)}{(1+\cos(\theta))^{4/3}(2-\cos(\theta))^{5/3}} \qquad (5.14)$$

A solution for $\theta(t)$ is obtained solving Equation (5.12) in a similar way as done with Equation (4.16). The initial boundary condition was fixed at a time value determined from the asymptotic solution obtained for Newtonian fluid. Once a solution for the evolution of the sintering angle with time is obtained, the evolution of the neck radius with time can easily be derived from Equations (4.20) (4.21) and (4.22).

5.3 Results and Discussion

Based on the use of the convected Maxwell constitutive equations, the model developed using this viscoelastic approach predicts that the sintering rate varies as a non-linear function of the material relaxation time and the term $\eta a_o/\Gamma$, which will be referred to as the characteristic sintering time. Figure 5.1 shows that, for small values of strain rate, the sintering model obtained using the upper convected Maxwell model (UCM) predicts an initial increase followed by a decrease of the coalescence rate.

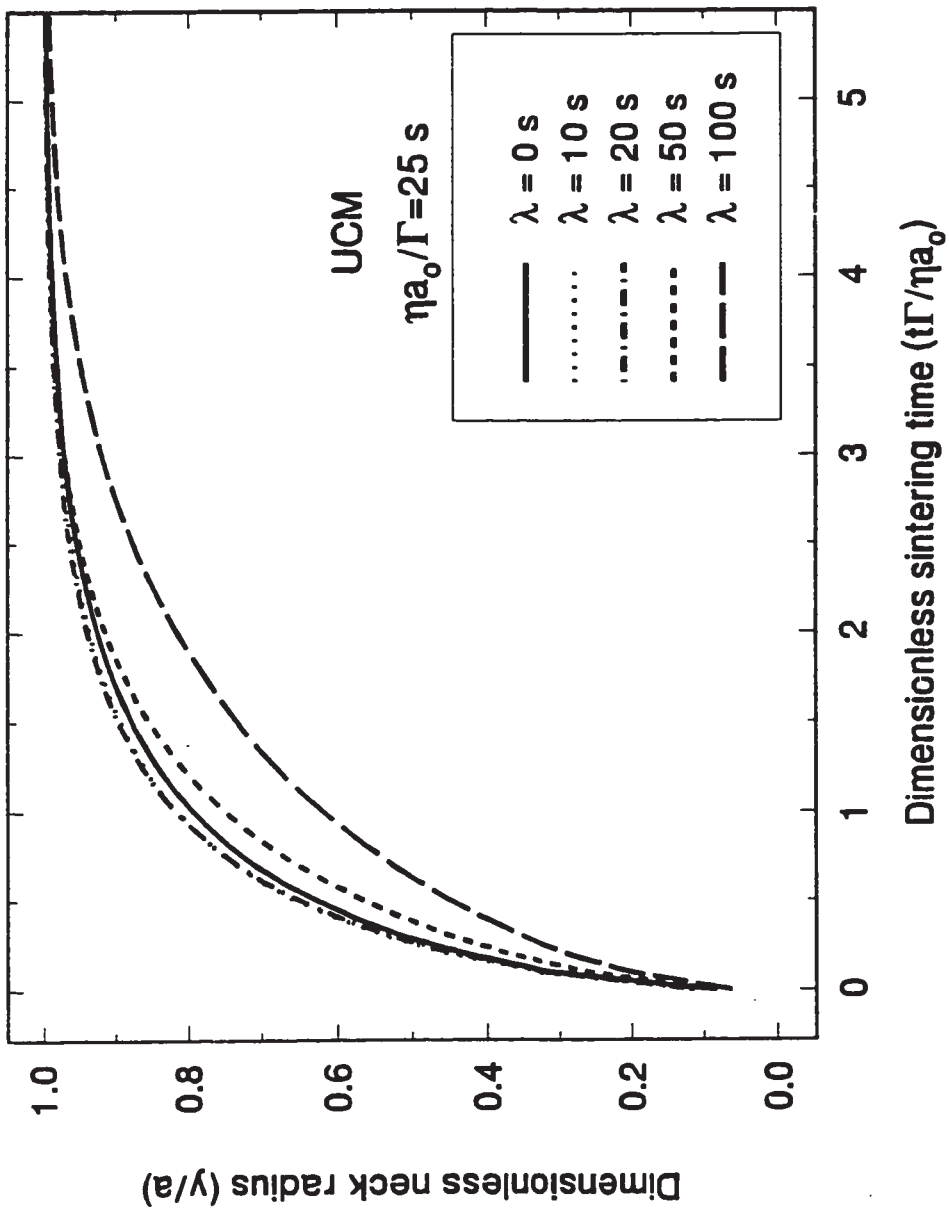

Figure 5.1 Modified-Frenkel model predictions with the upper convected Maxwell model ($\eta a_o/\Gamma$ =25 s).

It is interesting to note that in exit flow from tubes, increase and decrease of swelling has been observed as the Deborah number ($De=\lambda\dot{\gamma}$) increases with this particular viscoelastic model (Crochet and Keunings, 1980, Caswell and Viriyayuthakorn, 1983).

On the other hand, the sintering model obtained using the lower convected Maxwell model (LCM) predicts that the sintering rate decreases monotonically as the material relaxation time increases (Figure 5.2). Either with the UCM or the LCM, the sintering model predicts that as the characteristic time increases, the contribution of the relaxation time on the sintering rate diminishes, as illustrated in Figures 5.3 and 5.4. In Figures 5.5, 5.6, and 5.7, values of the material relaxation time were selected to give a fairly good comparison with experimental data. The predictions obtained from the current approach can simulate the trends experimentally observed for polymer sintering, as presented in the current work (Figures 5.5, 5.6 and 5.7) with the sintering rate decreasing as the relaxation time increases. Also, the model with the UCM explains the opposite effect of that reported in the literature (Mazur and Plazek, 1994).

The viscoelastic approach used to model polymer sintering is based on flow field and geometric assumptions. These assumptions appear reasonable, based on the numerical results presented by several authors (Jagota and Dawson, 1990, Martínez-Herrera and Derby, 1995). Yet, the predictions should be considered with caution. The use of viscoelastic constitutive equations usually results in the formulation of non-linear and implicit problems. In the present quasi-steady state approach, the time derivative of the stress tensor has been neglected in the formulation of the sintering problem. This simplification reduced greatly the complexity of the differential equation.

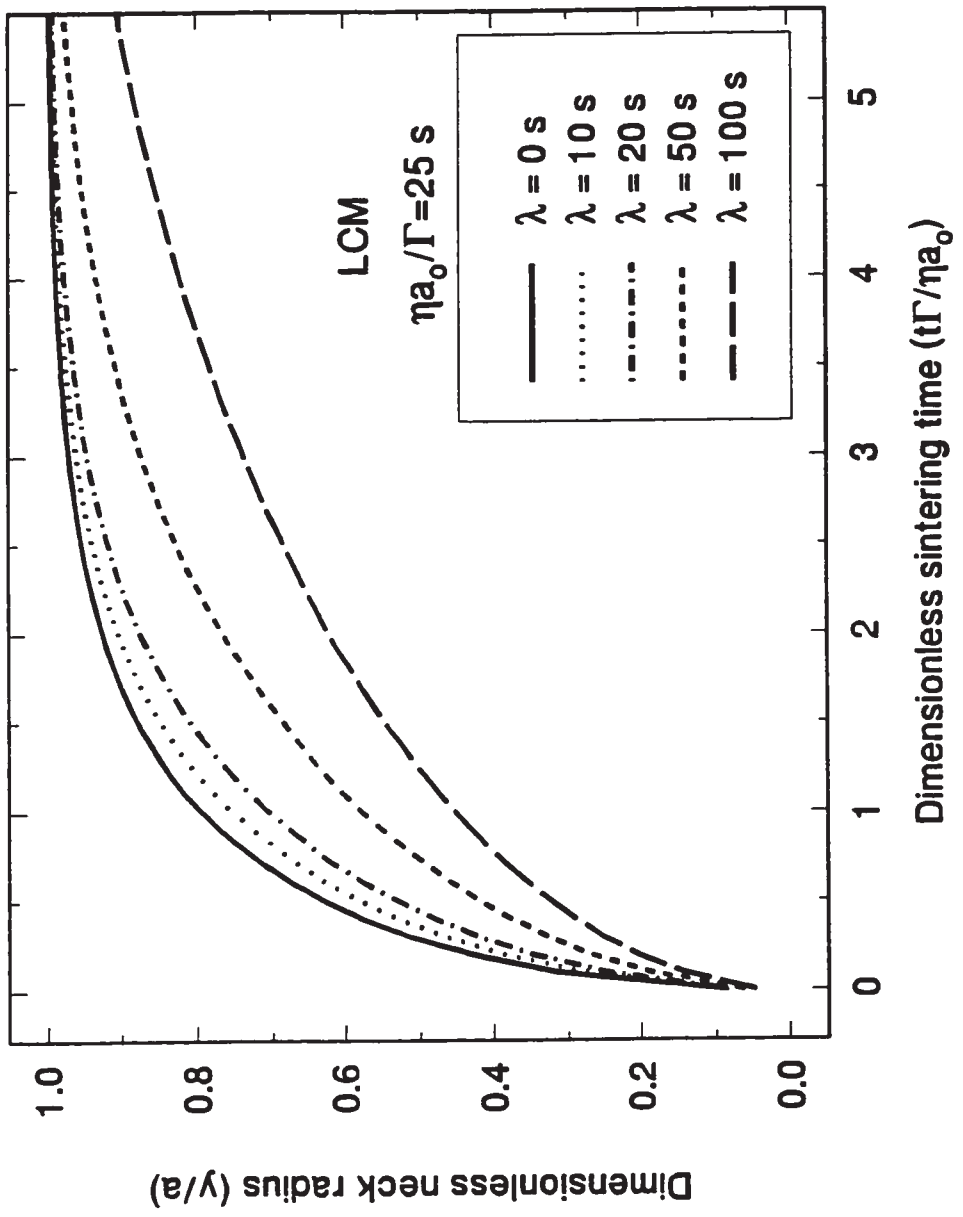

Figure 5.2 Modified-Frenkel model predictions with the lower convected Maxwell model ($\eta a_o/\Gamma = 25$ s).

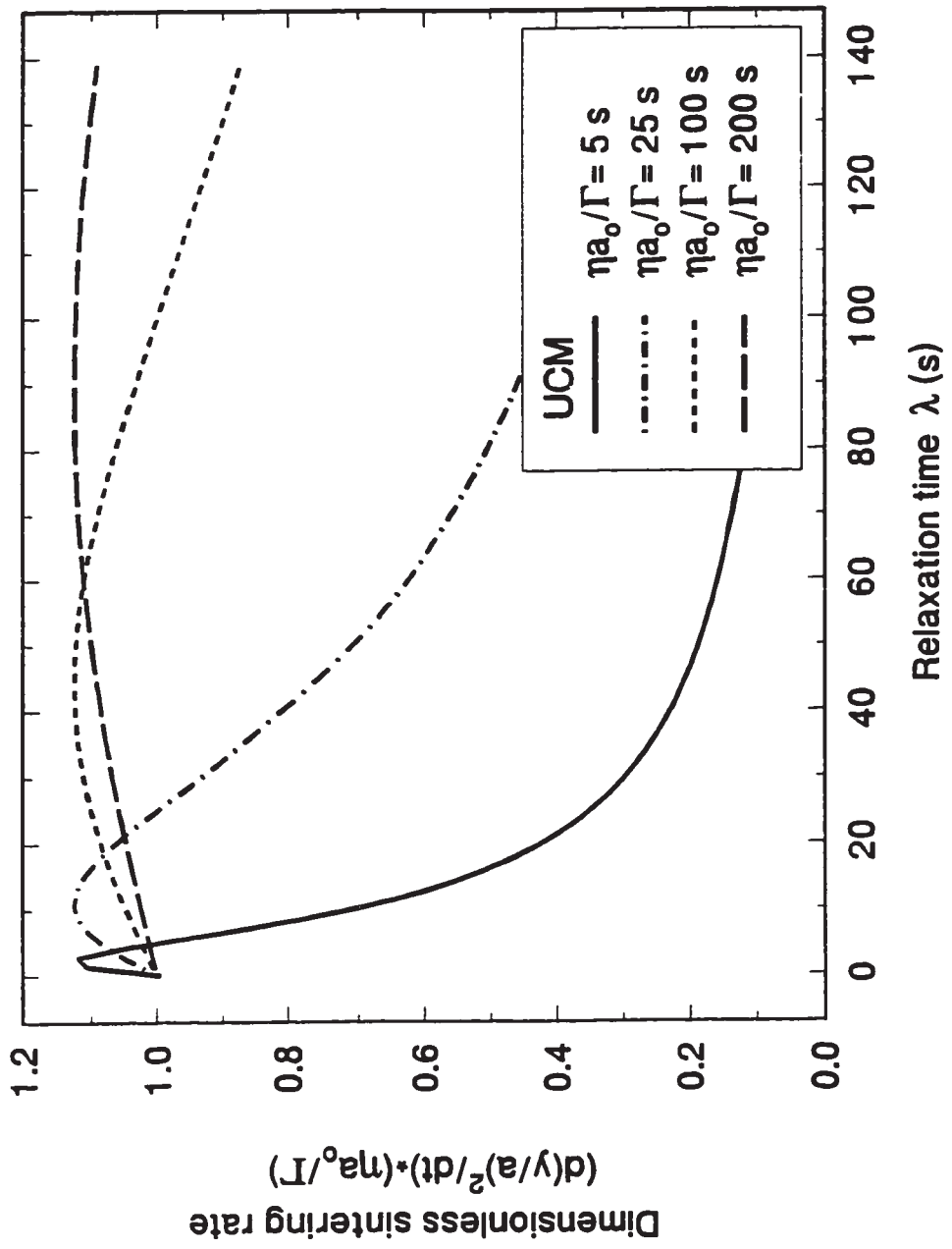

Figure 5.3 Frenkel-Eshelby model predictions with the upper convected Maxwell model.

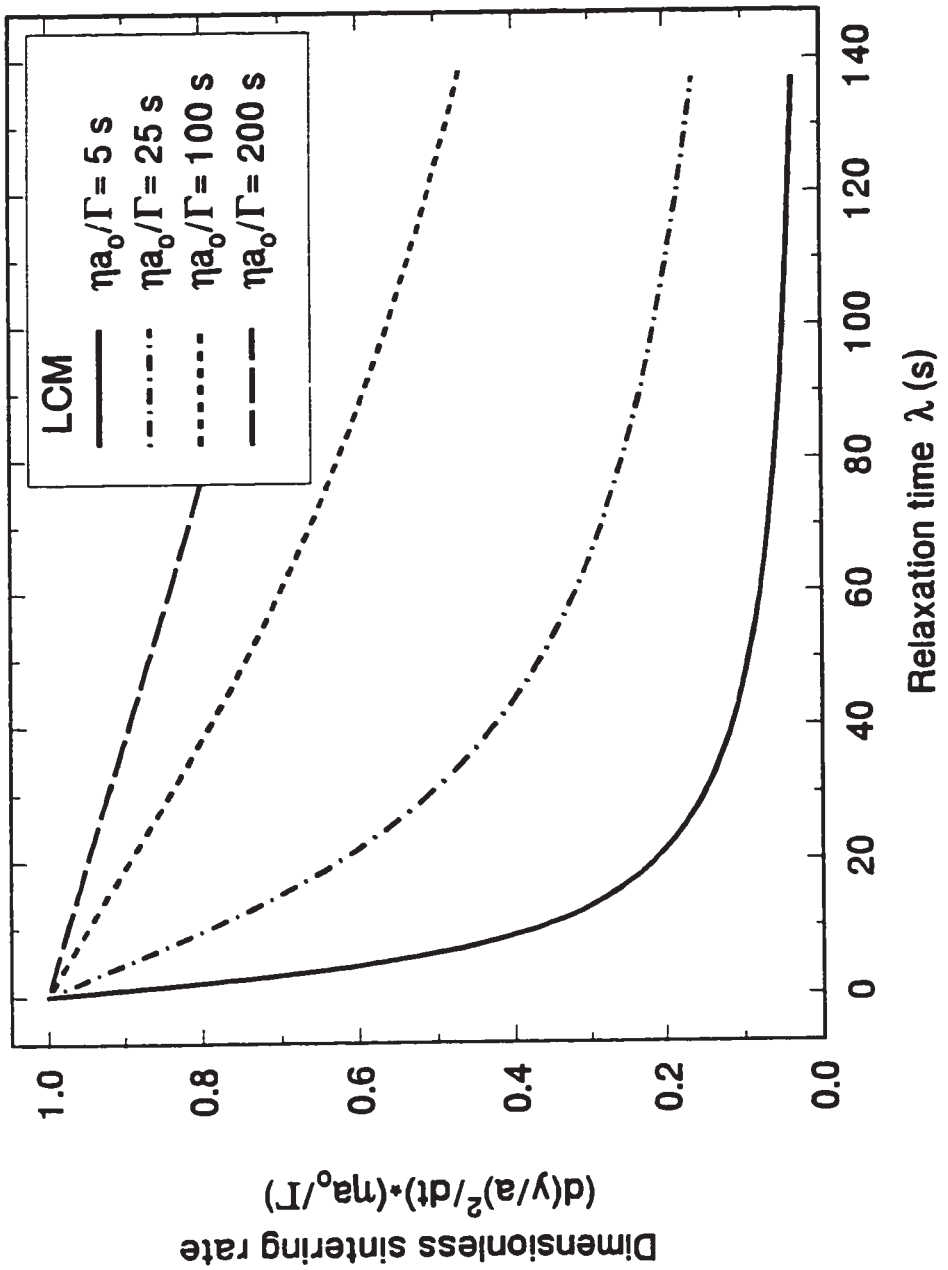

Figure 5.4 Frenkel-Eshelby model predictions with the lower convected Maxwell model.

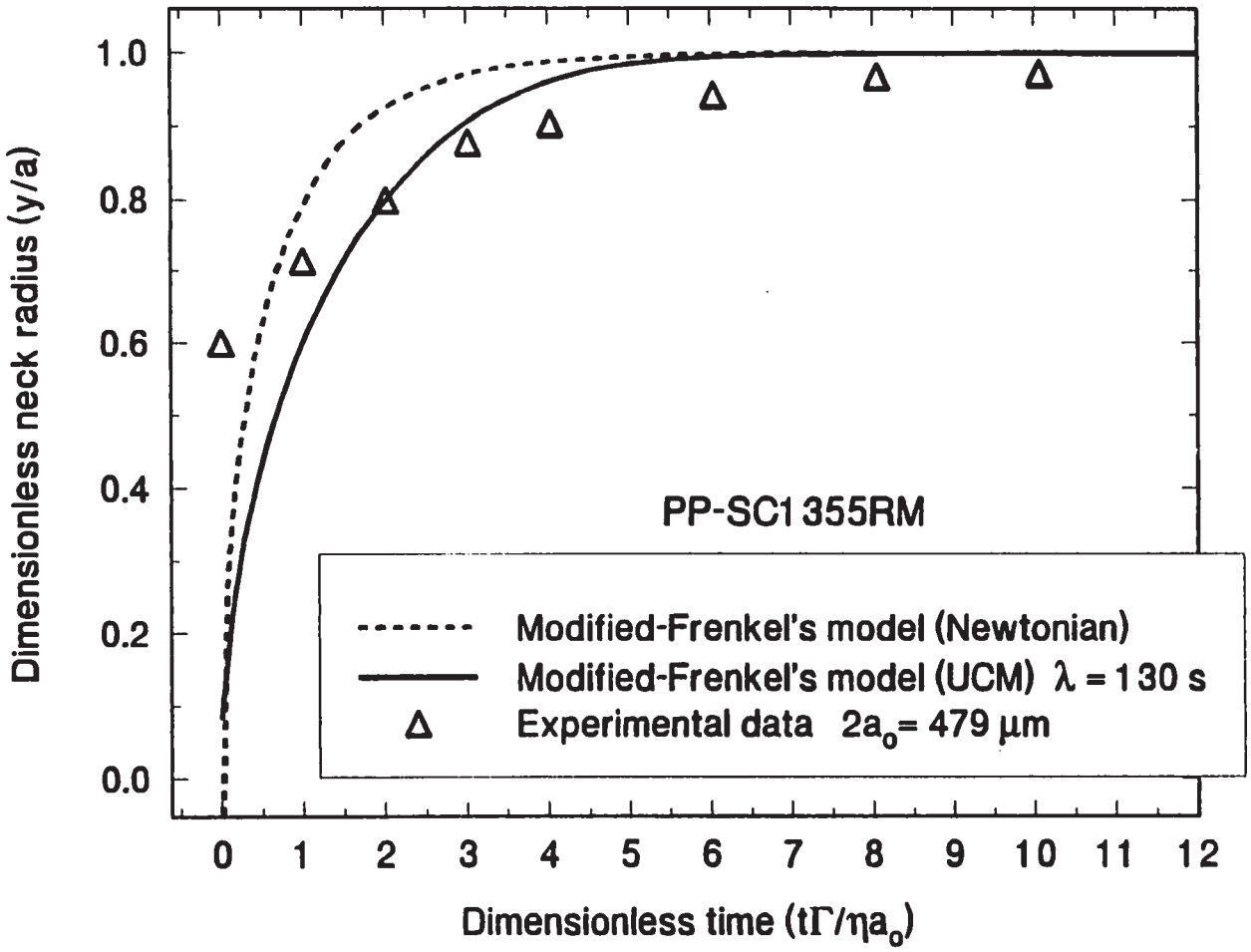

Figure 5.5 Comparison of the modified-Frenkel model with the upper convected Maxwell model ($\eta a_o/\Gamma$=29.9 s, λ=130 s) with experimental data obtained with resin PP-SC1355RM powder particles at 190°C.

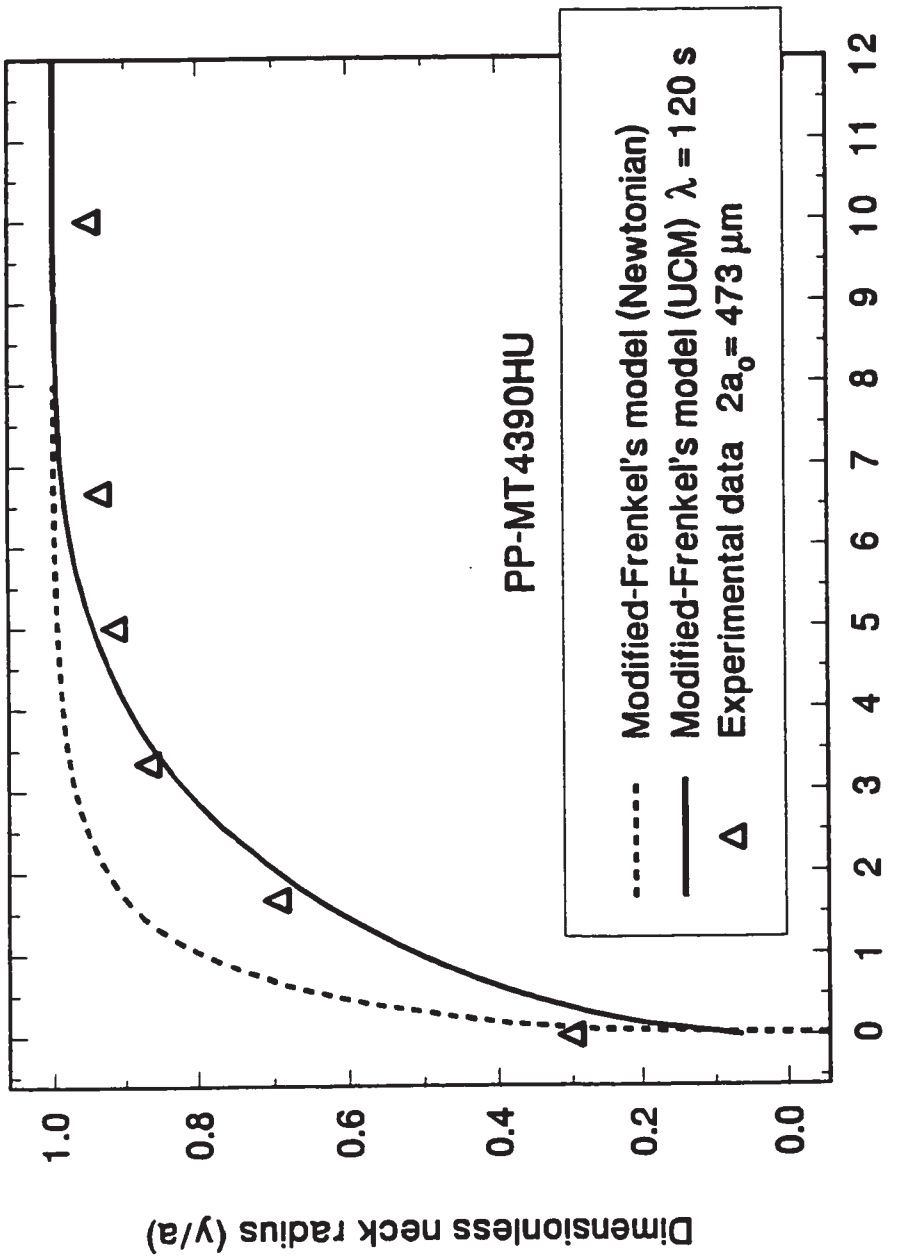

Figure 5.6 Comparison of the modified-Frenkel model with the upper convected Maxwell model ($\eta a_o/\Gamma = 18$ s, $\lambda = 120$ s) with experimental data obtained with resin PP-MT4390HU powder particles at 190°C.

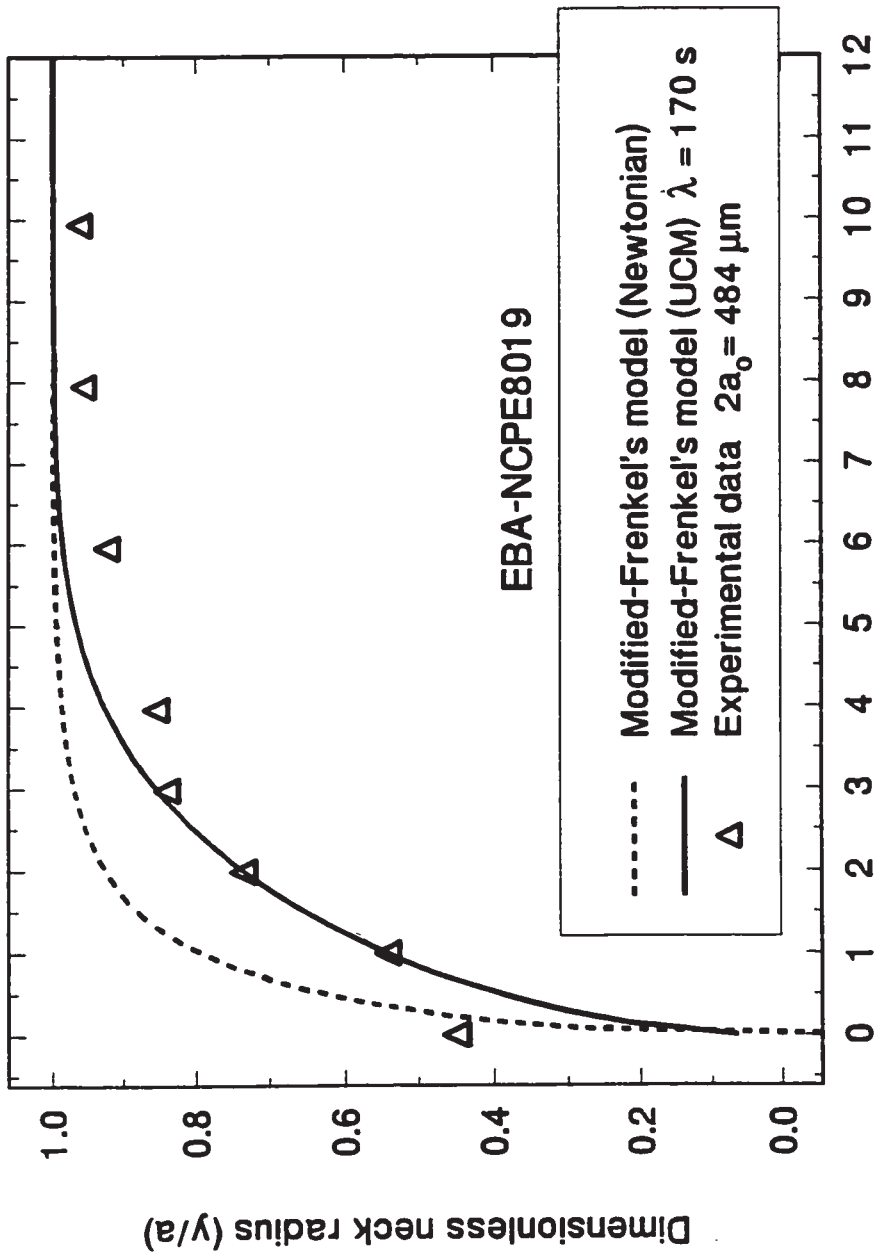

Figure 5.7 Comparison of the modified-Frenkel model with the upper convected Maxwell model ($\eta a_o/\Gamma = 30.2$ s, $\lambda = 170$ s) with experimental data obtained with resin EBA-NCPE8019 powder particles at 170°C.

Without this assumption, a more involved numerical algorithm would need to be implemented.

An attempt has been made to use the Phan-Thien Tanner (PTT) constitutive equation (Phan-Thien and Tanner, 1977, Phan-Thien, 1978) in modeling since it better represents the response of the fluid properties in elongational flow (Tanner, 1988). However, the model's predictions with the PTT are very close to the ones with the UCM. The use of the Phan-Thien Tanner constitutive equation in a sintering model would probably be relevant if the stress history were considered in the problem formulation.

5.4 Summary

The role of viscoelasticity in polymer sintering has been considered in the present work. Some authors have suggested that elastic deformations take place during polymer sintering (Mazur and Plazek, 1994). Although this suggestion has had some success to qualitatively validating the results obtained for sintering of acrylic resins (Mazur and Plazek, 1994), it can not explain the experimental results obtained in the present study with the copolymer resins. Alternatively, the resin elasticity could be viewed as its capacity to retain energy. Based on this conjecture, the stresses induced by the surface curvature would require longer time to cause deformations and would therefore slow down the sintering process.

A viscoelastic model has been proposed to describe polymer sintering. It has been developed based on Frenkel's approach, and it uses the convected Maxwell model.

A quasi-steady state approximation is used in the model formulation. With the upper convected Maxwell model, the viscoelastic sintering model predicts an increase followed by a decrease of the sintering rate as the material relaxation time increases. However, with the lower convected Maxwell model, the predicted sintering rate steadily decreases as the relaxation time increases. Moreover, based on the present viscoelastic sintering model, the coalescence rate becomes nearly independent on the material relaxation time as the characteristic sintering time (i.e., $\eta a_o/\Gamma$) increases. The current viscoelastic model has been successful in predicting the sintering rate obtained experimentally in the current work.

CHAPTER 6

CONCLUSIONS AND RECOMMENDATIONS

6.1 Conclusions

As a result of the research carried out in this thesis, the following conclusions have been made in regard to the experimental and modeling work done on polymer sintering in the context of the rotational molding process.

It has been confirmed that both the resin viscosity and viscoelasticity play a role in polymer sintering. It was found that as the viscosity of the resin increases, the sintering rate decreases, but this effect diminishes as the particle size decreases. The copolymer resins used in this study were known to have a higher melt elasticity as the copolymer content increased. The effect of the resin elasticity on the sintering rate was less explicit than the resin viscosity. The findings of this experimental study give some guidelines for an appropriate choice of resin for a reduced rotational molding cycle.

The effect of the geometry on the sintering rate has also been investigated. It was found that powder particles and cylindrical particles sinter in a similar way. While this study was originally conducted for comparison purposes, it has led to the considereration of micropellets as an alternative to powder in the rotational molding process. Numerical analysis revealed that the processing conditions for micropellets are severe.

This may affect the micropellet rheological properties which in turn affect the sintering process.

Experiments have been performed with a sintering temperature programmed to simulate the molding conditions during the heating cycle of the rotational molding process. Results obtained from these sintering experiments gave an insight into how the resin sinter and how bubbles are being formed during the rotational molding process. The effect of surface conditioning on the sintering process has been investigated. If significant, adhesion forces between the particles and the sintering surface would slow down the sintering process. Experimental results obtained with a glass surface, a glass surface with a lubricant, and a polymeric surface revealed that surface conditioning had little influence on the sintering process.

A sintering model has been developed based on Frenkel's approach to describe the complete sintering process. For a Newtonian fluid, the proposed model's predictions are close to those from theoretical and numerical results presented in the literature. Newtonian sintering models were found to be in good agreement with most of the experimental data obtained with rotational molding grade polyethylene. However, the Newtonian sintering model predicts a faster coalescence than that observed with the copolymer resins. This result suggests that properties other than the material surface tension and viscosity play a role in polymer sintering. The role of viscoelasticity in polymer sintering has been considered. It is expected that a longer time will be required for a resin to deform when given an applied stress if this resin has a high capacity in storing energy.

Viewing the sintering process as creeping flow may explain the reason why resins with high elasticity were found to sinter at a lower rate than that predicted by the Newtonian models.

An approach to modeling the sintering process for viscoelastic material has been proposed. Predictions using the convected Maxwell constitutive equations vary non-linearly as a function of the material relaxation time and the sintering characteristic time, defined as the product of the material viscosity with the initial particle radius divided by the surface tension. The proposed viscoelastic model predictions were found to fit the experimental results obtained in the current work.

6.2 Recommendations for future work

On the basis of the work carried out in this project, several comments and suggestions for future work may be made.

The material surface tension is an essential property in the sintering process. Tabulated data for the surface tension of polyethylene have been found in literature. However, for other resins such as polyvinyl chloride or polycarbonate, the data found in the literature were viewed with caution. To determine the relative effect of the material properties on the sintering rate for all resins, accurate measurements of the material surface tension need to be performed. This material property is essential in assessing the validity of theoretical models for polymer sintering.

The proposed viscoelastic sintering model is based on the use of the convected Maxwell constitutive equation with the approximation of a quasi-steady state flow as a first approximation. However, the sintering process is transient in nature. The model should be extended to consider the time derivative for the stress tensor in the problem formulation. Moreover, the flow in the sintering process is essentially extensional and therefore, the use of a constitutive equation which provides a realistic prediction for this type of flow would be relevant.

Not all of the effects of molding conditions on the sintering rate have been quantified. The current study was limited to the sintering of two particles at atmospheric pressure. In rotational molding, sintering occurs in a packing of particles where pressure is sometime applied. The contribution of forces such as pressure and gravity, and the effect of powder compaction on the sintering process should be examined.

It has been found that some resins sinter in a similar way although they were known to produce parts with different porosity in the rotational molding process. It appears that the results obtained for the sintering of two particles are not sufficient to characterize the resin processability in rotational molding. Experiments and models for the sintering of two particles do not address the process of bubble removal in a polymer melt. Consequently, in order to gain a better understanding of the rotational molding process, further studies should be performed on the process of bubble removal.

The proposed sintering models are based on the assumption that the material properties are constant. However, in rotational molding the material passes from a solid state into a melt state.

The solution of the heat transfer process and the sintering process in rotational molding would provide a useful tool to predict the effect of molding and material properties on the molding cycle and the molded part porosity.

REFERENCES

Allen, D. K., Metallurgy theory and practice, Am. Tech. Soc., Chicago (1969).

Anon., "Metallocene PEs could put a new spin on rotomolding", Modern Plastics, February, 30 (1997).

Argento, C., S. Mazur, and A. Jagota, "Problems in viscoelastic neck growth", in Sintering technology, Eds. R. M. German, G. L. Messing, R. G. Cornwall, M. Dekker, N. Y., (1996).

Association of Rotational Molders, The introductory guide to designing rotationally molded plastics parts, Chicago, IL (1982)

Association of Rotational Molders, Trouble-shooting manual, Chicago, IL (1989)

Ashby, M. F., "A first report on sintering diagrams", Acta Metall., **22**, 275 (1974).

Barnetson, A., P. R. Hornsby, "Observations on the sintering of ultra-high molecular weight polyethylene (UHMWPE) powders", J. Mater. Sci. Letters, **14**, 80 (1995).

Bawiskar, S., and J. L. White, "Comparative study of warpage, global shrinkage, residual stresses, and mechanical behavior of rotationally molded parts produced from different polymers", Polym. Eng. Sci., **34**, 815 (1994).

Bawiskar, S., and J. L. White, "Simulation of heat transfer and melting in rotational molding", Intern. Polym. Proc., **10**, 62 (1995).

Bellehumeur, C. T., M. K. Bisaria, and J. Vlachopoulos, "An experimental study and model assessment of polymer sintering", Polym. Eng. Sci., **36**, 2198 (1996).

Beruto, D., R. Botter, and A. W. Searcy, "The influence of thermal cycling on densification: further tests of a theory", in Ceramic powder science, **2**, Eds. G. L. Messing, E. R. Fuller, and H. Hausner, 911 (1988).

Bird, R. B., R. C. Armstrong, and O. Hassager, Dynamics of polymeric liquids, John Wiley & Sons, N. Y., **1** (1987).

Bisaria, M. K., E. Takács, C. T. Bellehumeur, and J. Vlachopoulos, "Anatomy of a rotomolding cycle", Rotation, **3**, (4), 12 (1994).

Bordia, R. K., and A. Jagota, "Crack growth and damage in constrained sintering films", J. Am. Ceram. Soc., **76**, 2475 (1993).

Brink, A. E., K. J. Jordens, and J. S. Riffle, "Sintering high performance semicrystalline polymeric powders", Polym. Eng. Sci., **35**, 1923 (1995).

Bross, P., and H. E. Exner, "Computer simulation of sintering processes", Acta Metall. **27**, 1013 (1979).

Burden, R. L., and J. D. Faires, Numerical Analysis, PWS Publ., Boston (1985).

Caswell, B., and M. Viriyayuthakorn, "Finite element simulation of die swell for a Maxwell fluid", J. Non-Newtonian Fluid Mech., **12**, 13 (1983).

Chen, C. H., J. L. White, and Y. Ohta, "Mold pressurization as a method to reduce warpage in rotational molding of polyethylene", Polym. Eng. Sci., **30**, 1523 (1990).

Coble, R. L., "Sintering crystalline solids. I. Intermediate and final state diffusion models", J. Appl. Phys., **32**, 787 (1961).

Coble, R. L., "Ceramic and metal sintering: mechanisms of material transport and density-limiting characteristics", in Fundamental phenomena in the materials sciences, **1**, Plenum Press, N. Y., 25 (1964).

Cosgrove, G. J., J. A. Strozier, and L. L. Seigle, "An approximate analytical model for the late-stage sintering of an array of rods by viscous flow", J. Appl. Phys., **47**, 1258 (1976).

Crawford, R. J., Rotational moulding of plastics, John Wiley & Sons, N. Y. (1992).

Crawford, R. J., "The emerging technology of rotational molding in the 90's", ARM's 21st Annual Fall Meeting, Vienna (1996).

Crawford, R. J., and P. J. Nugent, "Computer simulation of rotational moulding process for plastics", Plast. Rubb. Proc. Appl., **11**, 107 (1989).

Crawford, R. J., P. J. Nugent, and W. Xin, "Prediction of optimum process conditions for rotomolded products", Intern. Polym. Proc., **6**, 107 (1991).

Crawford, R. J., and P. J. Nugent, "A new process control system for rotational moulding", Plast. Rubb. Comp. Proc. Appl., **17**, 23 (1992) (a).

Crawford, R. J., and P. J. Nugent, "Impact strength of rotationally moulded polyethylene articles", Plast. Rubb. Proc. Appl., **17**, 33 (1992) (b).

Crawford, R. J., and J. A. Scott, "An experimental study of heat transfer during rotational moulding of plastics", Plast. Rubb. Proc. Appl., **5**, 239 (1985).

Crawford, R. J., and J. A. Scott, "The formation and removal of gaz bubbles in a rotational moulding grade of polyethylene", Plast. Rubb. Proc. Appl., **7**, 85 (1987).

Crochet, M. J., and R. Keunings, "Die swell of a Maxwell fluid: numerical prediction", J. Non-Newtonian Fluid Mech., **7**, 199 (1980).

Crolla, G., and G. Menges, "Sintering of PVC", J. Vinyl Tech., **11**, 125 (1989).

Daniels, E. S., and A. Klein, "Development of cohesive strength in polymer films from latices: effect of polymer chain interdiffusion and crosslinking", Prog. Org. Coat., **19**, 359 (1991).

De With, G., and A. J. Corbijn, "Fibre-on-plate experiments: relation and surface tension", J. Mater. Sci., **30**, 1742 (1995).

Dedrick, J. H., and A. Gerds, "A study of the mechanisms of sintering of metallic particles", J. Appl. Phys., **20**, 1042 (1949).

Eadie, R. L., and G. C. Weatherly, "Contributions of grain boundary and volume diffusion to shrinkage rates during sintering", in Sintering and catalysis, Ed. G. C. Kuczynski, Plenum Press, N. Y., 239 (1975).

Easterling, K. E., and A. R. Thölen, "A study of sintering using hot-stage electron microscopy", Metal Sci. J., **4**, 130 (1970).

Engineering design handbook - Rotational molding of plastic powders, Department of the army headquarters, United States Army Material Command, AMC Pamphlet 706-312 (1975).

Eshelby, J. D., Discussion in paper by A. J. Shaler "Seminar on the kinetics of sintering", Metals Trans., **185**, 806 (1949).

Espinasse, I., P. Cassagnau, and A. Michel, "Crosslinking of ethylene-vinylacetate and ethylene-methacrylate blends in rotomolding operations", Preprint Polym. Process. Soc. 9th Annual Meeting, (1991).

Exner, H. E., and G. Petzow, "Shrinkage and rearrangement during sintering of glass spheres", in Sintering and Catalysis, Ed. G. C. Kuczynski, Plenum Press, N. Y., 279 (1975).

Fisk, P. M., "The principles of film formation", in The science of surface coatings, Ed. H. W. Chatfield, London (1962).

Fortelný, I., and A. Živný, "Coalescence in molten quiescent polymer blends", Polymer, **21**, 4113 (1995).

Frenkel, J., "Viscous flow of crystalline bodies under the action of surface tension", J. Phys., **9**, 385 (1945).

Gala Industries, "Micropellets - An alternative rotomolding product form", Rotation , **4**, (4), 9 (1995).

German, R. M., and J. F. Lathrop, "Simulation of spherical powder sintering by surface diffusion", J. Mater. Sci., **13**, 921 (1978).

German, R. M., G. L. Messing and R. G. Cornwall, Eds., Sintering technology, M. Dekker, N. Y. (1996).

Graham, G. A. C., "The contact problem in the linear theory of viscoelasticity", Int. J. Eng. Sci., **3**, 27 (1965).

Gogos, G., L. Olson, X. Liu, and V. R. Pasham, "Computational model for rotational molding of thermoplastics", Proc. SPE ANTEC 97, Toronto, **3**, 3216 (1997).

Guggenheim, E. A., "The principle of corresponding states", J. Chem. Phys., **13**, 253 (1945).

Hahn, K., Ley, G., H. Schuller, and R. Oberthür, "On particle coalescence in latex films", Colloid & Polym. Sci., **264**, 1092 (1986).

Halldin, G. W., and I. L. Kamel, "Powder processing of ultra-high molecular weight polyethylene I. Powder characterization and compaction", Polym. Eng. Sci., **17**, 21 (1977).

Harkin-Jones, E., and R. J. Crawford, "Mechanical properties of rotationally molded Nyrim", Polym. Eng. Sci., **36**, 615 (1996).

Harkin-Jones, E., and R. J. Crawford, "Rotational molding of liquid plastic systems: an assessment of material moldability", Adv. Polym. Tech., **15**, 71 (1996).

Hata, T., and T. Kasemura, "Surface and interfacial tensions of polymer melts and solutions", in Polymer science and technology, Ed. L. H. Lee, **12A**, (1980).

Hinsken, H., S. Moss, J. R. Pauquet, and H. Zweifel, "Degradation of polyolefins during melt processing", Polymer Degradation and Stability, **34**, 279 (1991).

Hiram, Y., and A. Nir, "A simulation of surface tension driven coalescence", J. Colloid Interface Sci., **95**, 462 (1983).

Hopper, R. W., "Coalescence of two equal cylinders: exact results for creeping viscous plane flow driven by capillarity", Comm. Am. Ceram. Soc., **67**, C-263 (1984).

Hopper, R. W., "Plane Stokes flow driven by capillarity on a free surface", J. Fluid Mech., **213**, 349 (1990).

Hopper, R. W., "Plane Stokes flow driven by capillarity on a free surface. Part 2. Further developments", J. Fluid Mech., **230**, 355 (1991).

Hopper, R. W., "Stokes flow of a cylinder and half-space driven by capillarity", J. Fluid Mech., **243**, 171 (1992).

Hopper, R. W., "Coalescence of two viscous cylinders by capillarity: Part I, Theory", J. Am. Ceram. Soc., **76**, 2947 (1993) (a).

Hopper, R. W., "Coalescence of two viscous cylinders by capillarity: Part II, Shape evolution", J. Am. Ceram. Soc., **76**, 2953 (1993) (b).

Hornsby, P. R., and A. S. Maxwell, "Mechanism of sintering between polypropylene beads", J. Mater. Sci., **27**, 2525 (1992).

Hornsby, P. R., and R. I. Davidson, "Development and application of accelerated polymer sintering technology", Plast. Rubb. Comp. Proc. Appl., **25**, 13 (1996).

Jagota, A., and P. R. Dawson, "Micromechanical modeling of powder compact - I. Unit problems for sintering and traction induced deformation", Acta Metal., **36**, 2551 (1988) (a).

Jagota, A., and P. R. Dawson, "Micromechanical modeling of powder compact - II. Truss formulation of discrete packings", Acta Metal., **36**, 2563 (1988) (b).

Jagota, A., P. R. Dawson, and J. T. Jenkins, "An anisotropic continuum model for the sintering and compaction of powder packings", Mech. Mater., **7**, 255 (1988).

Jagota, A., and P. R. Dawson, "Simulation of the viscous sintering of two particles", J. Am. Ceram. Soc., **73**, 173 (1990).

Jagota, A., K. R. Mileska, and R. K. Bordia, "Isotropic constitutive model for sintering particle packing", J. Am. Ceram. Soc., **73**, 2266 (1990).

Jagota, A., and G. W. Scherer, "Viscosities and sintering rates of a two-dimensional granular composite", J. Am. Ceram. Soc., **76**, 3123 (1993).

Jagota. A., "Simulation of the viscous sintering of coated particles", J. Am. Ceram. Soc., **77**, 2237 (1994).

Jagota, A., and G. W. Scherer, "Viscosities and sintering rates of composite packings of spheres", J. Am. Ceram. Soc., **78**, 521 (1995).

Jandel Scientific Software, "SigmaScan/Image, Image measurement software", (1992).

Janney, M. A., and H. D. Kimrey, "Microwave sintering of alumina at 28 GHz", in Ceramic powder science, **2**, Eds. G. L. Messing, E. R. Fuller, and H. Hausner, 904 (1988).

Jarvis, N. L., R. B. Fox, and W. A. Zisman, Adv. Chem. Ser., **43**, 317 (1964).

Jayaraman, G. S., J. F. Wallace, P. H. Geil, and E. Baer "Cold compaction molding and sintering of polystyrene", Polym. Eng. Sci., **16**, 529 (1976).

Johnson, D. L., and T. M. Clarke, "Grain boundary and volume diffusion in the sintering of silver", Acta Metall., **12**, 1173 (1964).

Johnson, D. L., "New method of obtaining volume, grain-boundary, and surface diffusion coefficient from sintering data", J. Appl. Phys., **40**, 192 (1969).

Johnson, D. L., "A general model for the intermediate stage of sintering", J. Am. Ceram. Soc., **53**, 574 (1970).

Johnson, D. L., W. B. Sanderson, E. L. Kemer, and J. Knowlton, "Plasma sintering of ceramics", in Defect properties and processing of high-technology nonmetallic materials, Materials Research Soc. Symp. Proc., **24**, Eds. J. H. Crawford, Y. Chen, and W.A. Sibley, 273 (1984).

Johnson, K. L., K. Kendall, and A. D. Roberts, "Surface energy and the contact of elastic solids", Proc. R. Soc. Lond. A, **324**, 301 (1971).

Joseph, D. D., Fluid dynamics of viscoelastic liquids, Springer-Verlag, N. Y. (1990).

Kausch, H. H., and M. Tirrell, "Polymer inderdiffusion", Ann. Reviews Mater. Sci., **19**, 341 (1989).

Khakhar, D. V., J. J. McCarthy, T. Shinbrot, and J. M. Ottino, "Transverse flow and mixing of granular materials in a rotating cylinder", Phys. Fluids, **9**, 31 (1997).

Kelly, P. Y., "A microscopic examination of rotomoulded polyethylene", Du Pont Canada (undated).

Kemer, E. L., and D. L. Johnson, "Microwave plasma sintering of alumina", Am. Ceram. Soc. Bull., **64**, 1132 (1985).

Kendall, K, and J. C. Padget, "Latex coalescence", Int. J. Adhesion and Adhesives, July, 149 (1982).

Kendall, K., and J. C. Padget, "Contact of polymer latex particles with metals", J. Adhesion, **22**, 39 (1987).

Kim, J. S., and D. L. Johnson, "Plasma sintering of alumina", Ceram. Bull., **62**, 620 (1983).

Kingery, W. D., and M. Berg, "Study of the initial stage of sintering solids by viscous flow, evaporation-condensation, and self-diffusion", J Appl. Phys., **21**, 1205 (1955).

Kingery, W. D., H. K. Bowen, and D. R. Uhlmann, Introduction to ceramics, John Wiley & Sons, N. Y. (1976).

Kontopoulou, M., A study of the parameters involved in the rotational molding of plastics, Master Eng. Thesis, McMaster University, Chemical Engineering, Canada (1995).

Kontopoulou, M., M. Bisaria, and J. Vlachopoulos, "An experimental study of rotational molding of polypropylene/polyethylene copolymers", to appear in Intern. Polym. Proc., **12**, (1997) (a).

Kontopoulou, M., Takács, C. T. Bellehumeur, and J. Vlachopoulos, "A comparative study of the rotomolding characterics of various polymers", Proc. SPE ANTEC 97, Toronto **3**, 3220 (1997) (b).

Kuczynski, G. C., "Self-diffusion in sintering of metallic particles", Metals Trans., **1**, 169 (1949) (a).

Kuczynski, G. C., "Study of the sintering of glass", J. Phys., **20**, 1160 (1949) (b).

Kuczynski, G. C., and I. Zaplatynsyj, "Sintering of glass", J. Am. Ceram. Soc., **39**, 350 (1956)

Kuczynski, G. C., B. Neuville, and H. P. Toner, "Study of sintering of poly(methyl methacrylate)", J. Appl. Polym. Sci., **14**, 2069 (1970).

Kuczynski, G. C., "Physics and chemistry of sintering", Adv. Colloid Interface Sci., **3**, 275 (1972).

Kuiken, H. K., "Viscous sintering: the surface-tension-driven flow of a liquid form under the influence of curvature gradients at its surface", J. Fluid Mech., **214**, 503 (1990).

Lange, F. F., "Sinterability of agglomerate powders", in Defect properties and processing of high-technology nonmetallic materials, Materials Research Soc. Symp. Proc., **24**, Eds. J. H. Crawford, Y. Chen, and W.A. Sibley, 247 (1984).

Lange, F. F., "De-sintering, a phenomenon concurrent with densification within powder compacts: a review", in Sintering technology, Eds. R. M. German, G. L. Messing, R. G. Cornwall, M. Dekker, N. Y., (1996).

Larson, R. G., Constitutive equations for polymer melts and solutions, Butterworths, Boston (1988).

Leaversuch, R. D., "Rotomolders fuse science and craft, enhance quality", Modern Plastics, October, 59 (1995).

Leco Instruments, "LECO 2001", Mississauga, Ontario, Canada (1992).

Lee, E. H., and J. R. M. Radoc, "The contact problem for viscoelastic bodies", Trans. ASME, Sept., 438 (1960).

Liu, Y. S., J. Feng, and M. A. Winnik, "Study of polymer diffusion across the interface in latex films through direct energy transfer experiments", J. Chem. Phys., **101**, 9096 (1994).

Liu, S. J., "A study of the sintering behavior of polyethylene", Rotation, **5**, (4) 20 (1996).

Lontz, J. F., "Sintering of polymer material", in Fundamental phenomena in the materials sciences, **1**, Plenum Press, N. Y., 25 (1964).

Mackenzie, J. K., and R. Shuttleworth, "A phenomenological theory of sintering", Proc. Phys. Soc., **62**, 833 (1949).

Macosko, C. W., Rheology: principles, measurements, and applications, VCH Publ., N. Y., (1994).

Martínez-Herrera, J. I., and J. J. Derby, "Analysis of capillary-driven viscous flows during the sintering of ceramic powders", AIChE J., **40**, 1794 (1994).

Martínez-Herrera, J. I., and J. J. Derby, "Viscous sintering of spherical particles via finite element analysis", J Am. Ceram. Soc., **78**, 645 (1995).

Maxwell, B. "Melt elasticity measurements, the compliment and supplement to melt flow measurements", SPE ANTEC 95, Boston, **1**, 1078 (1995).

Mazur, S., and D. J. Plazek, "Viscoelastic effects in the coalescence of polymer particles", Prog. Org. Coat., **24**, 225 (1994).

Mazur, S., "Coalescence of polymer particles", in Polymer powder technology, John Wiley & Sons, (1995).

McCarthy, J. J., T. Shinbrot, G. Metcalfe, J. E. Wolf, and J. M. Ottino, "Mixing of granular materials in slowly rotated containers", AIChE J., **42**, 3351 (1996).

Meissner, J., "Polymer melt elongation - Methods, results, and recent developments", Polym. Eng. Sci., **27**, 537 (1987).

Muller, B., and H. Howard, "Plastics formulating and compounding for rotational molding", Plastics Formulating & Compounding, Nov-Dec., 37 (1995).

Nagy, T., and J. L. White, "The effect of colorants on the properties of rotomolded polyethylene parts", Polym. Eng. Sci., **36**, 1010 (1996).

Narkis, M., "Sintering behavior of poly(methyl methacrylate) particles", Polym. Eng. Sci., **19**, 889 (1979).

Narkis, M., M. Puterman, H. Boneh, and S. Kenig, "Rotational molding of thermosetting three-phase syntactic foams", Polym. Eng. Sci., **22**, 417 (1982).

Nelson, J. C., N. K. Vail, J. W. Barlow, J. J. Beaman, D. L. Bourell, and H. L. Marcus, "Selective laser sintering of polymer-coated silicon carbide powders", Ind. Eng. Chem. Res., **34**, 1641 (1995).

Nichols, F. A., and W. W. Mullins, "Morphological changes of a surface of revolution due to capillarity-induced surface diffusion", J. Appl. Phys., **36**, 1826 (1965).

Nugent, P. J., A study of heat transfer and process control in the rotational moulding of polymer powders, Ph.D. thesis, Queen's University of Belfast, Department of Mechanical and Manufacturing Engineering, Belfast, Northern Ireland (1990).

Nugent, P. J., R. J. Crawford, and L. Xu, "Computer prediction of cycle times during rotational molding of plastics", Adv. Polym. Tech., **11**, 181 (1992).

O'Neill, S., and R. J. Crawford, "Investigation of cooling during rotational moulding", ARM's 21st Annual Fall Meeting, (1996).

Pekcan Ö., M. A. Winnik, and M. D. Croucher, "Fluorescence studies of coalescence and film formation in poly(methyl methacrylate) nonaqueous dispersion particles", Macromolecules, **23**, 2673 (1990).

Petke, F. D., and R. B. Ray, "Temperature dependence of contact angles of liquids on polymeric solids", J. Colloid Interface Sci., **31**, 216 (1969).

Phan-Thien, N. and R. I. Tanner, "A new constitutive equation derived from network theory", J. Non-Newtonian Fluid Mech., **2**, 353 (1977).

Phan-Thien, N., "A nonlinear network viscoelastic model", J. Rheol., **22**, 259 (1978).

Pietsch, W., "Successfully use, agglomeration for size enlargement", Chem. Eng. Prog., April, 29 (1996).

Pokluda, O., C. T. Bellehumeur, and J. Vlachopoulos, "A modification of Frenkel's model for sintering", AIChE J., (accepted, 1997).

Progelhof, R. C., and J. L. Throne, "Parametric concepts in liquid rotational molding", Polym. Eng. Sci., **16**, 680 (1976).

Progelhof, R. C., G., Cellier, and J. Throne, "New technology in rotational molding powder densification", SPE Annual Tech. Conf., San Francisco (1982).

Rabinovitz, E., and Z. Rigbi, "Rotational reaction molding of polyurethane", Plast. Rubb. Proc. Appl., **5**, 365 (1985).

Rahaman, M. N., "Effect of rigid inclusions on sintering", in Ceramic powder science, **2**, Eds. G. L. Messing, E. R. Fuller, and H. Hausner, 887 (1988).

Rao, M. A. and J. L. Throne, "Principles of rotational molding", Polym. Eng. Sci., **12**, 237 (1972).

Rastogi, A. K., and L. E. St. Pierre, "Interfacial phenomena in macromolecular systems III, The surface free-energies of polymers", J. Colloid Interface Sci., **31**, 168 (1969).

Reed, J. S., Introduction to the principles of ceramic processing, John Wiley & Sons, N. Y. (1988).

Roe, R. J., "Surface tension of polymer liquids", J. Phys. Chem., **72**, 2013 (1968).

Rosenzweig, N., and M. Narkis, "Coalescence phenomenology of spherical polymer particles by sintering", Polym. Comm., **21**, 988 (1980).

Rosenzweig, N., and M. Narkis, "Dimensional variations of two spherical polymeric particles during sintering", Polym. Eng. Sci., **21**, 582 (1981) (a).

Rosenzweig, N., and M. Narkis, "Sintering rheology of amorphous polymers", Polym. Eng. Sci., **21**, 1167 (1981) (b).

Rosenzweig, N., and M. Narkis, "Newtonian sintering simulator of two spherical particles", Polym. Eng. Sci., **23**, 32 (1983).

Ross, J. W., W. A. Miller, and Weatherly, G. C., "Dynamic computer simulation of viscous flow sintering kinetics", J. Appl. Phys., **52**, 3884 (1981).

Russell, T. P., V. R. Deline, W. D. Dozier, G. P. Felcher, G. Agraval, R. P. Wool, and J. Q. Mays, "Direct observation of reptation at polymer interface", Nature, **365**, 235 (1993).

Scherer, G. W., "Sintering of low-density glasses: I, Theory", J. Am. Ceram. Soc., **60**, 236 (1977) (a).

Scherer, G. W., D. L. Bachman, "Sintering of low-density glasses: II, Experimental study", J. Am. Ceram. Soc., **60**, 243 (1977) (b).

Scherer, G. W., "Sintering of low-density glasses: III, Effect of a distribution of pores sizes", J. Am. Ceram. Soc., **60**, 243 (1977) (c).

Scherer, G. W., "Viscous sintering of a bimodal pore-size distribution", J. Am. Ceram. Soc., **67**, 709 (1984).

Scherer, G. W., and T. Garino, "Viscous sintering on a rigid substrate", J. Am. Ceram. Soc., **68**, 216 (1985).

Scott, J. A., A study of the effect of process variables on the properties of rotationally moulded plastic articles, Ph.D. Thesis, Queen's University of Belfast, Department of Mechanical and Industrial Engineering, Belfast, Northern Ireland (1986).

Siegmann, A., I. Raiter, M. Narkis, and P. Eyerer, "Effect of powder particle morphology on the sintering behaviour of polymers", J. Mater. Sci., **21**, 1180 (1996).

Spence, A. G., Analysis of bubble formation and removal in rotationally moulded products, Ph.D. Thesis, Queen's University of Belfast, Department of Mechanical and Industrial Engineering, Belfast, Northern Ireland (1994).

Spence, A., and R. J. Crawford, "The effect of processing variables on the formation and removal of bubbles in rotationally molded products", Polym. Eng. Sci., **36**, 993 (1996).

Sperling, L. H., Introduction to physical polymer science, John Wiley & Sons, N. Y. (1986).

Sun, D. W., and R. J. Crawford, "Computer simulation of rotational moulding heat transfer processes", Plast. Rubb. Comp. Proc. Appl., **19**, 47 (1993) (a).

Sun, D. W., and R. J. Crawford, "Analysis of the effects of internal heating and cooling during the rotational molding of plastics", Polym. Eng. Sci., **33**, 132 (1993) (b).

Sundararaj, U., and C. W. Macosko, "Drop breakup and coalescence in polymer blends: the effects of concentration and compatibilization", Macromolecules, **28**, 2647 (1995).

Takács, E., C. T. Bellehumeur, and J. Vlachopoulos, "Differences in rotomoldability of polyethylene micropellets and powders", Rotation, **5** (3), 17 (1996).

Tanaka, A., "Rotational molding of ABS resin", Japan Plastics, January (1974).

Tanner, R. I., Engineering Rheology, Oxford Univ. Press, N. Y. (1988).

Throne, J. L., "Some factors influencing cooling rates of rotational molding parts", Polym. Eng. Sci., **12**, 335 (1972).

Throne, J. L., "Rotational molding heat transfer - An update", Polym. Eng. Sci., **16**, 257 (1976).

Throne, J. L., Plastics process engineering. Marcel Dekker, N. Y. (1979).

Throne, J. L., and J. Gianchandani, "Reactive rotational molding", Polym. Eng. Sci., **20**, 899 (1980).

Throne, J. L., and M. S. Sohn, "Characterization of rotational molding grade of polyethylene powder", Advances Polym. Tech., **9**, 181 (1989).

Throne, J. L., "Study of the compaction and sintering of two high-performance thermoplastic polyimides", Adv. Polym. Tech., **9**, 281 (1989).

Thümmler, F., and W. Thomma, "The sintering process", Metall. Reviews, **12**, 69 (1967).

Timoshenko, S. P., and J. N. Goodier, "Theory of elasticity", McGraw-Hill, N. Y. (1970).

Ting, J. M., and R. Y. Lin, "Effect of particle-size distribution on sintering, Part I Modelling", J. Mater. Sci., **29**, 1867 (1994).

Ting, T. C. T., "The contact stresses between a rigid indenter and a viscoelastic half-space", J. Appl. Mech., December, 845 (1966).

Truss, R. W., K. S. Han, J. F. Wallace, and P. H. Geil, "Cold compaction molding and sintering of ultra high molecular weight polyethylene", Polym. Eng. Sci., **20**, 747 (1980).

Tuminello, W. H., "Relating rheology to molecular weight properties of polymers", in Encyclopedia of fluid mechanics, **9**, Ed. N. Cheremisinoff, (1990).

Tzoganakis, C., J. Vlachopoulos, and A. E. Hamielec, "Effect of molecular weight distribution on the rheological and mechanical properties of polypropylene", Polym. Eng. Sci., **29**, 390 (1989).

Utracki, L. A., and Z. H. Shi, "Development of polymer blend morphology during compounding in a twin-screw extruder. Part I: Droplet dispersion and coalescence - A review", Polym. Eng. Sci., **32**, 1824 (1992).

Van de Vorst, G. A. L., R. M. M. Mattheij, and H. K. Kuiken, "A boundary element solution for two-dimensional viscous sintering", J. Comp. Phys., **100**, 50 (1992).

Van de Vorst, G. A. L., "Integral method for a two-dimensional Stokes flow with shrinking holes applied to viscous sintering", J. Fluid Mech., **257**, 667 (1993).

Van de Vorst, G. A. L., Modelling and numerical simulation of viscous sintering, Ph.D. thesis, Eindhoven University of Technology, The Netherlands (1994).

Vick, L. W., and R. G. Kander, "Physical aging effects in the compaction and sintering of polycarbonate powder", Plast. Eng., August, 23 (1996).

Vlachopoulos, J., C. T. Bellehumeur, and M. Kontopoulou, "The role of rheology in rotomolding", Proc. 12th Int. Cong. Rheol., Quebec, 693 (1996).

Vlachopoulos, J., N. Silvi, and J. Vleck, "POLYCAD®: A finite element package for molten polymer flow", in Computer-aided engineering for polymer processing, application to extrusion and other continuous processes, Hanser Verlag, Munich, (1992).

White, J. L., S. Bawiskar, and T. Nagy, "Rotational molding of ABS resins", University of Akron, Akron, Ohio, (undated).

Wilson, T. L., and P. G. Shewmon, "The role of interfacial diffusion in the sintering of copper", Trans. Metall. Soc. AIME, **236**, 48 (1966).

Wu, S., Org. Coat. Plast. Chem., **31**, 27 (1971).

Wu, S., Polymer interface and adhesion, Marcel Dekker, N. Y. (1982).

Xu, L., Rotational moulding of thick wall products, Ph.D. Thesis, Queen's University of Belfast, Department of Mechanical and Industrial Engineering, Belfast, Northern Ireland (1994).

Xu, L., and R. J. Crawford, "Analysis of the formation and removal of gas bubbles in rotationally moulded thermoplastics", J. Mater. Sci., **28**, 2067 (1993).

Xu, L., and R. J. Crawford, "Computer simulation of the rotational moulding process", Plast. Rubb. Comp. Proc. Appl., **21**, 257 (1994).

Xu, L., and R. J. Crawford, "The development of the computer simulation program for the rotomolding process", SPE ANTEC 97, Toronto, **3**, 3205 (1997).

Yan, W. H., "The contact problem for viscoelastic bodies", J. Appl. Mech., June, 395 (1966).

IMAGE EVALUATION TEST TARGET (QA-3)

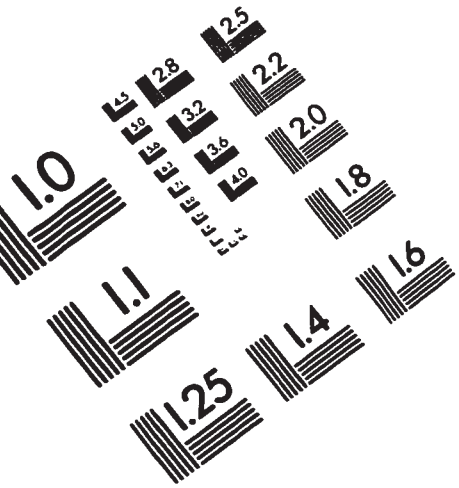

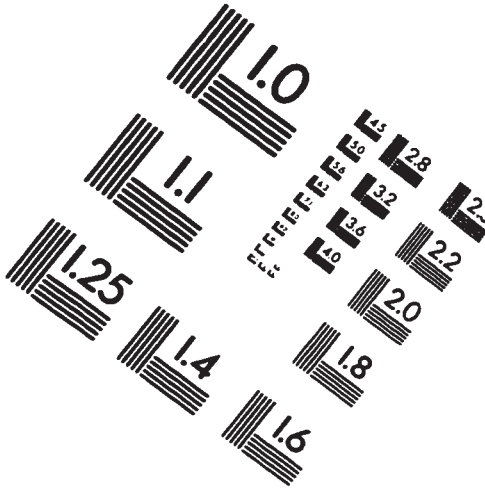

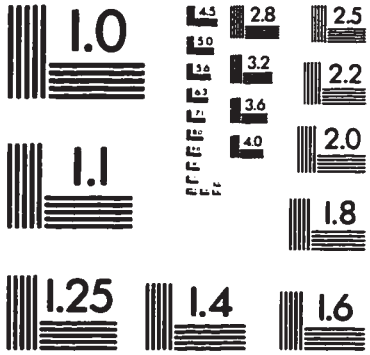

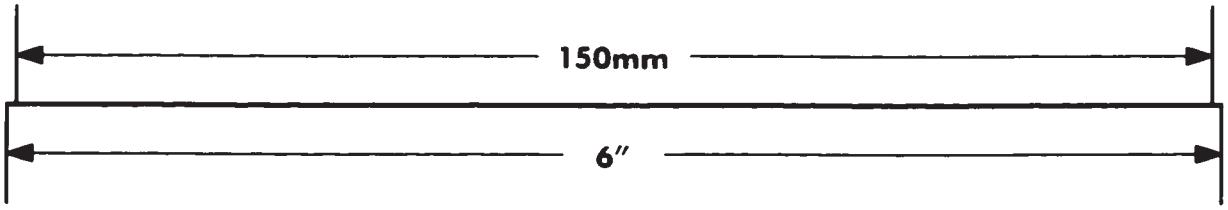

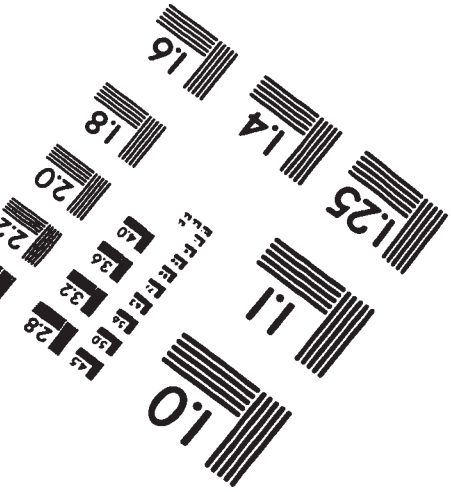

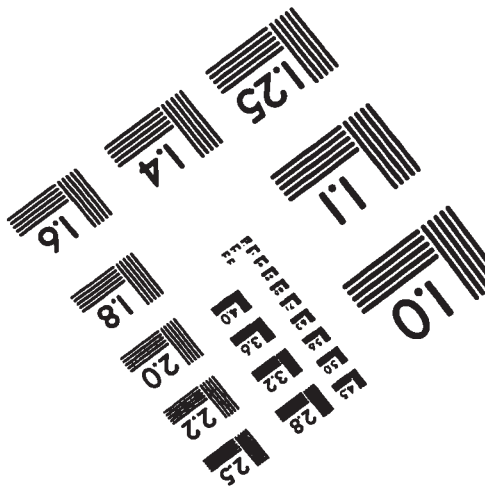

APPLIED IMAGE, Inc
1653 East Main Street
Rochester, NY 14609 USA
Phone: 716/482-0300
Fax: 716/288-5989